Thesis for the Master's degree in Molecular Biosciences

The Role of Cid13 in the G1/S Checkpoint in Fission Yeast

Riikka Taipale

60 study points

Department of Molecular Biosciences
Faculty of mathematics and natural sciences

UNIVERSITY OF OSLO 02/2012

The Role of Cid13 in the G1/S Checkpoint in Fission Yeast

Riikka Taipale

60 study points

Department of Molecular Biosciences
Faculty of mathematics and natural sciences

UNIVERSITY OF OSLO 02/2012

2012

The Role of Cid13 in the G1/S Checkpoint in Fission Yeast

Supervisors: Beáta Grallert, Erik Boye

http://www.duo.uio.no/

Trykk: Reprosentralen, Universitetet i Oslo

ABSTRACT

This study was carried out at the Department of Cell Biology at the Institute of Cancer Research at the Oslo University Hospital as a part of my Master's degree in molecular biosciences at the University of Oslo. Our group is working with cell cycle studies in fission yeast *Schizosaccaromyces pombe* and the main focus is on the G1/S checkpoint which was recently characterized. This checkpoint is activated in G1 phase in response to ultraviolet C (UVC) irradiation which delays the cell-cycle progression in late G1.

The G1/S checkpoint is dependent on the Gcn2 kinase which phosphorylates eukaryotic translation initiation factor eIF2α and this phosphorylation leads to downregulation of general translation. Despite the general downregulation of translation some mRNAs are still translated normally or even at an increased rate after UVC irradiation.

One of these mRNAs is *cid13* and here we explore the importance of Cid13 in response to UVC irradiation in G1. Cid13 belongs to a family of poly(A) polymerases and its only known target is the mRNA of *suc22*, the small subunit of ribonucleotide reductase (RNR). Cytoplasmic polyadenylation is known to increase mRNA half-life leading to increased translation. Cid13 has been suggested to regulate dNTP production by increasing the amount of Suc22 and therefore the total amount of RNR in the cells. RNR is regulated on several levels but no translational regulation has been identified so far.

Here we show that deletion of *cid13* leads to loss of G1/s checkpoint and increased UVC sensitivity. We also show that Suc22 levels are increased in a Cid13 dependent manner after UVC irradiation. However, the levels of dNTPs do not show a corresponding increase. These observations led us to conclude that Cid13 must have other targets important for an appropriate response to UVC irradiation in G1.

ABBREVIATIONS

ADP	Adenosine diphosphate
AMP	Adenosine monophosphate
ATP	Adenosine triphosphate
APS	Ammonium persulphate
BCA	Bicinchoninic acid
BSA	Bovine serum albumin
bp	Base pair
CDK	Cyclin-dependent kinase
cDNA	Complementary DNA
CDP	Cytidine diphosphate
clonNAT	Trade name for antibiotic nourseothricin
CMP	Cytidine monophosphate
CTP	Cytidine triphosphate
DMSO	Dimethyl sulphoxide
dATP	2'-deoxyadenosine 5'-triphosphate
dCTP	2'-deoxycytidine 5'-triphosphate
cGTP	2'-deoxyguanosine 5'-triphosphate
dTTP	2'-deoxythymidine 5'-triphosphate
DNA	Deoxyribonucleic acid
DTT	Dithiotreitol
EDTA	Ethylenediaminetetraacetic acid
e.coli	*escherichia coli*
eIF2α	Eukaryotic initiation factor 2α
EMM	Edinburg minimal medium
EtBr	Ethidium bromide
EtOH	Ethanol
fw	Forward
g	Gram
G1	First gap phase
G2	Second gap phase
GDP	Guanosine diphosphate
GMP	Guanosine monophosphate
GTP	Guanosine triphosphate
HU	Hydroxyurea
Kb	Kilo base
kDa	Kilo Dalton
Leu	Leucine
LiAc	Lithium Acetate
Log	Logarithmic
M	mol/l
M phase	Mitosis

Mb	Mega base
MEA	Malt extract agar
MetOH	Methanol
min	Minute(s)
mL	Milliliter
MQ-H_2O	MilliQ- H_2O
mRNA	Messenger RNA
nat^r	clonNAT resistance
nat^s	clonNAT sensitivity
NEB	New England Biolabs
Nm	Nanometer
OD	Optical density
ORC	Origin Recognition Complex
PA	Polyacrylamide
PABP	Poly(A) binding protein
PAGE	Polyacrylamide gelelectrophoresis
PCR	Polymerase Chain Reaction
PEG	Polyethylene glycol
PNK	Polynucleotide kinase
Pre-RC	Pre-replication complex
PVDF	Polyvinylidine fluoride
RNA	Ribonucleic acid
Rnase A	Ribonuclease A
rev	Reverse
SDS	Sodium dodecyl suplhate
S phase	DNA synthesis phase
S. cerevisiae	*Saccaromyces cerevisiae,* budding yeast
S. pombe	*Schizosaccaromyces pombe,* fission yeast
TEMED	Tetramethylethylenediamine
TBE	Tris/Borate/EDTA
TDP	Thymidine diphosphate
TMP	Thymidine monophosphate
TTP	Thymidine triphosphate
Ura	Uracil
UVC	Ultraviolet C
YE	Yeast extract
x g	Times gravity
µl	Microliter
˚C	Degrees celsius

Gene names in *S. pombe* are written in *small letters* and *italic.*

TABLE OF CONTENTS

1 INTRODUCTION

1.1 Overview

In this introduction chapter I will first describe fission yeast as a model organism. I'll also give an introduction to the cell cycle, checkpoints and G1/S transition in fission yeast before continuing to ribonucleotide reductase and its function and regulation. The emphasis will be in transcription regulation and subcellular localization of both RNR subunits and in the role of Spd1 as an RNR inhibitor. The role of Cid13 in RNR regulation will be elucidated and also some other properties of Cid13 essential to this study will be introduced.

After the introduction I have described all materials (chapter 3) and methods (chapter 4) used in this study. Chapter 5 presents the results from the experiments we have set out to investigate our working hypothesis presented in the chapter 2, Aim of study. In the end, I will discuss my results in light of recent knowledge from the field and suggest some additional mechanisms for how Cid13 is involved in G1/S checkpoint and regulation of dNTP pools in fission yeast.

1.2 Fission yeast as a model organism

The fission yeast, *Schizosaccaromyces pombe*, is a single-celled eukaryote fungus widely used as a model organism in cell biology. The purpose of using model organisms is that it is easier to establish basic principles in simple model organisms than in complicated human cells. In general, model organisms provide a platform for complex genetic studies in a simple system.

S. pombe cells are rod-shaped, 7-15 nm in length and covered with a cell wall. The cell division occurs by binary fission producing two daughter cells; therefore the name fission yeast. Fission yeast is commonly used to study teh cell cycle, cell division and DNA repair as homologues of several fission yeast genes engaged in these mechanisms have been found to be directly involved in human cells (PombeNet at forsburgs Lab, appendix I). Dysfunctions in cell-cycle regulation and DNA repair often lead to genetic abnormalities and severe diseases such as cancer. Relevance of these studies to human

health has been commonly recognized and in 2001 Sir Paul Nurse was honored with the Nobel Prize in Physiology or Medicine for the cell-cycle studies in *S. pombe*.

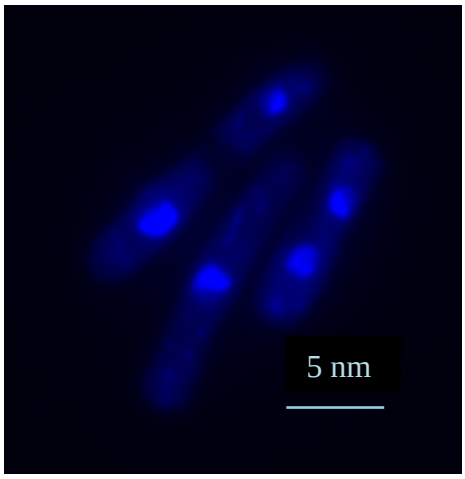

Figure 1.1. Fluorescence microscope picture of *S. pombe* cells in different cell cycle phases. Nuclei stained with DAPI giving a bright blue signal.

Model organisms are chosen because of their advantages to use in the laboratory. Fission yeast is small and has a simple genome which is easy to manipulate. A genome of about 12 Mb is divided between three chromosomes containing approximately 5100 genes, the smallest number of protein coding genes yet recorded for a eukaryote (www.pombase.org) (Wood et al. 2002). PomBase is a recently established internet-based scientific resource that provides detailed and updated information on the fission yeast genome (appendix I).

Being a non-pathogenic fungus, fission yeast can be handled with little precautions. Short generation time and feasible growth conditions provide an effective source of cellular material at a low cost. Classical genetic methods can easily be applied and unlike most other microorganisms, *S. pombe* cells can be maintained in either a haploid or diploid state providing additional advantages. During the last three decades, an increasing number of molecular biologists have chosen fission yeast as their model organism and, as a result, a wide variety of genetic tools are commonly available.

1.3 Fission yeast cell cycle

The cell cycle of *S. pombe* is similar to the general eukaryotic cell cycle consisting of four phases: G1 (first gap-phase), S (synthesis/DNA replication), G2 (second gap phase) and

M (mitosis). This series of events is tightly regulated in order to produce two daughter cells in equal size after each cycle.

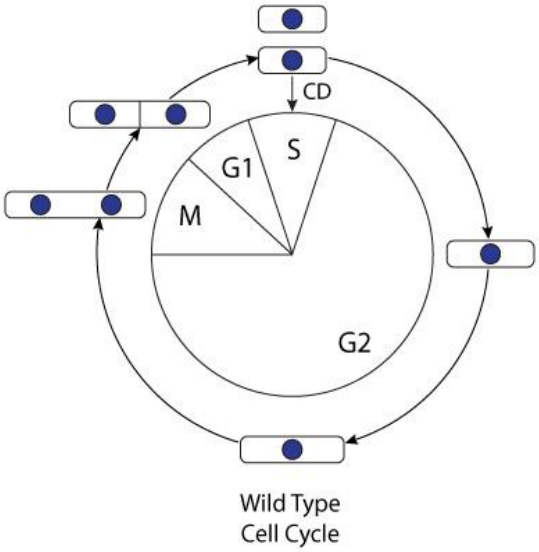

Figure 1.2. A schematic drawing of fission yeast cell cycle. In the laboratory conditions haploid cells spend most of the time in G2. Note that the septation and cell division occur in G1 and S, respectively.

Generally, fission yeast is haploid and under favorable growth conditions the cell cycle is rapid, only 2-4 hours. The cells spend up to 70% of that time in G2 phase producing new cellular material before they enter mitosis where the chromosomes are segregated and equally distributed to produce two separate nuclei with 1C DNA content each. The first gap phase following mitosis is short, but crucial in order to make a decision whether to enter a new cycle or to exit the cell cycle and go into a stationary phase. Fission yeast can also enter the meiotic cell cycle, mate and sporulate, but this occurs only in response to nutrient starvation. Diploid cells can also be used in laboratory.

DNA is replicated in S phase resulting in 2C DNA content in each nucleus. Because of the short G1 phase, the cytokinesis in cycling fission yeast cells takes place during S phase. This special feature can be utilized in modern cell-cycle studies by flow cytometry.

1.3.1 Cell-cycle regulation and checkpoints

The cell-cycle control system is similar in all eukaryotes even if complexity and timing of events vary greatly from one cell type to another. The purpose is to ensure that cell-cycle events occur in the right order and only once per cycle. Periodic gene expression seems to be a universal feature of cell-cycle regulation (Breeden 2003) and more than 400 fission yeast genes are found to be periodically expressed (Rustici et al. 2004).

Cyclin-dependent kinases (CDKs) are the main components of the cell-cycle control system. CDKs are expressed during the whole cell cycle, but their activities rise and fall as the cell progresses through the cell cycle. These changes are regulated by cyclins, CDK inhibitors (CDIs) and phosphorylation. A CDK can be active only when it has a cyclin bound to it. Cyclin protein levels oscillate during one cycle and they are specific to particular cell-cycle phases leading to changes in cyclin-CDK complexes that are being assembled. Activation of one type of cyclin-CDK complex again triggers a new cell-cycle event. (Alberts 2008)

Only one CDK, Cdc2 (Nurse 1990), and four cyclins (Cig1, Cig2 Cdc13 and Puc1 (Martin-Castellanos et al. 1996)) have been identified in *S. pombe*. In addition to CDKs and cyclins, the only known CDK inhibitor in fission yeast, Rum1, is a central player in the cell-cycle control system. Rum 1 inhibits Cdc2/Cdc13 and Cdc2/Cig2 complexes and targets Cdc13 to degradation to allow cells to remain in the G1 phase (Benito et al. 1998). In late G1 and early S phase Rum1 itself is targeted to degradation by Cdc2/Cig1 and Cdc2/Puc1 complexes (Benito et al. 1998). After the inhibition of Cdc2/Cdc13 by Rum1 declines and part of the Cdc13 is degraded in M/early G1, the inhibition is taken over by kinases Mik1 and Wee1 (Baber-Furnari et al. 2000) (Rhind and Russell 2001). They inactivate Cdc2/Cdc13 complex in S and G2 phase and this inhibitory phosphorylation is removed in the end of G2 phase by the phosphatase Cdc25 to allow cells to enter mitosis. In general, degradation of cyclins and CDK inhibitors is important for moving from one cell-cycle phase to another.

The events in the cell cycle of most organisms are ordered into pathways in which the initiation of late events depends on the completion of early events. Dependencies are revealed by perturbations of specific events, for example by application of chemicals, or by the study of mutants that specifically inhibits a particular event in the cell.

Checkpoints are control mechanisms that enforce dependency in the cell cycle events and actively halt cell cycle progression when activated. As an example, the checkpoint gene *rad3* is responsible for delaying mitosis until completion of DNA replication, and the deletion of *rad3* abolishes this dependency (al-Khodairy and Carr 1992). Elimination of checkpoints may lead to cell death, incorrect distribution of chromosomes or other organelles, or increased susceptibility to environmental perturbations such as DNA damaging agents (Hartwell and Weinert 1989).

DNA damage and inhibition of DNA replication are the most studied factors triggering a checkpoint signaling cascade that delays the cell-cycle. This delay is thought to provide cells time to repair the DNA damage or time to complete one cell-cycle phase before proceeding to the next. This is important to avoid chromosomal instability and aberrant cell proliferation, which can cause cancer.

Several DNA damage checkpoints are described in fission yeast (Harris et al. 1996; Rhind and Russell 1998; Caspari and Carr 1999). They all target CDK activity and they are dependent on so-called checkpoint Rad proteins. They were initially identified because their loss of function resulted in defects in cell cycle arrest in response to genotoxic treatments. Nowadays, checkpoint proteins are also known to regulate multiple DNA repair and replication functions. Knowledge of checkpoint signaling and DNA repair pathways are important for determining responses to current cancer therapies, most of which target DNA (Kastan and Bartek 2004).

In the presence of DNA damage, the intra-S checkpoint slows down DNA replication providing time to complete S phase. The S-M checkpoint prevents mitosis as long as DNA replication is incomplete (also called DNA replication checkpoint) and the G2-M checkpoint prevents the cells from entering mitosis if DNA damage is present.

An additional DNA damage checkpoint, the G1/S checkpoint, has been described in *S. pombe*, that doesn't target CDK activity (Nilssen et al. 2003; Tvegard et al. 2007). Checkpoint activation occurs by a still unknown mechanism and leads to activation of the translation regulator Gcn2 kinase. When activated, Gcn2 phosphorylates the eukaryotic translation initiation factor eIF2α, which is the only known substrate for Gcn2. This checkpoint is not a general DNA damage checkpoint as it is induced by some (UVC, MMS, H_2O_2) but not all (IR, PUVA) DNA-damaging agents.

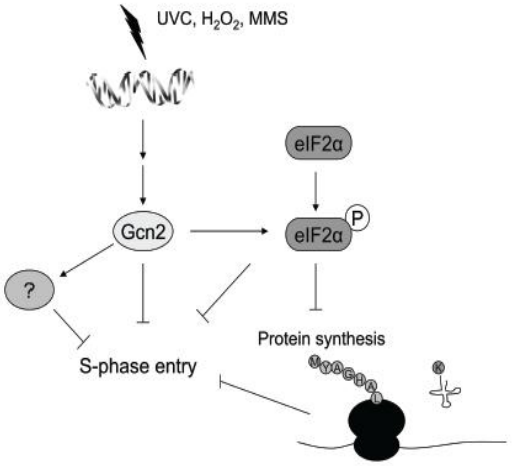

Figure 1.3. A current model for G1/S checkpoint activation. (Krohn 2008, Rothe 2011)

1.3.2 G1/S transition

G1 is a crucial phase in the cell cycle as cells need to make the decision whether to continue into another cycle or to enter the stationary phase. This decision is made at a specific time window in early G1 called Start in yeast or the restriction point in mammals (Alberts 2008).

If extracellular conditions are favorable and signals to grow and divide are present, cells commit to another cell cycle and the G1 is devoted for preparation of DNA replication. This includes the assembly of the Origin Recognition Complex (ORC) which allows recruitment of several other proteins leading to pre-replication complex (pre-RC) assembly at the replication origins.

The main transcription factor for genes involved in the G1/S transition is Cdc10. Temperature sensitive Cdc10 mutants in fission yeast are frequently used in cell-cycle studies to synchronize the cells in the G1 phase (*cdc10* block, see 4.1.5.). In permissive temperature (25˚C), the Cdc10 mutants grow normally, but when changed to restrictive temperature (36˚C), Cdc10 is inactivated leading to cell-cycle arrest in G1 phase.

After releasing the wild type cells from the *cdc10* block, they are shown to peak in S phase approximately 60 minutes later and this corresponds to the appearance of phosphorylated Cdc2 (Krohn et al. 2008). Activation of the G1/S checkpoint leads to a 30-minutes delay into S phase.

Cdt1 (Cdc10-dependent transcript 1) is a replication licensing factor which is expressed only in G1. Degradation of Cdt1 during the S phase is an important mechanism to prevent rereplication (Arias and Walter 2006). Proteolysis of Cdt1 in the S phase is dependent on the Cul4 ubiquitin ligase complex, whose function in turn is dependent on the regulatory protein Cdt2. Transcription of *cdt2* is increased in S phase and in response to DNA damage. Cdt2 is also required in the G1/S transition in order to degrade Spd1, a ribonucleotide reductase (RNR) inhibitor (see 1.4), and hence to activate RNR is the S phase (Liu et al. 2005).

1.4 Ribonucleotide reductase

Eukaryotic ribonucleotide reductase, RNR, is a heterotetrameric enzyme which catalyzes the last and ratelimiting step in the de novo deoxyribonucleotide synthesis from ribonucleotides (Figure 1.4.). It provides the cell with a balanced supply of dNTPs (deoxyribonucleoside triphosphates) for DNA replication and repair, and abnormalities that affect the function or regulation of RNR may lead to genetic abnormalities, cancer and cell death. Several medical therapies, against malaria for instance, target RNR as its function is essential for cell survival.

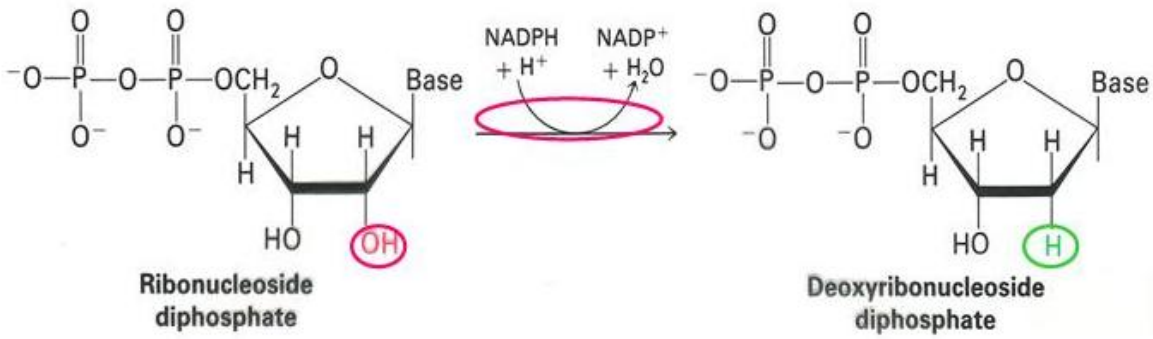

Figure 1.4. The reaction catalyzed by ribonucleotide reductase: NTP → dNTP.

Fission yeast RNR consists of two large regulatory subunits encoded by *cdc22* and two small catalytic subunits encoded by *suc22* (Fernandez Sarabia et al. 1993). These two genes were first identified in screens for mutations in cell-cycle genes (Gordon and Fantes 1986), and DNA sequence comparisons with other organisms led to the observation that they are closely related to RNR genes. The small subunit Suc22 is localized primarily in the nucleus and it is relocalized to the cytoplasm during the S-phase

or following DNA damage checkpoint activation leading to tetramerisation of RNR and production of dNTPs (Liu et al. 2003).

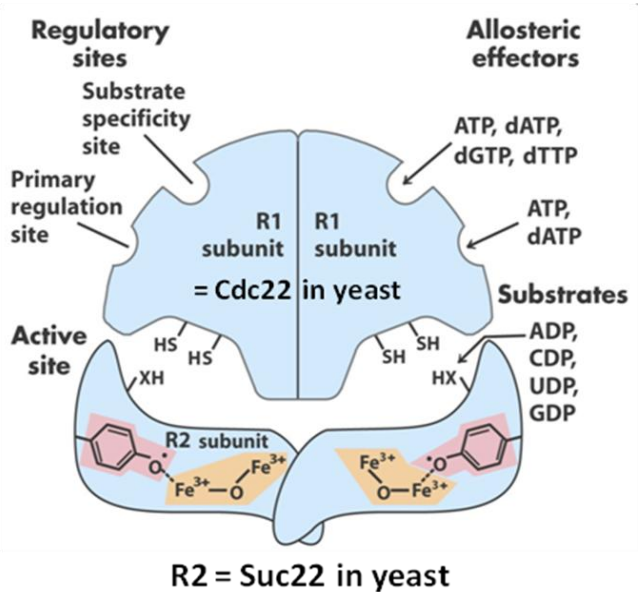

Figure 1.5. A schematic drawing of eukaryotic ribonucleotide reductase class 1a. A dimer of large subunits, Cdc22 in *S. pombe*, forms the regulatory part of the enzyme. A dimer of small subunits, Suc22 in *S. pombe*, provides the catalytic sites of the enzyme.

(www.biochem.arizona.edu)

The reduction reaction catalyzed by RNR is strictly conserved in all living organisms (Torrents et al. 2002) . This reaction is initiated by generation of a free radical and it is oxygen-dependent in fission yeast RNR (Harder and Follmann 1990). The small catalytic subunit of class I eukaryotic RNRs contains a diferric iron center and a tyrosyl radical, which is buried inside the hydrophobic environment and stabilized by an iron center (reviewed in (Stubbe and Riggs-Gelasco 1998)). The chemotherapeutic agent hydroxyurea (HU) is an inhibitor of RNR activity, because it quenches the free radical (Harder and Follmann 1990). When cells are exposed to HU, they arrest the cell cycle in S phase. This is due to shortage of nucleotides which causes replication stress activating the DNA replication checkpoint.

Substrates for RNR are ADP, GDP, CDP and UDP. Catalysis of ribonucleoside 5'-diphosphates (NDPs) involves a reduction at the 2'-carbon of ribose 5-phosphate to form the reduced 2'-deoxyribonucleoside 5'-diphosphates (dNDPs) (figure 1.4.). Both the overall concentration and the balance among the individual dNTPs are tightly regulated to ensure high fidelity DNA replication and repair. It has been recently reported that the DNA replication checkpoint is not activated by extreme and mutagenic dNTP pool imbalances, but only when one of the dNTPs is limiting (Kumar et al. 2010). Eukaryotic

cells with class Ia RNR have an allosteric control mechanism to selectively turn on and off synthesis of particular dNTPs as they accumulate.

1.4.1 Transcription regulation of RNR subunits

Transcription of RNR genes is tightly regulated during the cell cycle. Regulation of transcription is the first regulatory step defining the amount of available mRNAs for translation. Both RNR subunits are to some extent subjected to periodical regulation of transcription.

The length of the *cdc22* transcript is about 3.3 kb and the *suc22* transcript is about 1.5 kb. In earlier cell-cycle studies it was found that the level of *cdc22* transcript varies strikingly during the normal cell cycle reaching the maximum at the G1-S boundary while the level of 1.5 kb *suc22* transcript is constant (Gordon and Fantes 1986). Studies in *S. cerevisiae* have shown that the mRNA levels of RNR2, the small subunit of RNR, show a modest 2-fold fluctuation, and reaches a maximum in S phase (Elledge et al. 1993).

However, another *suc22* transcript was found in later studies and confirmed to derive from the same *suc22* gene. When *S. pombe* cells were exposed to hydroxyurea (HU), a 1.9 kb transcript was detected at very low levels in addition to the previously described 1.5 kb transcript (Fernandez Sarabia et al. 1993). In 1996, Harris et al. showed that the level of the 1.9 kb transcript fluctuates in a similar manner as the level of the *cdc22* transcript peaking at the G1/S transition. They also suggest that it is not HU itself that causes induction of the large *suc22* transcript, but the fact that HU-treated cells arrest in S phase and therefore the 1.9 kb transcript of *suc22* starts to accumulate and reaches a level at which can be detected.

The 1.5 kb and 1.9 kb mRNA species of *suc22* differ in their 5’ untranslated regions (UTRs). The large transcript is a product of *suc22* with start site some 550 nucleotides upstream of that of the smaller transcript and contains two MCB (MluI cell cycle box; ACGCGT) elements 5' to the start. Similar MCB elements are found in the *cdc22* promoter region. The role of MBC motifs in regulation G1/S transcription in fission yeast has been studied in more detail using *cdc22* as an example (Maqbool et al. 2003). These motifs bind a transcription factor complex DSC1 (DNA synthesis control) and contains products of several genes, for example *cdc10* (Lowndes et al. 1992). Several MBC-element containing genes are known to be induced also in response to DNA damage.

As mentioned earlier the *cdc22* promoter region contains two MBC elements. It is proposed that these elements affect the transcription of *cdc22* differently: MBC2 ensures basal transcription, while MBC1 stimulates cell-cycle dependent transcription (Maqbool et al. 2003). *Cdc22* transcription is also induced in response to HU treatment. This is consistent with the fact that *cdc22* expression increases in S phase, which is where HU-treated cells accumulate.

Transcription of the larger *suc22* mRNA and *cdc22* is confirmed to become induced also outside S phase in response to heat shock and DNA damage caused by the UV mimetic agent 4-nitroquinoline oxide (4-NQO). Both heath shock and DNA damage during G2 prevents the cells from entering mitosis because of the checkpoint activation (Harris et al. 1996). The DNA damage checkpoint and the DNA replication checkpoint pathways share several components while heat shock response is based on the presence of the heat shock consensus element upstream of the large transcript start site. Harris et al. (1996) showed that induction of the large *suc22* transcript is dependent on an intact DNA damage checkpoint. Also Caf1, a component of the Ccr4-Not transcription factor complex, is shown to be required for activation of 1.9 kb *suc22* mRNA transcription in response to HU (Takahashi et al. 2007). Interestingly, Caf1 is also an RNase which shortens poly(A) tails.

Both Cdc22 and Suc22 function is required for cells to entry S phase and to complete DNA replication and loss-of-function mutants of either gene are lethal (Fernandez Sarabia et al. 1993). When studying the DNA sequence of both *suc22* transcripts no additional translation initiation codon can be found upstream of that for the smaller transcript. This indicates that both transcripts give rise to the same protein product.

1.4.2 Cytoplasmic polyadenylation of *suc22* mRNA by Cid13

Cytoplasmic extension of poly(A) tail leads to translational activation and provides a rapid mechanism to upregulate protein expression without need for new transcription. It also counteracts the deadenylation of active mRNAs that are otherwise destined for degradation. Translational regulation is an important mechanism in some specialized cell types as mammalian embryonic cells (Kronja and Orr-Weaver 2011) and there is increasing evidence that it plays some role also in cell-cycle regulation of somatic cells. Translational regulation additionally coordinates cell cycle progression with growth.

Because progression through the cell cycle is linked to the attainment of certain size, translational regulation of gene expression couples cell growth and cell cycle progression with the supply of nutrients in the cell's environment.

Nuclear polyadenylation of mRNA is catalyzed by canonical poly(A) polymerases (PAPs). During the past ten years, a new Cid1 family of PAPs that regulate specific mRNAs both in the nucleus and in the cytoplasm has been characterized. The first member of these non-canonical poly(A) polymerases was described in fission yeast and it was found to be involved in the replication checkpoint (Wang et al. 2000). A few years later, Saitoh et al. (2002) identified another member of PAPs, Cid13, which is found to localize both in the cytoplasm and the nucleus and its only known target is the 1.9 kb transcript of *suc22*.

It has been shown that *cid13Δ* cells exposed to HU are not able to upregulate the 1.9 kb *suc22* transcript to the same extent as *cid13+* cells (Saitoh et al. 2002). Also the abundance, half-life, and poly(A) tail of the 1.9 kb *suc22* mRNA was found to be substantially reduced in *cid13Δ* cells. Saitoh et al. (2002) conclude from these observations that Cid13 controls dNTP synthesis and HU tolerance. They also argue that cytoplasmic polyadenylation of *suc22* may provide a mechanism to rapidly enhance dNTP synthesis in response to DNA damage.

Taken together, cells respond to DNA damage by inducing transcription of an additional *suc22* transcript. This may be one mechanism to provide more RNR and eventually produce more dNTPs for DNA repair. It is not yet known whether cytoplasmic polyadenylation of this transcript with Cid13 strengthens this effect in response to DNA damage.

1.4.3 Spd1 as RNR inhibitor

Regulation of RNR involves several different mechanisms. RNR inhibitors are among the most important regulators of RNR activity. Inhibitors can target translation of RNR subunits, destroy the catalytic activity (e.g. HU; see 1.4.) or inhibit tetramerization. A significant proportion of RNR regulation in cycling cells thus occurs post-translationally.

The most studied RNR inhibitor of fission yeast is Spd1 which seems to both inhibit and enhance tetramerization leading to inhibition of enzyme activity. Spd1 is a small

intrinsically disordered protein, which is able to interact with both RNR subunits. Earlier studies suggested that Spd1 is responsible for nuclear sequestration and anchoring of Suc22 keeping RNR inactive outside S phase and when DNA damage is not present (Liu et al. 2003). Nuclear co-localization of Suc22 and Spd1 was observed, but no direct interaction was shown. In 2006, Hakansson et al. showed that Spd1 binds to Cdc22 with much higher affinity than to Suc22 and they suggested that Spd1 is mostly localized in the cytoplasm and controls RNR activity directly by binding the RNR large subunit Cdc22.

One of the recent hypotheses postulates that Spd1 first mediates formation of immature, inactive RNR complex. Then, Spd1 degradation would leave the subunits in the optimal conformation for catalytic activity (Nestoras et al. 2010). This model takes into consideration that Spd1 can interact with both subunits as predicted earlier, and that this interaction occurs in the cytoplasm. Nestoras et al. (2010) also show that there is no correlation between the observed interaction of RNR subunits, RNR inhibition, and Suc22 nuclear import.

Spd1 is degraded in S phase and after DNA damage to allow upregulation of dNTP levels. Degradation is mediated by the activity of the $CRL4^{Cdt2}$ ubiquitin ligase complex (Holmberg et al. 2005) and can be achieved in two ways. First, Cdt2 levels peak in S phase (see 1.3.2.) and it binds to the ubiquitin ligase complex activating it. Second, Cdt2 levels increase in response to DNA damage checkpoint activation and leads to activation of the ubiquitin ligase complex.

It has also been reported that Caf1, a component of the Ccr4-Not transcription factor complex (see also 1.4.1.), plays a role in Spd1 degradation in response to replication stress caused by HU treatment. Takahashi et al. (2007) suggest that Caf1 is required for HU-induced release of nuclear Suc22-Spd1 and cytoplasmic translocation of Suc22, and that the exonuclease activity possessed by Ccr4-Not complex is responsible for the Spd1 degradation ability. They have also studied the synergistic effect of Caf1 and Cid13. Both *caf1Δ* and *cid13Δ* single mutants are HU-sensitive, while the double mutant does not show any increased HU-sensitivity indicating that Caf1 and Cid13 may act in the same pathway.

Salguero et al (2011, in press) have suggested a link between Spd1 degradation and DNA damage. They report that the DNA-bound polymerase processivity factor PCNA triggers

proteolysis of Spd1 by the $CRL4^{Cdt2}$ ubiquitin ligase complex. They argue that the PCNA-Spd1 interaction can potentially target RNR to sites of DNA synthesis. This provides an opposing argument to the generally accepted view that active RNR is cytoplasmic. Further work is required to elucidate this apparent contradiction.

1.5 Cid13 expression is not affected by UVC irradiation or exposure to HU

UVC irradiation of fission yeast cells in G1 phase trigger the G1/S checkpoint and leads to a delay in cell-cycle progression (Nilssen et al. 2003). Activation of Gcn2 kinase with UVC leads to phosphorylation of eIF2α and repression of general translation after irradiation, but it is not clear whether this is required for the checkpoint. Ongoing studies focusing on the translational response after UVC irradiation in G1 have shown that Cid13 mRNA is maintained in the polysome fraction suggesting that translation of Cid13 is not affected by UVC (Knutsen, JH., unpublished). Actively transcribed mRNA has multiple ribosomes bound to it and this formation is called a polysome. This finding led us to investigate whether Cid13 is required to upregulate dNTP pools in response to DNA damage caused by UVC and whether dNTP levels affect the G1/S checkpoint activation.

During an unperturbed cell cycle, expression and localization of Cid13 is known to be constant and it is found not to be affected by exposure to HU. Deletion of *cid13* leads to sensitivity to long-term exposure to HU, but the cells are not significantly affected by short-term HU exposure causing replication stress which cells can cope with an intact S-M checkpoint. Both Saitoh et al. (2002) and Read et al. (2002) suggest that Cid13 acts independently of checkpoints and that it probably has other targets than *suc22* mRNA.

1.6 DNA damage and dNTP pools

All organisms are exposed to various DNA damaging agents during their lifetime. This is a constant threat to genome integrity and the damage must be repaired immediately to avoid chromosomal instability and eventual cell death. To survive the DNA damage, checkpoints and reparation systems must be intact. Most DNA repair pathways are highly conserved across the species underlining their importance for cell survival.

In this study, UVC irradiation is used as a DNA-damaging agent, and the standard dose of 1100 J/m^2 is given to the cells in liquid medium. Exposure to this dose corresponds to a survival rate of 10-20% in wild type cells. UVC irradiation leads to formation of cyclobutane pyrimidine dimers, CPDs (figure 1.6.) and 6-4 photoproducts on DNA, and causes damage on other macromolecules in the cells as well. In fission yeast UV-induced DNA damage is repaired by nucleotide excision repair (NER) pathway and/or by UV-damage DNA endonuclease-dependent excision repair (UVER) pathway. Many other organisms posses enzymes called photolyases which are able to remove UV-induced DNA damage, but no such enzymes are found in fission yeast and mammalian cells.

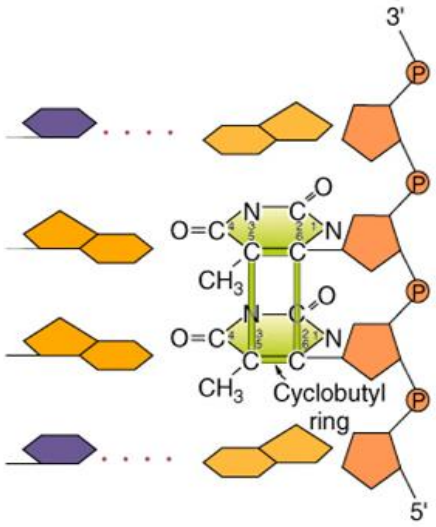

Figure 1.6. Ultraviolet light is absorbed by the nucleic acid bases. This can induce chemical changes as bond formation between adjacent pyrimidines within one strand. The most frequent of these so called photoproducts are cyclobutane pyrimidine dimers, CPDs, shown here.

High-fidelity DNA repair is dependent on sufficient pools of free dNTPs in the cells. This can be achieved by increasing the RNR activity, which again can be achieved in several ways (1.4.). Outside the S phase, levels of dNTPs are generally much lower than levels of their precursors, NTPs.

Transcriptional activation of RNR subunits as well as degradation of RNR inhibitor Spd1 is linked both to the cell cycle and to the checkpoint response (Harris et al. 1996). Regulation of nucleotide pools in response to DNA damage in fission yeast is not studied extensively. However, it has been shown that asynchronous *S. pombe* cells increase dNTP levels twofold in response to 4-NQO, while in *S. cerevisiae* the increase is 6-8-fold. When G1-arrested fission yeast cells enter the S phase, an equal 2-fold increase in dNTP levels is observed. The low increase in dNTP pools in response to DNA damage,

compared to many other organisms, has been suggested to be caused by the relatively tight feedback inhibition of the fission yeast RNR. (Hakansson et al. 2006).

Upregulation of dNTPs in response to 4-NQO treatment is apparently dependent on activation of the DNA damage checkpoint which leads to RNR activation via degradation of Spd1. It is not yet known whether UVC-induced DNA damage in G1, and the subsequent G1/S checkpoint activation, leads to activation of RNR and increased dNTP pools, and whether this correlates with repair activity in the cells.

2 AIM OF STUDY

The aim of this study is to explore the possible physiological effects of Cid13 on Suc22 expression and dNTP pools in response to UVC irradiation in G1 phase. The working hypothesis is the following:

If *cid13* is deleted

→ 1.9 kb *suc22* mRNA is less stable

→ less translation of Suc22

→ less RNR activity

→ less dNTPs

→ less DNA repair

→ G1/S checkpoint is affected

The following questions are elucidated to test the hypothesis:

1) Does Cid13 contribute to cell survival after UVC irradiation in G1?
2) Does Cid13 contribute to cell-cycle delay in entry into S phase after UVC irradiation in G1?
3) Does Cid13 affect Suc22 levels and localization in response to UVC irradiation in G1?
4) Does Cid13 contribute to upregulate dNTP pools in response to UVC irradiation in G1?

3 MATERIALS

3.1 Yeast strains

Table 3.1. The following *S. pombe* strains were used in this study.

Strain	Referred to as	Genotype	Supplier
#489	wild type	*cdc10-M17*	Lab collection
#1005	wild type	*cdc10-M17 ura4-D18 h+*	Lab collection
#1138	*gcn2Δ*	*cdc10M-17 gcn2::ura4+ ura4-D18 h-*	Lab collection
#1639	*cid13Δ*	*cdc10-M17 cid13::leu2+ ura4-D18 leu1-32 h-*	Lab collection
#1353	*rad3Δ*	*cdc10-M17 rad3::ura4+ ura4-D18 h+*	Lab collection
#1697	wild type	*cdc10-M17 suc22:GFP:natMX6 ura4-D18 h+*	This study
#1673	*gcn2Δ*	*cdc10M-17 gcn2::ura4+ suc22:GFP:natMX6 ura4-D18 h-*	This study
#1674	*cid13Δ*	*cdc10-M17 cid13::leu2+ suc22:GFP:natMX6 ura4-D18 leu1-32 h-*	This study

3.2 Plasmids and primers

3.2.1 Plasmids and template sequences

1) The following plasmids were used as templates to amplify transforming DNA. Plasmid #136 was used to amplify *ura4+* and plasmid #309 was used to amplify GFP-clonNAT tag.

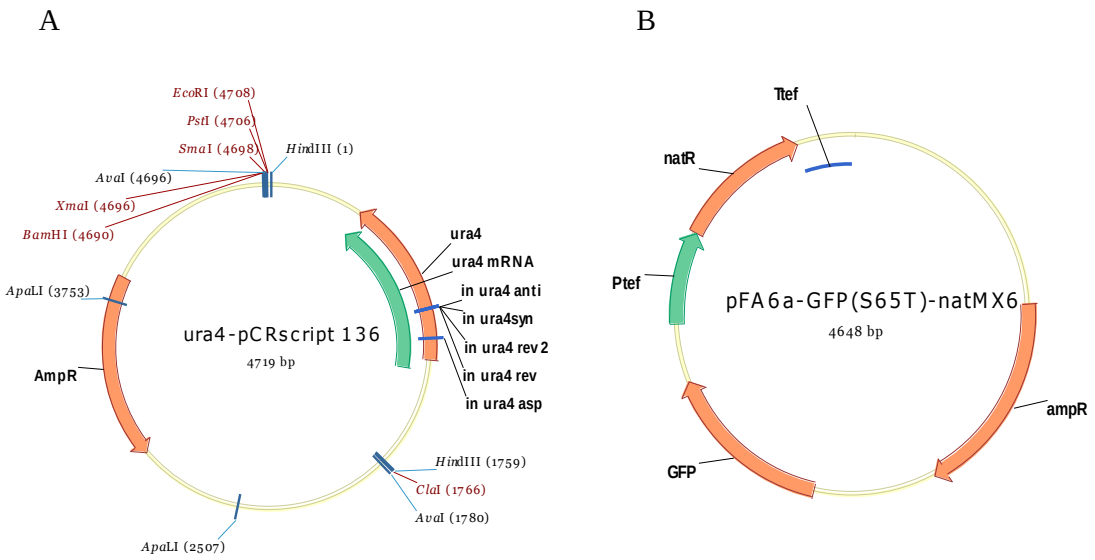

Figure 3.1. A) A map of plasmid #136: ura4-pCRscript 136. B) A map of plasmid #309: pFA6-GFP(S65T)-natMX6.

2) For *ura4+* deletion from *suc22:GFP:ura4+*, *S. pombe* genomic DNA was used as a template.

3) DNA sequence for tA template for polymerase assay:

3’ – CCATCCCGAAGCGTCGGCAGGTTAATAATAATAA - 5’

3.2.2 Primers

Table 3.2. Primers used to amplify the C terminal GFP-clonNAT tag for *suc22*.

Primer name	Direction	Sequence	Supplier
Suc22 tag fwd	forward	5’-ACTACCAAATTGCTGGCGTTATGT CGGGTACCAAGCGCGCTGAGAAGGATGA TCATACATTTACAATCGATGAGGACTTT – CGGATCCCCGGGTTAATTAA- 3’	DNA Technology A/S
Suc22 tag rev	reverse	5’ -TATTGCTAAATAGGTTATCAGTAA TCAATAATATTTTTTTTTTGCTTTAACTTA TCTAAAAACCAAAAATAACTAGTCAT – GAATTCGAGCTCGTTTAAAC- 3’	DNA Technology A/S

Table 3.3. Primers used to amplify *ura4+* deletion cassette to remove *nat*^{r} (clonNAT) from Suc22:GFP:clonNAT tag.

Primer name	**Direction**	**Sequence**	**Supplier**
A + b	forward	5' –CGAAAAGAGAGACCACATGGTC CTTCTTGAGTTTGTAACAGCTGCTGGGAT TACACATGGCATGGATGAACTATACAAA TAG - gctttaaattaaaatggttc- 3'	DNA Technology A/S
D + c	reverse	5' –TATTGCTAAATAGGTTATCAGTAA TCAATAATATTTTTTTTTGCTTTAACTTT AACTTATCTAAAAACCAAAAATAACTAG TCAT - ctataatagttaatattttagtc- 3'	DNA Technology A/S

Table 3.4. Primers used to amplify wt sequence to remove *ura4+* which is used to replace *nat*^{r}.

Primer name	**Direction**	**Sequence**	**Supplier**
A + e	forward	5'-CGAAAAGAGAGACCACATGGTCCT TCTTGAGTTTGTAACAGCTGCTGGGATTA CACATGGCATGGATGAACTATACAAATA G - atgactagttatttttggtt- 3'	DNA Technology A/S
F	reverse	5' – GATAAGTCAACCATAAATCG- 3'	DNA Technology A/S

Table 3.5. Primer for polymerase assay (4.4.).

Primer name	**Sequence**	**Supplier**
p22	5' – GGTAGGGCTTCGCAGCCGTCCA - 3'	Lab collection, University of Copenhagen

3.3 Enzymes

Following table (3.6.) contains the enzymes used in this study, apart from the enzymes included in kits (chapter 3.7. Kit).

Table 3.6. Enzymes

Enzyme	**Supplier**
S.H.P/H.PJ. Helix Pomatia Juice (helikase)	BioSepra
Zymolase	MP Biomedical
Ribonuclease A	Sigma-Aldrich
Xma I	New England Biolabs
PNK	Lab collection, University of Copenhagen
Klenow fragment of DNA polymerase I (5000 U/mL)	New England Biolabs

3.4 Antibodies

Table 3.7. Antibodies used to immunodetection and visualization of proteins in this study.

Type of antibody	**Antigen**	**Source**	**Concentration**	**Supplier**
Primary	GFP	rabbit	1:2500	abcam
	cdc2-P	rabbit	1:400 (preabsorbed)	Cell Signaling Technology
	cdc2	rabbit	1:1000	Santa Cruz Biotechnology, INC.
	eIF2α-P	rabbit	1:3000	Invitrogen
	Tubulin	mouse	1:30 000	Sigma-Aldrich
Secondary	Anti-rabbit, IgG alkaline phosphatase linked whole antibody	goat	1:10 000	GE Healthcare
	Anti-mouse, IgG+IgM alkaline phosphatase linked whole antibody	goat	1:5000	GE Healthcare

3.5 Molecular weight standards

The molecular weight standards in table 3.8. were loaded to the gel to be able to estimate size and amount of DNA or protein in a sample. Pictures of the ladders are provided in the appendix 2.

Table 3.8. Molecular weight standards used in this study.

Molecular weight standard	Range	Supplier
O'GeneRuler 1kb DNA Ladder, ready-to-use	250 – 10 000 bp	Fermentas
PageRuler Prestained Protein Ladder	10 – 170 kDa	Fermentas
Novex Sharp Protein Standard	3.5 – 260 kDa	Invitrogen

3.6 Chemicals and reagents

Chemical/reagent	Supplier
2-propanol	Sigma-Aldrich
5-fluoroorotic acid	Sigma-Aldrich
Acetic acid	VWR
Agarose type 1	Sigma-Aldrich
Annealing buffer	Lab collection, University of Copenhagen
APS	Bio-Rad
Bio-safe Coomassie Brilliant Blue Stain	Bio-Rad
DMSO	Sigma-Aldrich
DTT	Sigma-Aldrich
ECF substrate	GE Healthcare
ECF dilution buffer	GE Healthcare
EDTA	Sigma-Aldrich
Ethanol	Kemetyl Norge AS
GelRed	Life Technologies
Hoechst 33258	Sigma-Aldrich

Membrane blocking agent	GE Healthcare
Methanol	Merck
NEBuffer #2	New England Biolabs
NEBuffer #4	New England Biolabs
PNK-buffer	Lab collection, University of Copenhagen
Ponceau S	Bio-Rad
Polyacrylamide	Sigma-Aldrich
Sheared herring testes DNA	Intergen
Sytox Green	Invitrogen
TEMED	Bio-Rad
Urea	Sigma-Aldrich

3.7 Kit

Kit	**Supplier**
AccuPrime Pfx DNA Polymerase	Invitrogen
iProof™ High-Fidelity DNA Polymerase	BioRad
QIAquick PCR Purification Kit	QIAGEN
Pierce BCA Protein Assay Kit	Thermo Scientific
ATP Determination Kit	Biaffin GmbH & Co KG
illustra AutoSeq™ G-50 Dye Terminator Removal Kit	GE Healthcare

3.8 Solutions

3.8.1 Yeast growth media and agar plates

Growth media	Ingredients
EMM medium	32.3 g/L EMM Supplemented with 225 µg/mL amino acids when needed
EMM agar plates	48.8 g/L EMM agar
MEA agar plates	30% malt extract, 20g/L agarose
YE 50 medium	0.5% Yeast Extract, 30 g/L glucose, 250 mg/mL histidine, 250 mg/mL leucine, 250 mg/mL adenine, 250 mg/mL uracil, 250 mg/mL lysine
YE 50 agar	As YE medium above, in addition: 20 g/L agar
YE 50 agar with clonNAT	YE 50 agar supplemented with 100 µg/ml clonNAT
YE 50 agar with hydroxyurea	YE 50 agar supplemented with hydroxyura to 5 or 7 mM
YE 50 agar with 5-FOA	YE 50 agar supplemented with 1mg/mL 5-fluoroorotic acid

3.8.2 Buffers and other solutions

Solution	Ingredients
Agarose gel solution, 1%	1% agarose 1 x TAE buffer
Citrate/phosphate pH 5.6	7.1 g/L Na_2HPO_4 11.5 g/L citric acid
Citrate/phosphate/EDTA/sorbitol	50 mM citrate/phosphate pH 5.6 40 mM EDTA pH 8.0 1 M sorbitol
Denaturing sample buffer (2x)	125 mM Tris-HCL pH 6.8 20% glycerol 4% SDS 0.1% (w/v) bromphenol blue 200 mM DTT
Denaturing sample buffer (1x)	For 5 mL: 1 mL 200 mM Tris-HCl pH 8

	2.5 mL 2x sample buffer 1.5 mL MQ-H_2O
DNA loading buffer (6x)	0.5M EDTA pH 8.0 40% (w/v) sucrose 0.25% bromphenol blue
EDTA pH 8.0 (0.5 M)	146.12 g/L EDTA NaOH to pH 8.0
LiAc/TE (10x)	1 M lithium acetate 1x TE Acetic acid to pH 7.5
Loading buffer for protein samples	2 mL 87% glycerol 50 µL 10% bromphenol blue 1 mL H_2O
PEG/LiAc/TE	40% PEG 4000 1x LiAc/TE
PBS (1x)	137 mM NaCl 2.7 mM KCl 4.3 mMNa_2HPO_4 1.47 mM KH_2PO_4
Potassium acetate pH 5 (5 M)	118 g KAc 46 mL acetic acid (to pH 5)
Resuspension buffer	20 mL 1x TE 5 mL Tris pH 6.8 (0.5 M) 6 mL 10% SDS 1 mL 87% glycerol 2 mL H_2O
Running buffer (10x)	30.2 g/L tris 144 g/L glycine 1% (w/v) SDS
Sodium Acetate pH 5.2 (3 M)	40.8 g NaAc*3 H_2O to 100 mL H_2O Adjust to pH 5.2 with glacial acetic acid
STOP buffer (2x)	20 mM Tris-HCl pH 8.0 150 mM NaCl 50 mM NaF 10 mM EDTA 1 mM NaN_3
TAE buffer (10x)	48.4 g Tris base 11.4 mL glacial acetic acid (17.4 M) 3.7 g EDTA

	Dilute the buffer to 1 L MQ-H_2O
TBS-T	20 mM Tris-HCl pH 7.5 8 g/L NaCl 0.05% (v/v) Tween-20
TE pH 7.5 (10x)	0.1 M Tris-HCl pH 8.0 0.01 M EDTA pH 8.0 HCl to pH 7.5
Transfer buffer	50 mM Tris 380 mM glycine 0.1% (w/v) SDS 20% (v/v) methanol

4 METHODS

4.1 Cell biology methods

4.1.1 Growth and maintenance of *S. pombe* cells

Liquid cultures

Liquid Yeast extract medium (YE) is a rich growth medium providing optimal growth conditions to *S. pombe*. Wild type cells have a generation time of three hours in YE, while some mutant strains need up to five hours. Liquid Edinburgh minimal medium (EMM), with additional supplements when needed, is a well defined, but poorer growth medium than YE. Therefore the generation time is somewhat longer when cells are grown in EMM than in YE.

To start a liquid culture a loop of cells is inoculated in YE medium at 25˚C overnight without shaking to grow cells to early stationary phase. This pre-culture is used to prepare a main culture in either YE or EMM, depending the experiment, with desired volume and cell number. The main culture is grown at 25˚C overnight in a shaking water bath.

The volume/cell number can be calculated from the optical density of the liquid culture in 595 nm (Hitachi U-1900 Spectrophotometer was used in this stuty). As *S. pombe* divides to two equal daughter cells during one generation the cell number doubles during one generation time in logarithmically growing culture. The following equation is used to calculate the correct volume of the inoculum:

$$V_{preculture} = \frac{V_{total} * OD_{desired}}{OD_{preculture} * 2^{n}},$$

where $V_{preculture}$ is the volume of the preculture used as inoculum, V_{total} is the total volume of the new culture, $OD_{desired}$ is the desired optical density of the new culture measured at 595 nanometers at defined time point and $OD_{preculture}$ is the OD_{595nm} measured for the pre-culture. The number of generations, n, is defined by the time cells are grown in liquid medium divided by the generation time of that particular strain.

The pre-culture should have OD_{595nm} 0.1-1.0 when it is used to prepare a main culture because *S. pombe* cells grow slowly at low cell density, and if the culture has reached the stationary phase the cells are allowed to reenter the cell cycle for one generation time before further inoculation.

Growth on malt extract agar (MEA)

Conjugation and sporulation of *S. pombe* cells cannot take place except under nutrient starvation. MEA is a poor growth medium allowing cells several rounds of vegetative growth before they run out of nutrients. The cells with opposite mating type are then able to conjugate and sporulate. MEA plates were used in this study for making new strains by crossing and for identifying the mating type (see 4.1.2.).

Strain maintenance

For long-time storage *S. pombe* strains are maintained frozen at -80˚C in YE 50 medium mixed with 50% sterile glycerol in 1:1 ratio. A small cell culture is grown to late-logarithmic phase before adding glycerol and the cell suspension is moved to a cryotube for storage.

To reisolate cells from frozen culture a small amount of cell suspension is scraped from the frozen stock and the patch is incubated on a YE agar plate for 1-4 days, depending on the strain, in 25˚C. When growth is visible cells are streaked out to form single colonies on a fresh YE agar plate and incubated 2-3 days before further use. YE agar plates can be stored in the fridge for at least 8 weeks, but it is recommended to streak out a fresh plate before each experiment. In this study YE agar plates have been also used for selection purposes when supplemented with hydroxyurea or clonNAT. Strains do not store well on EMM agar plates (with or without supplements), but these are widely used for selection for auxotrophs (see 4.1.3.). See chapter 3.8.1. for description of growth media.

4.1.2 Crossing, random spore analysis and identification of the mating type

To introduce new genes or replace existing genes in fission yeast cells I can cross two strains with different genotypes and select for progeny I am interested in. Genetic crossing can only occur between two strains with different mating types, h+ and h-. Malt

extract (ME) is used as growth medium as it is nutritionally poor medium and when the cells starve they begin to mate and sporulate.

1) Mix a toothpick full of cells of each two strains in 300-400 µl of MQ-H_2O. Pipette 20 µl to a MEA plate and incubate at 25˚C for two days.
2) Inoculate a toothpick full of cells with helikase in 0,5 ml of MQ-H_2O; either with 1 µl helikase at 25˚C ON or with 5 µl helikase from two to three hours in 36˚C.
3) Look for spores under the microscope.
4) Spin down 1 min at 21 000 x g and resuspend the pellet in 1 ml MQ-H_2O.
5) Plate out 20 µl and streak for single colonies. Incubate at 25˚C until colonies appear.
6) Replica plate to selective plate(s) (4.1.3).

To identify the mating type of the new cells these can be crossed with both h+ and h- strains and examined further.

1) Pick several candidates from the plates and cross them with known h+ and h- strains. Incubate at 25˚C for two days. See figure 4.1 for streaking pattern.
2) Add crystalline iodine to the Petri dish and incubate 1-5 minutes. Iodine vapor will break down starch in spore walls and turn that area dark violet. This will tell you if the mating and sporulation has taken place.

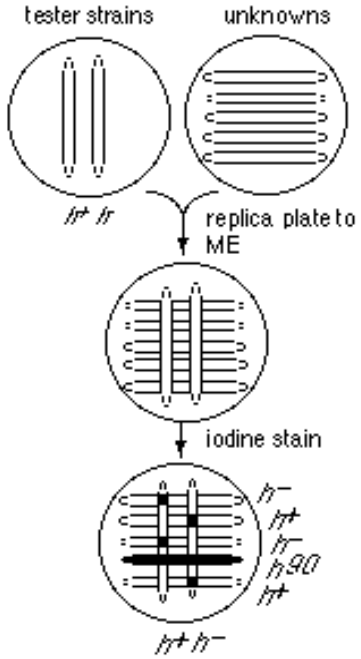

Figure 4.1. Streaking pattern for identifying the mating type of new strains after the genetic cross. Two strains with the opposite mating type will sporulate and the areas with spores will turn dark when treated with iodine. The heterothallic h90 strain is able to switch the mating type and sporulate within the own strain. (Figure: (Forsburg 2003)

4.1.3 Replica plating

Replica plating is a technique that allows screening for nutritionally defective mutants called auxotrophs or for other selectable phenotypes. A number of auxotrophic markers exist in *S. pombe* and the most commonly used are genes for adenine, leucine, lysine and uracil. In this study replica plating has been used to identify colonies with desired genotype after transformation.

In replica plating a pattern of *S. pombe* colonies on a YE plate is copied to a selective plate using sterile filter paper. EMM agar plates with or without supplements are used for screening amino acid auxotrophs while YE agar plates with clonNAT are used for screening for cells with clonNAT resistance marker. YE agar plates with 5-fluoroorotic acid (5-FOA) are used to counterselect *ura4* -expressing cells because the *ura4* gene product in *S. pombe* (orotine-5'-monophosphate decarboxylase) converts 5-FOA to 5-fluorouracil, which is toxic. After 1-3 days incubation at 25˚C auxotrophs will show no growth in the absence of the required supplement.

4.1.4 Transformation

Transformation of *S. pombe* cells with foreign DNA was done after the following protocol previously described by Bähler et al. (1998) with slight adjustments. Cells were grown in 25˚C for two days and the fresh log -phase culture was used for transformation. OD_{595} was adjusted to 0.2-0.4 to achieve the preferred cell number pr transformation (2 – 4 x 10^8 cells / 100 µL). The expected recombination frequency after lithium acetate transformation of fission yeast is 10^4 to 10^5 per microgram DNA.

1) Spin down 50 ml cell culture at 1700 x g for 4 min.
2) Wash once with equal volume of MQ-H_2O. Spin down at 1700 x g for 4 min.
3) Resuspend the cell pellet in 1 mL of MQ-H_2O and transfer to Eppendorf tube. Spin down at 21 000 x g for 1 min.
4) Wash with 1 mL LiAc/TE. Spin down at 21 000 x g for 1 min.
5) Resuspend the cell pellet in 100 µL of LiAc/TE.
6) Add 2 µL of sheared herring testes DNA and 10 µL (100-300 ng) of transforming DNA and mix gently. Incubate at RT for 10 min.
7) Add 260 µL of 40% PEG/LiAc/TE and mix gently. Incubate at 25˚C for 30 min.
8) Add 43 µL of DMSO and heat-shock the cell suspension at 42˚C for 5 min. Spin down at 21 000 x g for 1 min.
9) Wash with 1 mL YES. Spin down at 21 000 x g for 1 min.
10) Resuspend in 0,5 mL YES. Transfer the cell suspension to 10 mL YES and incubate at 25 °C in shaking water bath for 2 hours (e.g. transformation with *ura4+* cassette).

    OR

    Resususpend in 0,5 mL MQ-H_2O. Transfer the cell suspension to 30 mL ½ YES + ½ MQ-H_2O and incubate at 25˚C ON.
11) Spin down the cells at 1700 x g for 4 min and resuspend in 1 mL YES.
12) Plate out to appropriate plates; 30 µl, 100 µl, 300 µl and 200 µl of non-concentrated culture (taken out before step 11).
13) Incubate at 25˚C for 6 days.
14) Replica plate or streak out to selective plates if necessary.

4.1.5 Synchronization of *S. pombe* cells

To study effects of UVC irradiation in different cell-cycle phases cells are synchronized before irradiation. In this study I have used temperature-sensitive strains (*cdc10-M17*) which means that they have a specific mutation in the transcription factor gene *cdc10* which is required for entry to S phase. This mutant gene functions normally at the permissive temperature (25˚C), but becomes inactive and cells cannot enter S phase at the non-permissive temperature (36^{o}C).

Cells are first grown in 25˚C to log phase over two days. Cultures are then shifted up to 36˚C for one generation time. Meanwhile, cells will proceed until G1 and then arrest the cell cycle. The generation time in YE medium is shorter than that in EMM and there is also some differences in generation times between different strains. Too long time in restrictive temperature leads to leakage from the arrest. Because *cdc10* mutants still continue to grow, they become abnormally large and most of the cells finish the cytokinesis during the arrest. Optimal length and efficiency of the arrest for each strain can be confirmed with flow cytometry, which is able to separate cells in different cell-cycle phases based on measured DNA content and light scattering (see 4.1.9.). See appendix 3-5 for flow cytometry analyses.

4.1.6 UVC -irradiation of S. *pombe* cells in G1 phase in solid medium

This method is used to compare survival rate of different fission yeast strains after UVC irradiation in G1.

Cells were grown in liquid YE medium at 25˚C for two days. OD_{595nm} of the fresh log-phase cultures was adjusted to 0.25 and cultures were incubated further at 36˚C to arrest cells in G1 before UV irradiation (see 4.1.5 and appendix 3).

3-fold dilution series were pipetted to a microtiter plate with a flat bottom. These samples were then spotted with a 48-pinned device to four air-dried YE plates and irradiated (UV crosslinker, Hoeger): 0 J/m^2 (control), 50 J/ m^2, 100 J/ m^2, 200 J/ m^2. The plates were incubated at 25˚C 5-6 days.

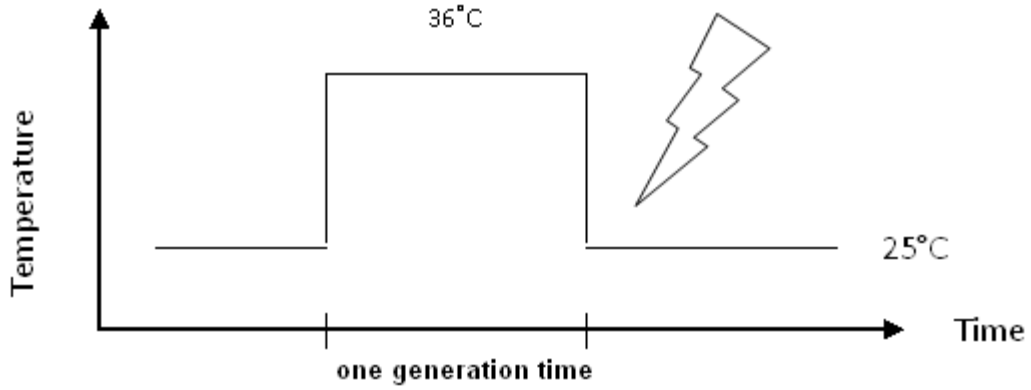

Figure 4.2. UVC irradiation of the cells synchronized with *cdc10* block. Cells are incubated at restrictive temperature, 36˚C, for one generation time and irradiated immediately after release to permissive temperature, 25˚C.

4.1.7 UVC -irradiation of S. *pombe* cells in G1 phase in liquid medium

In this study, cells were irradiated in liquid medium when the cell culture was used to collect samples for immunoblotting, microscopy, flow cytometry, and dNTP measurement.

Cells were grown in liquid medium as described in 4.1.1. The preculture in YE was gradually diluted into EMM. YE contain high concentrations of amino acids and other macromolecules which absorb UV light and may decrease the irradiation dose absorbed by the cells. Therefore, EMM is used as a standard medium for irradiation in our lab. Synchronization of the cell culture was done as described in 4.1.5. and the cells were irradiated immediately after release from *cdc10* block (figure 4.2.). The OD_{595nm} of the cell culture was adjusted to 0.15 - 0.3 before irradiation. Liquid culture was poured to a Petri dish and irradiated under constant stirring. A Petri dish with appropriate size to the volume of the culture was used as the thickness of the liquid layer should be 3 mm.

UVC irradiation at 254 nm was used (Sylvania Fluorescence Lamp, UVC light). The intensity of the UVC light (W/m^2) was measured with UVX radiometer (AH Diagnostic) to be able to calculate the duration of irradiation. In this study, the standard dose for fission yeast, 1100 J/m^2, was used.

4.1.8 Sensitivity to hydroxyurea

Fission yeast cells are sensitive to hydroxyurea with concentration-dependent manner. This property can be used to select for specific mutants by a simple plate assay. Deletion of *cid13* is one of the mutations leading to HU sensitivity at relatively low concentrations when wt cells still grow well (Read et al. 2002; Saitoh et al. 2002), and this knowledge is used in this study.

1) Grow a preculture in 10 mL YE as described in 4.1.1.
2) On the third day of inoculation, adjust the OD_{595nm} of the cell culture to 0.3 and prepare a 5-fold dilution series.
3) Pipette 8 µL cell-suspension to YE plates containing 5 mM or 7 mM HU.
4) Incubate for 5 days at 25˚C.

4.1.9 Flow cytometry

Flow cytometry is a technique for counting, examining, and sorting microscopic particles, as cells, suspended in a stream of fluid. Flow cytometry uses the principles of light scattering, light excitation, and emission from fluorescent molecules. When the cells intercept the beam of exciting light they scatter light and the fluorochromes are excited to a higher energy state. This energy is released as a photon of light at a specific wavelength and converted to electrical pulses by optical detectors. The acquired data can be analyzed by flow cytometer software.

Flow cytometers use the principle of hydrodynamic focusing for presenting cells to a laser (or other light source). The sample is injected into the center of a sheath flow. The combined flow is reduced in diameter, forcing the cell into the center of the stream, allowing precise alignment of the jet of cells and the exciting light. (figure 4.3.)

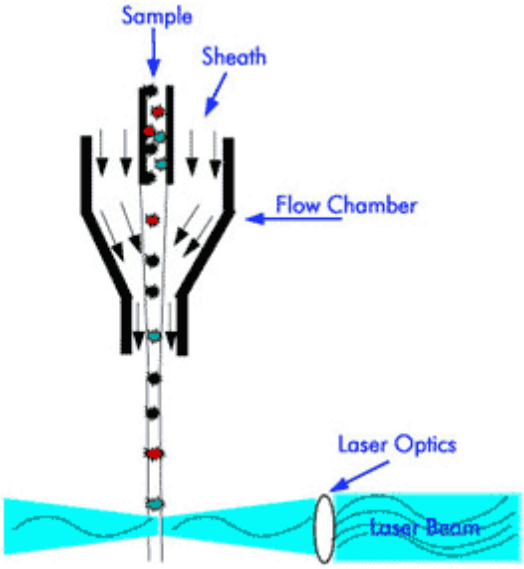

Figure 4.3. A scematic drawing of the flow chamber and the laser beam in the sensor area (http://biology.berkeley.edu/).

A new analysis method for *S. pombe* cells was recently published by Knutsen et al. (2011). It is based on the measurements of the width as well as the total area of the DNA-associated fluorescence signal which allows the discrimination between cells in G_1 and in G_2 phase that have two and one nuclei, respectively. Therefore, the cell-cycle progression of fission yeast can be followed in detail. This method is used in this study to follow the synchrony of the cell cultures when arrested in G1 and the cell-cycle progression after the arrest (see Appendix 3).

In this study, flow cytometry was also applied to monitor the expression levels of GFP-tagged proteins (see 5.4.2 and appendix 4).

The following protocol was used to prepare cell samples for flow cytometry:

1) Take 1 mL of logarithmically growing cell suspension and centrifuge at 21 000 x g for 2 min. Alternatively, take 500 µL of methanol fixed cells (resuspended in PBS) and centrifuge at 21 000 x g for 2 min and proceed directly to step 4.
2) Discard the supernatant and resuspend the cells by adding 1 mL ice cold 70% ethanol while vortexing. Samples can be stored in the fridge.
3) Take 500 µL of the sample over to a new Eppendorf tube and centrifuge at 21 000 x g for 2 min.
4) Discard supernatant and resuspend pellet in 1.0 mL 20 mM EDTA. Centrifuge at 21 000 x g for 2 min.

5) Discard supernatant and resuspend pellet in 1.0 mL 20 mM EDTA. Centrifuge at 21 000 x g for 2 minutes.
6) Discard supernatant and resuspend pellet in 0.5 mL 20 mM EDTA containing 0.1 mg/mL DNAse-free RNase A and incubate at 36˚C ON.
7) Add 0.5 mL 20 mM EDTA containing 2 µM Sytox Green; final concentration of 1.0 µM Sytox Green in sample. NB! When analyzing GFP-tagged cells Hoechst 33258 is used; final concentration of 5 µM Hoechst in sample.
8) Transfer the samples to 5 mL plastic tubes and sonicate in a water bath for 5 min.
9) Run the samples (LSR II Flow Cytometer, BD Bioscience) as described in the core facility manual.

4.2 DNA methods

4.2.1 Genomic mini-prep

The following procedure was used to isolate genomic DNA from *S. pombe* cells to use as a template DNA for PCR.

1) Grow a 2 mL culture to late-logarithmic phase in YE.
2) Pellet at 21 000 x g for 1 min.
3) Wash once with STOP buffer or ice cold water.
4) If STOP buffer was used, wash once with citrate/phosphate/EDTA/sorbitol.
5) Resuspend cells in 1.0 mL citrate/phosphate/EDTA/sorbitol containing 2.5 mg Zymolase. Transfer to an Eppendorf tube and incubate at 37˚C for 30 minutes. Check for ghosts by adding a drop of 10% SDS on the microscopy slide; 1µL SDS to 9 µl of the digested cells.
6) Pellet cells at 21 000 x g for 10 seconds. Remove the supernatant.
7) Resuspend the pellet in 0.5 mL TE.
8) Add 25 µL 20% SDS, mix by inverting tube several times; do not vortex. Incubate at 65˚C for 15 minutes.
9) Add 175 µL 5M potassium acetate (pH 5), vortex well and keep on ice for 15 min.
10) Centrifuge at 21 000 x g for 10 min at 4˚C.
11) Transfer 0.5 mL of the supernatant to another Eppendorf tube.
12) Add 0.5 mL ice-cold 2-propanol (isopropanol) and mix.

13) Pellet by centrifuging at 21 000 x g for 10 min at 4˚C.
14) Remove all of the supernatant.
15) Wash pellet with 500 µl of 70% EtOH. Centrifuge at 21 000 x g for 5 min at 4˚C. Remove the supernatant.
16) Let the pellet air-dry before resuspending in 40 µL TE.
17) Run 10 µl on agarose gel to check the quality of your DNA.

4.2.2 Polymerase Chain Reaction (PCR)

PCR is a rapid technique to amplify a specific DNA sequence in an enzymatic reaction. It is very sensitive so very little starting material is needed. Two oligonucleotide primers that flank the region of double-stranded DNA to be amplified must be complementary to a sequence in the opposite strand.

In the first step the double-stranded DNA is heat-denaturated to obtain single strands to which primers can bind. In the second step the temperature is decreased to allow the primers to anneal. In the third step these primers are extended by DNA polymerase at a temperature optimal to polymerase used. Primer extension occurs in the 5' → 3' direction in the presence of all four deoxyribonucleotides. Because of the high temperature used in the denaturation step only heat-tolerant DNA polymerases can be used. These three steps are repeated 20-40 times resulting in an exponential amplification of the sequence of interest.

In this study two different PCR kits were used when trying to find the optimal conditions for each reaction to occur. Denaturation, annealing and elongation times and temperatures are dependent on the template/product composition and length, and the DNA polymerase used. BioRad C100 Thermal Cycler was used to run PCR in this study.

Amplification and integration of GFP + clonNAT tag

The DNA sequence for GFP + clonNAT tag was amplified by PCR. The template and primers are described in figure 3.1.B and table 3.2., respectively.

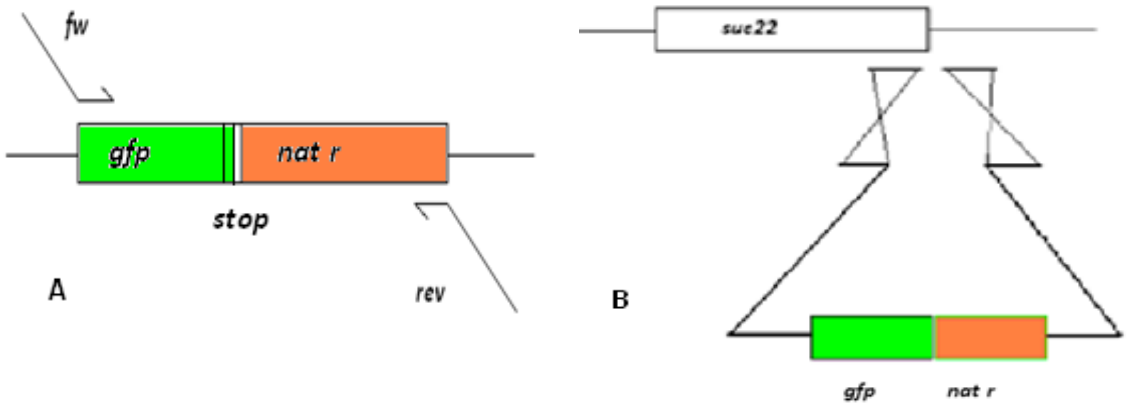

Figure 4.4. PCR-based gene targeting. **A)** A DNA sequence containing *gfp* and *nat*^{r} was amplified from a plasmid (see chapter 3.2.) by PCR. The forward primer consists of a 80 nt long targeting tail homologous to the 3' end of *suc22* and a 20 nt long sequence complementary to the *gfp* 5' end. The reverse primer has a similar 80 nt targeting region homologous to sequence immediately downstream of suc22 and 20 nt long sequence complementary to 3' end of nat^{r}. The amplified sequence have a length of 2494 nt. **B)** Targeting the amplified DNA sequence with homologous recombination. The resulting strains will carry the GFP tagged *suc22* gene and a resistance gene for clonNAT. Drawings are not in scale.

Replacing clonNAT marker with **ura4+** *cassette*

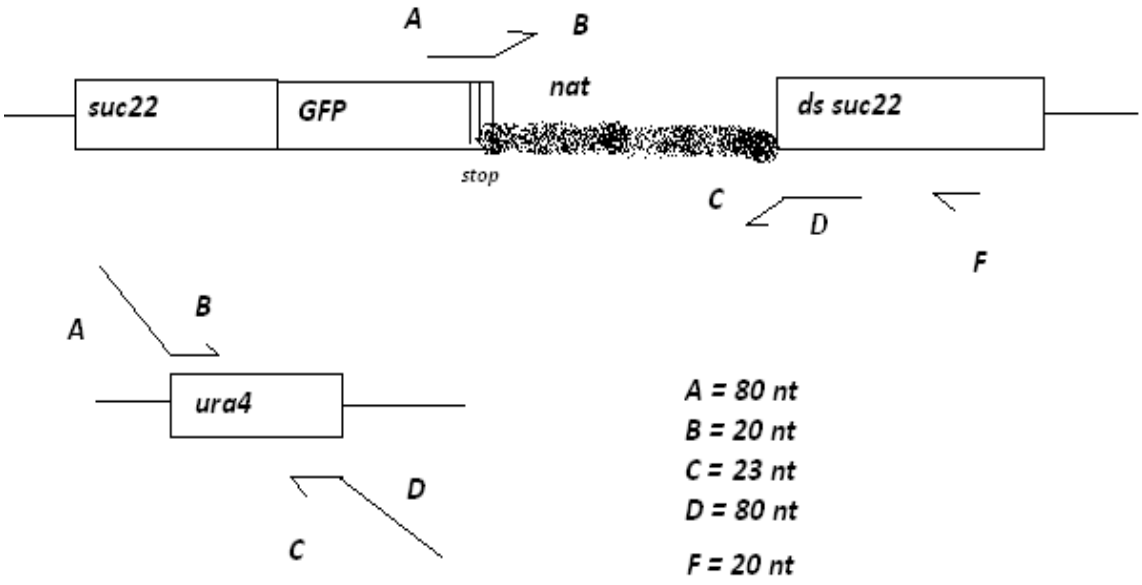

Figure 4.5. (previous page) The primers for amplifying *ura4+* and how they are designed. Primer sequences and template are shown in table 3.3. and figure 3.1., respectively. Both primers consist of two parts to be able to anneal and target the DNA correctly. A + b primer has a long tail (part A) targeting to 3' end of *gfp* including the translation stop codon for the fusion protein suc22-GFP and the rest of the primer is equal to *ura4+* sense strand at the 5' end (part b). c + D primer has a similar structure with a long tail (part D) targeting to downstream sequence of *suc22* (*ds suc22*) and the other part is equal to *ura4+* antisense strand at the 3' end (part c). PCR-product is 1212 + 160 nt (*ura4+* and primers, à 80 nt) = 1332 nt long. Note: primer F is used in the next step (figure 4.6).

Removing* ura4+ *from suc22-GFP sequence

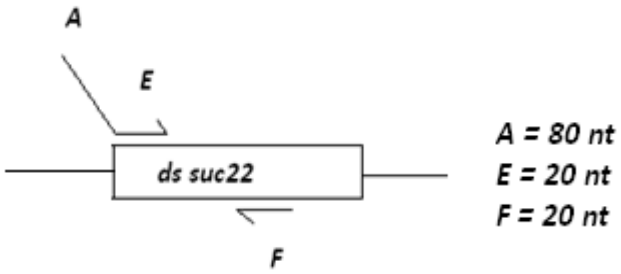

Figure 4.6. Primers to amplify the wild type sequence to remove *ura4+*. The wt genomic DNA was used as a template to amplify the targeting sequence. Primer sequences are described in table 3.4. The forward primer consists of two parts, **A + e**, where **A** is complementary to the very end of the GFP gene and part **e** targets the 5' end of the *suc22* downstream sequence. Reverse primer targets further down in *ds suc22*. When the cells are transformed this sequence will recombine with the host DNA and remove *ura4+* from that. The PCR product is 354 + 80 nt = 434 nt long.

4.2.3 Agarose gel electrophoresis

Agarose gel electrophoresis is used to separate DNA fragments in an electric field. Negatively charged DNA molecules will migrate towards the positive electrode when an electric current is applied. Agarose gels are usually capable of resolving differences around 50 nucleotides depending on the size of the DNA fragments and the concentration of agarose; a higher percentage of the agarose will separate smaller DNA fragments. Smaller fragments will migrate faster than large fragments. Agarose gel electrophoresis can also be used to identify and purify a DNA fragment of interest. 1% agarose gels were used in this study.

The gel is stained with the fluorescent nucleic-acid stain GelRed to visualize the DNA bands under 365 nm UV light (ChemiGenius Bio Imaging System, Syngene).

1) Prepare and cast a gel in a gel chamber.
2) Remove the comb and fill the chamber with electrophoresis buffer (1xTAE).
3) Mix DNA samples with 6x loading buffer before loading onto the gel. Load the molecular weight standard to be able to approximate the size and DNA concentration of the samples.
4) Run the gel at 80-120V for 45-60 minutes.
5) Remove the gel from the electrophoresis chamber and incubate in GelRed (diluted 1:10 000) for at least 20 minutes before imaging.

4.2.4 Purification of DNA

DNA samples must be purified after PCR or other enzymatic reactions to remove primers, unbound nucleotides, and enzymes. Both the QIAquick PCR Purification Kit and manual purification were used in this study. The purification kit was used to purify genomic DNA after the mini-prep (4.2.1.) and manual purification was used to purify PCR products (4.2.2.).

Protocol for manual purification of DNA:

1) Collect the PCR-amplified DNA in a 2 mL tube and measure the volume.
2) Add 1/10 volume 3 M NaAc (pH 5.2).
3) Add 2.5 volume 96% EtOH.
4) Centrifuge at 21 000 x g for 25 min at 4˚C. Remove the supernatant.
5) Wash the pellet with 500 µL of 70% EtOH. Centrifuge at 21 000 x g for 10 min to get a good pellet. Remove the supernatant.
6) Dry pellet thoroughly before resuspending it to MQ-H_2O. (For example: if start volume is 500 µL, resuspend DNA to 32 µL H_2O).
7) Run 2 µL on an agarose gel to make sure you got a right product.
8) Store the DNA at -20˚C.

4.2.5 Restriction analysis

Restriction enzymes are endonucleases which cleave double-stranded DNA within a specific recognition sequence. Using a known restriction enzyme it is possible to foresee the length of the resulting DNA sequences. It is important to use a buffer that is compatible with enzyme activity. This information is provided by the producer. Sometimes BSA is added to the reaction mixture to enhance the enzymatic activity.

In this study restriction analysis was applied to verify one PCR product which showed an unexpected migration length in agarose gel. The following 10 µL reaction mixture was set up and incubated for 30 minutes at 37˚C:

1 µL	purified DNA
1 µL	BSA (10x)
0.5 µL	XmaI restriction endonuclease
1 µL	NEBuffer #4
6.5 µL	H_2O

After incubation the reaction mixture was analyzed by agarose gel electrophoresis.

4.3 Protein methods

4.3.1 TCA extraction of proteins

TCA (trichloroacetic acid) precipitation of total cell protein is a widely used method.

1) Add 300 µl of acid-washed glass beads and 200 µl 20% TCA.
2) Ribolyze 9 x 30 s at a speed 6.5 (FastPrep FP120 ribolyzer, Thermo Scientific), cool down 20-30 s between each run.
3) Check cell breakage under the microscope. Ribolyze several rounds if needed.
4) Add 400 ul 5% TCA.
5) Put a 1.5 ml screw cap tube in the bottom of a 15 ml falcon tube. Puncture the bottom of the ribolyzer tube with a needle (ø 0.5mm) and set it on top of the 1.5

ml screw cap tube. Centrifuge at 1700 x g for 2 minutes. Glass beads will stay in the upper tube.

6) Retrieve the screw-cap tube from the bottom of the Falcon tube with tweezers. Discard the tube with glass beads. Put the lids on the screw-cap tubes and centrifuge at 21 000 x g for 10 min.
7) Discard supernatant (use suction).
8) If samples will be analyzed with BCA Protein Assay Kit (4.3.2), resuspend the pellet in 300µl resuspension buffer.

   OR

   If samples will be run on the SDS-PAGE without concentration measurement, 200µl of 1 x denaturing sample buffer is added.
9) Boil the samples at 95˚C for 3-5 min. Centrifuge for 1 minute at 21 000 x g. Use the supernatant.
10) Store the samples at -80˚C or continue to SDS-PAGE.

4.3.2 Protein concentration measurement with BSA Protein Assay Kit

Total protein concentration in TCA-extracted samples can be measured with BCA Protein Assay Kit (Thermo Scientific). This kit takes advantage of reduction of Cu^{2+} to Cu^{1+} by protein in an alkaline medium and detection of the purple-colored reaction product (Cu^{1+}/BCA complex) after adding a reagent which contains bicinchoninic acid. The amount of reduced Cu is proportional to the amount of protein in the solution. This purple-colored solution absorbs light at the wavelength of 562 nm which can be measured by using a spectrophotometer.

A standard curve was created using known concentrations of BSA and measurement was done after the instruction from the manufacturer.

4.3.3 SDS-PAGE

SDS-polyacrylamide gel electrophoresis, SDS-PAGE, for short, is used to separate proteins according to the molecular weight. To eliminate the effect of different secondary and tertiary protein structures and charges, protein samples must be denatured and treated with a detergent. SDS is both a denaturing agent that binds to proteins and also gives

them a uniform negative charge. In addition, the reducing agent dithitreitol (DTT) is added to samples to disrupt the disulfide bonds that stabilize proteins. When electric field is applied to the gel all proteins starts to migrate towards the anode.

The migration of proteins in the electric field is affected by the size of the protein and the size of the pores in the gel. Pore size is dependent on the concentration of polyacrylamide. Small molecules will migrate faster than large molecules and the migration velocity is inversely proportional to the logarithm of the molecular weight.

Gels with both uniform and gradually chancing polyacrylamide concentration are available. It is important to use a gel with appropriate pore size according to the protein(s) of interest. The uppermost part of the gel has a higher concentration of polyacrylamide than the rest of the gel. This part is called stacking gel and it concentrates the loaded sample before entering to the separating gel. SDS-PAGE can also be used to estimate the molecular weight of the protein.

In this project, 10% pre-cast gels were used. (Exception: see 4.4.6 for casting and running the polyacrylamide-urea gel for dNTP measurement.)

Preparing samples for SDS-PAGE

If protein concentration of the samples is measured with BCA Protein Assay Kit (4.3.2) and the sample is resuspended in resuspension buffer, the following protocol is used:

1) Boil the samples in 95˚C for 3-5 min. Centrifuge for 1 minute at 21 000 x g. Move the supernatant to a new tube.
2) Pipette a volume equal to 10-30µg protein (depending of the experiment) to a 250µl tube, add MQ-H_2O to 12µl.
3) Mix one volume of loading buffer and one volume of 2.5M DTT. Add 3µl of that to each sample (= total sample volume 13µl).

When BCA Protein Assay Kit is not used, but equal volume of each sample is loaded to the gel in the first round, following protocol is used:

1) Resuspend the protein pellet in 200µl of 1x denaturing sample buffer.
2) Boil the samples ata 95˚C for 3-5 min. Centrifuge for 1 minute at 21 000 x g. Use the supernatant.
3) Load 10µl of each sample to the gel.

Running the SDS-PAGE

1) Assemble the gel chamber (BioRad) and fill with 1x running buffer between the gels and leave it for a couple of minutes to find out whether the buffer is leaking. If that is the case, the gel(s) must be mounted tighter.
2) Remove the comb from the gel and remove air bubbles from the wells with a syringe.
3) Load the molecular weight ladder to the first well.
4) Load the samples.
5) Fill the chamber with 1x running buffer until the anode.
6) Run in 160V for 50 min (BioRad Power Pac 200) or until the color front has ran out of the gel.
7) Disassemble the gel chamber. Remove the stacking gel and the gel front and soak the gel in transfer buffer for 15 min before continuing to the blotting step (4.3.4).

4.3.4 Semi-dry protein blotting

Immunoblotting is a method to transfer proteins from a gel to a membrane by an electric field. Proteins have negative charge because of the SDS added earlier so they migrate towards the anode. The transfer buffer contains methanol which increases the binding of proteins to the membrane and increases elution of SDS from the gel. Semi-dry blotting is used for proteins up to 100 kDa in size.

The membrane type must be chosen according the transfer system used. PVDF membranes were used in this project.

1) Soak the membrane in MetOH for 10 seconds and leave it to MQ-H_2O for 10 min.
2) Soak the gel, membrane and two thick filter papers in transfer buffer for 15 min.
3) Assemble the blotting sandwich as shown in the figure 4.7.
4) Run transfer for small gels in 15V for 40 min (BioRad Trans-Blot, Semi-Dry transfer Cell).

After the transfer the gel can be colored with Coomassie Blue to see how much protein is left in the gel. Likewise, the membrane can be reversibly colored with Ponceau S to detect the proteins in the membrane.

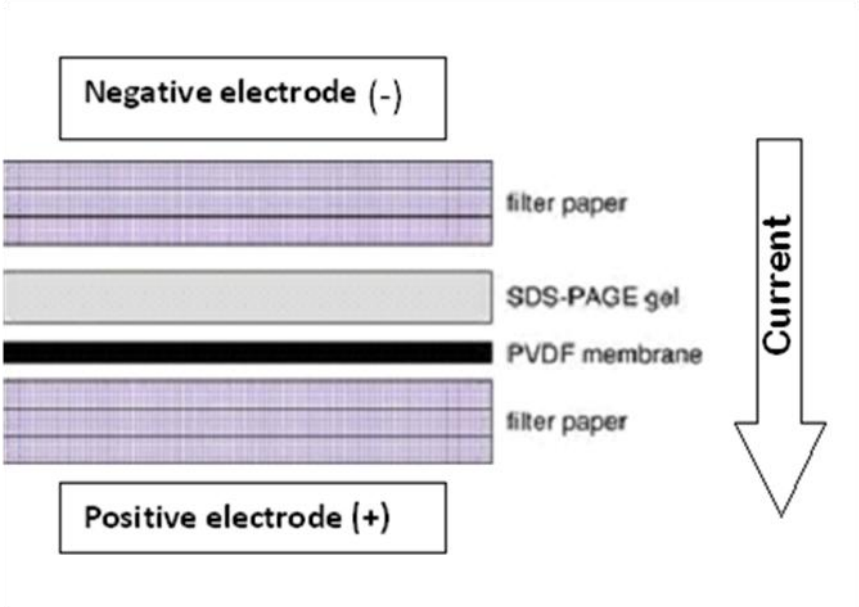

Figure 4.7. This figure shows the assembly of the blotting sandwich between the positive and the negative electrode. The arrow shows the direction of the current when the electric field is applied.

4.3.5 Immunodetection and visualization of proteins

After the transfer proteins are fixed and accessible for analysis. To be able to visualize the protein of interest on the membrane, specific antibodies are used. In this project indirect detection using two antibodies is applied.

To begin with, the membrane is blocked with a blocking agent to reduce nonspecific binding of antibodies to reduce the background. Common blocking agents contain BSA or non-fat milk which is mixed with TBS or PBS together with a detergent such as Tween-20.

After the blocking step the membrane is incubated with a primary antibody against the protein of interest. Excess antibody is then washed out and the secondary antibody is added. This antibody is the same for all primary antibodies from same species. The secondary antibodies used in this project are conjugated to alkaline phosphatase, an enzyme that, in the presence of its substrate ECF, catalyzes the formation of stable fluorophores which emit light when scanned by fluorescence imaging equipment (Chemi Genius, Syngene, VWR).

1) Block the membrane in 5% membrane blocking agent/TBS-T (TBS with 0,1% Tween) for 1 hour at RT.
2) Incubate the membrane with primary antibody, diluted to the appropriate concentration in TBS-T, overnight at 4˚C.
3) Wash the membrane 3 x 5 min with 5 mL TBS-T.
4) Incubate the membrane with secondary antibody, diluted to the appropriate concentration in TBS-T, for 1 hour at RT.
5) Wash the membrane 3 x 5 min with 5 mL TBS-T.
6) Put the membrane on a glass plate and remove the excess liquid with a paper towel before adding 1-2 mL ECF. Incubate for 5 minutes at RT.
7) Remove excess ECF with a paper towel or a filter paper.
8) Expose the membrane with transilluminator using EtBr filter.
9) Cover the membrane with aluminum foil and store in the fridge.

The membrane can be reprobed with another primary antibody for other purposes, like loading control.

1) Soak the membrane in methanol for 20-30 min. Rinse with MQ-H_2O.
2) Soak in TBS-T for 10 min.
3) Continue from the step 1. as described above.

4.4 Measuring dNTP pools with polymerase assay

This polymerase assay is described in detail by Roy et al. in 1999. It is based on the elongation of the ^{32}P 5’ –end-labeled oligonucleotide primers annealed to complementary oligonucleotide templates. Incorporation of dNTPs is catalyzed by the Klenow fragment

of *E. coli* DNA polymerase I. It is required that the amount of dNTP species to be analyzed is limiting resulting in reaction termination. Polymerase assay is very sensitive and allows quantification of low concentration of dNTPs. (Roy et al. 1999)

The wild type, *cid13Δ* and *gcn2Δ* cells were grown and UVC irradiated in G1 as described in 4.1.1. and 4.1.7. The cells were harvested 0, 30, 60 and 90 minutes after the irradiation.

This procedure consists of following steps:

1) Harvesting the cells to be analyzed.
2) The samples are normalized according to the ATP concentration. Standard ATP solutions are used to create a standard curve.
3) dNTP concentration (dATP in this study) is measured by polymerase assay which is based on elongation of radioactively labeled primers. These primers are annealed to a template specific for dNTP species to be analyzed.
4) The elongated primer/template fragments are separated by gel electrophoresis. Standard samples with known dNTP concentrations are used to create a standard curve for quantification.
5) The separated fragments are visualized and quantified. These results are adjusted according to the normalized values from the step 1.

This procedure was mainly run during one week visit at the University of Copenhagen in November 2011. Because of limited time frame amount of only one set of samples and one dNTP species (dATP) were analyzed.

4.4.1 Cell harvesting and ether extraction

The following protocol was used to harvest the cells and to remove TCA with ether. TCA must be removed properly as it destroys the enzymes used later in this experiment.

1) Filter 50 mL of the cell suspension under the vacuum (Millipore, Durapore HVLP membrane filter). Wash the membrane once with 50 mL ice-cold water.
2) Transfer the filter to a Falcon tube and rinse off the cells carefully with 500 µL 10% TCA/15 mM $MgCl_2$.
3) Transfer the cell suspension to 1.5 mL tube. Samples can be stored at -80˚C.

4) Sonicate the samples in the water bath at 4.5 for 15 s. Keep samples on ice during the rest of the procedure.
5) Centrifuge at 21 000 x g for 5-10 min. Take the supernatant over to a new tube (approx. 500 µL).
6) Add equal volume of diethyl ether, vortex 15 s.
7) Centrifuge at 21 000 x g for 1 min.
8) Remove the upper layer carefully to not to lose too much of the lower layer you are interested in.
9) Repeat steps 6.-8. seven (7) times. Samples can be stored at -80˚C.

4.4.2 ATP determination with Luciferase assay

To validate the amount of sample used further in this experiment, ATP level in all samples is measured. This is important to be able to compare results from different samples to each other in the end. Even if cell number is adjusted to particular OD when collecting cells, it is not accurate because of loss of sample on the way. Luciferase –assay (ATP Determination Kit, 3.7.) can be used to quantitative determination of small amounts of ATP. The assay is based on the following reaction:

$$Luciferin + ATP + O_2 \xrightarrow[mg2+,\ luciferase]{} oxyluciferin + AMP + pyrophosphate + CO_2 + light$$

Luminescence is measured with a luminometer giving a specific value for each sample. Standard ATP solutions are used to generate a standard curve to calculate ATP concentration in the analyzed samples.

4.4.3 Primer labeling and purification

22 nucleotides long synthetic oligonucleotide is used as a primer (p22; see 3.2.2. for primer sequence) and this oligo is labeled with radioactive phosphate, ^{32}P, at 5'-end. Labeling reaction is catalyzed by polynucleotide kinase (PNK) which is able to transfer the terminal phosphate (γ-^{32}P) of ATP to the 5′-hydroxyl terminus of a DNA molecule. After labeling reaction the primer is purified in a Sepharose column. Unbound ^{32}P is retarded in the matrix and labeled primer is in flow through.

Set up the labeling reaction:

2 µL	p22 (10 µM stock)
6 µL	PNK-buffer (10x)
6 µL	^{32}P-ATP
14.5 µL	H_2O
1.5 µL	PNK

Incubate at 37˚C for 1 h.

Purify the labeled primer from the reaction mixture in Illustra AutoSeq™ G-50 MicroSpin™ column according to the kit instructions.

4.4.4 Template-primer annealing

To measure amount of dATP in the samples template tA is used (see 3.2.1. for template sequence). This template allows quantification of dATP in the samples. The first 22 nucleotides are complementary to primer p22 and the additional sequence consist of triplet repeat 3'-$(TAA)_4$-5'. tA and p22 are annealed together before proceeding to primer elongation.

2 pmol/µL stock solution of primer/template (p22/tA) complex is prepared to know amount of primer elongated in a later step of the procedure. Following reaction mixture with total volume of 130 µL is set up:

12 µL	purified p22 primer
2.6 µL	100 mM p22 primers (not labeled)
5.6 µL	100 mM tA template
52 µL	annealing buffer (2.5x)
58.2 µL	H_2O

Keep in 90˚C heat block for 2 min, switch of the heater and allow cooling down to RT (at least 30 min). Keep the solution in the cold room ON if you continue day after. Note that unlabeled primer is added to the reaction mixture to get big enough volume to start the reaction.

4.4.5 Klenow dNTP reaction

This step of the procedure is the actual polymerase reaction where the elongation of the labeled primers with dNTPs occurs. Single-stranded end of the template, 3'-$(TAA)_4$-5', is filled with available dNTPs. As mentioned earlier, amount of dNTP species analyzed must be limiting while the other dNTP species must be added in excess to allow effective elongation to occur. In this study, dATPs were measured and dTTPs were added in excess.

For later quantification, standard solutions of dNTP mixture and dTTPs were used to make a standard curve.

1) Prepare reaction premix for 20 samples (20x):

	1x	20x
dNTPs / cell extract (= standard dNTPs / my sample)	10 µL	0
10x Klenow buffer (NEB#2)	2 µL	40 µL
100 pmol dTTP (100 µM stock)	1 L	20 L
Primer/template (p22/tA)	1.5 µL	30 µL
Klenow polymerase mix	1 µL	0
H_2O	4.5 µL	90 µL

2) For each sample, use either 10 µl cell extract or less cell extract and add H_2O to 10 µL. Add 9 µl reaction premix.
3) Make Klenow polymerase mix:

H_2O	25.6 µL
10x Klenow buffer (NEB#2)	3 µL
Klenow polymerase	2.4 µL

4) Add 1 µL Klenow mix to each sample and incubate at 27˚C for 20 min. Stop the reaction by incubating at 75˚C for at least 10 min.

5) Centrifuge shortly just to remove liquid from the lid after the heating.
6) Dry the samples in the speedwac (Eppendorf Concentrator 5301) with open lids for 30-45 min at 45˚C and resuspend the pellet in 12 µL of loading buffer. Samples can be stored at -20˚C at this stage.

4.4.6 Casting the polyacrylamide-urea gel and running the electrophoresis (PAGE)

This chapter is based on the same principle as SDS-PAGE described in 4.3.3, but in this protocol the gel is prepared manually. The electrophoresis using a large polyacrylamide-urea gel can separate DNA molecules with one nucleotide difference in length. In this study the Dedicated Height Sequencing Kit (C.B.S. Scientific Company) was used to run the electrophoresis.

A large gel is cast between two glass plates by pouring the liquid gel solution between the plates. To solidify the gel APS and TEMED are used as additives. APS create a radical which starts a polymerization chain reaction while TEMED stabilizes free radicals and improves polymerization. Before loading the samples the gel is preheated to avoid uneven migration of the samples.

Start with preparing the polyacrylamid-ura gel (10% PA / 1xTBE / 8M Urea):

1) Prepare first 100 ml of following solution and stir until urea is dissolved (takes 30-45 min) and add H_2O to 100 ml.

Urea	48 g
10x TBE	10 mL
33% PA	33 mL
H_2O	5 mL

2) Meanwhile, clean the big glass plates and set up a gel chamber with thin spacers between the plates and seal them together.
3) First, take 1.5 mL of urea/TBE/PA solution and add 1 µL TEMED and 10 µL APS. Use it immediately to seal the gel chamber inside to avoid leakage;

pipette 500 µl to each side of the chamber and wait until the solution reaches the bottom. Then you have 500 µl left in your tube and when that has solidified, the sealing is also solid. Then you can cast the gel.

4) Take the rest of the urea/TBE/PA solution (98.5 mL) and add 40 µL TEMED and 400 µL APS. Cast the gel immediately.
5) Set the gel chamber to the bench and lift the open side a little and start pouring carefully from the one corner all the time. This let the air come out of the chamber while it is filled with the gel. You may not need all the solution to fill the chamber.
6) Place the comb on top and seal the top with plastic film to avoid gel to dry while it is solidifying. When the rest of the solution has solidified, your gel is also solid.

Preparing the samples:

1) Put the samples with loading buffer on the heating block and set it to 90˚C and let it warm up. When temperature is around 50-60˚C, go through all samples and pipette up and down a couple of times as the dry pellet may not have dissolved properly. When the heat block reaches 90˚C, wait for 2 min and switch it off.
2) Carry your samples in the heat block to your preheated gel (1-3 hours at 2100 V) and load.
3) Run the gel at 2100 V for two to three hours.

Fixing and drying the gel:

1) Prepare the gel fixation buffer. Mix well.

H_2O	800 mL
Acetic acid	100 mL
MetOH	100 mL

2) Remove the inner/smaller glass plate very carefully as the gel is very thin. Put the glass plate with the gel into the buffer-bath and let it soak for about 5 min. Fixation buffer fixes the DNA to the gel and also removes urea from the gel. Urea makes the gel very fragile when the gel is dried. Lift up the glass plate with the gel and dry it a little with a filter paper. If the paper gets very wet, take a new one and tap especially in the corners in order to gel to stick to the filter paper. Then you are able to turn it around slowly and end up with the gel on the paper.

3) Put a dry filter paper to the gel dryer plate (Gel Dryer, Bio Rad) and the paper with the gel on top of it. Then, cut a piece of the plastic film and put it on top of the gel. Put the lid down and open the vacuum a little. Lift the lid carefully just to check that vacuum is created.

4) Let the gel dry under vacuum for 1h 40min.

5) When finished, shut down the vacuum first. Open the lid and lift one corner of the thick plastic carefully just to release the vacuum. Then lift the whole plastic and remove the thin plastic film carefully. The gel should be stuck on the filter paper under it. Move the paper with the gel to Storage Phosphor Screen.

4.4.7 Visualization and quantification of DNA

Samples labeled with 32P can be visualized by exposing the gel to photostimulable storage phosphorimaging plates (Storage Phosphor Screen) overnight. High energy radiation excites electrons in the plate resulting in an absorption band around 600 nm. Scanning of the plate with a helium-neon laser at 633 nm stimulates the electrons to return to the ground state and releases a photon at 390 nm. The intensity of that luminescence is recorded and stored as a digital image. The image is then analyzed with appropriate software (Total Lab Quant was used in this study). This imaging method is very sensitive and the imaging plates can be reused after exposing them to bright visible light.

When calculating the results the bands in each line are integrated. Radioactivity in each band and in each lane totally is determined. In each primer, dNTP can be incorporated

into one of three positions corresponding to the triplet-repeats (TAA) in the template leading to both aborted and full size products. Number of moles of elongated primer is proportional to the radioactivity in each band.

A formula for calculating amount (pmol) of dATP incorporated per pmol of primer/template complex (p22/tA in this study):

(band1+b2+b3) + 2 * (b4+b5+b6) + 3 * (b7+b8+b9) + 4 * (b10+b11+b12)

Where b = band and band number corresponds to the band for the first incorporated dNTP. As 3 pmol of p22/tA was used in this study, the sum is multiplied by three (3).

Standard samples are quantified first and standard curve with regression equation is created. This equation is used to calculate the input (= amount of dATP) in my samples. Then the pmol dATP/µl value for each sample is calculated (when 10 µL sample loaded into the gel, divide the input with 10). ATP concentration determined with luciferace assay is also recorded in pmol/µL so the ratio between dATP and ATP can now be calculated (dATP/ATP). This gives a specific value for each sample and these values are directly comparable with each other.

4.5 Microscopy

Several different microscopic techniques were used in this study. Light microscope (Axioscope, Zeiss, Germany) with 40x objective was used to follow the growth of *S. pombe* cells in liquid medium and to follow sporulation when performing genetic crosses. Phase contrast and fluorescence microscope (Leica DM6000B, Wetzlar, Germany) with 63x objective was used when studying GFP-tagged cells and nuclear staining with DAPI.

4.5.1 Methanol fixation of *S. pombe* cells

To study GFP-tagged cells in the fluorescence microscope the cells were fixed with methanol. The cell samples were collected at different time points so it was important to stop all cellular processes immediately and to be able to study those samples together later on. Polylysine slides with negatively charged, adhesive surface were used to achieve better attachment of cells to the slide.

1) Filter 3-5 mL of cell suspension in a Durapore HVLP filter (Millipore) and rinse the filter in a 50 mL tube with 10 mL ice cold methanol. Remove the filter and store the fixed cells in -20˚C.
2) Centrifuge the fixed cells at 710 x g for 8 min and remove the methanol. Resuspend the pellet in 1 mL PBS.
3) Spread 10 µl of cell suspension to a polylysine slide and let it dry. Put on a cover slip before analysis.

Samples can be DAPI-stained before analysis (see 4.5.2.).

4.5.2 DAPI staining

4'-6-Diamidino-2-phenylindole, DAPI, is a sensitive, fluorescent DNA-binding probe and can be used to stain both fixed and live cells. DAPI staining is used to visualize the chromosomes/nucleus under the fluorescence microscope. Its selectivity for DNA and high cell permeability allows efficient staining of nuclei with little background from the cytoplasm.

DAPI staining is a very easy method: Put a 2µL drop of DAPI solution on a cover slip and place it on top of the microscope slide with your sample. The sample is ready for analysis immediately.

5 RESULTS

5.1 Cell survival after UVC irradiation in G1

Our group has previously shown that Gcn2 is essential for the UVC-induced G1/S checkpoint. Our working hypothesis is that Gcn2 exerts its function partly by regulating RNR levels through Cid13. If Cid13 is indeed important for the response to UVC, a *cid13Δ* mutant is expected to be sensitive to UVC irradiation. To explore this proposition, I compared the survival rate of wild type, *cid13Δ*, *gcn2Δ* and *rad3Δ* cells after UVC irradiation in G1. The *rad3Δ* mutant strain is included in this experiment as a control. *rad3* is one of checkpoint genes (1.2.1.) and *rad3Δ* cells are known to be very sensitive to UVC irradiation (Bentley et al. 1996). Serial dilutions of synchronized cultures of the appropriate strains were spotted onto YE plates as described in chapter 4. 1. 5. Cells were exposed to four different doses of UVC, from 0 J/m^2 (non-irradiated cells) to 200 J/m^2. The highest dose given on a plate, 200 J/m^2, corresponds to the dose of 1100 J/m^2 given to the cells in liquid medium as measured by the survival rate of wt cells. The experiment was performed in three biological replicas, in two technical replicas each. Representative results are shown here.

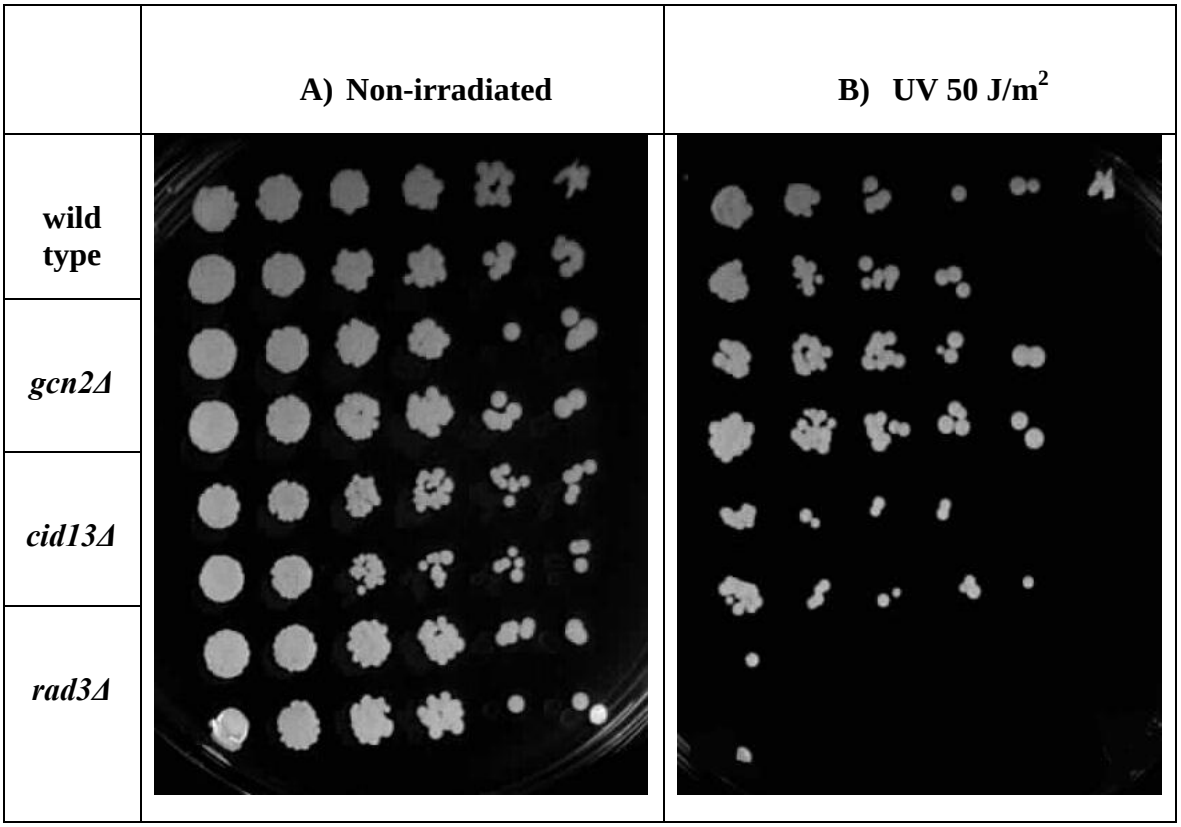

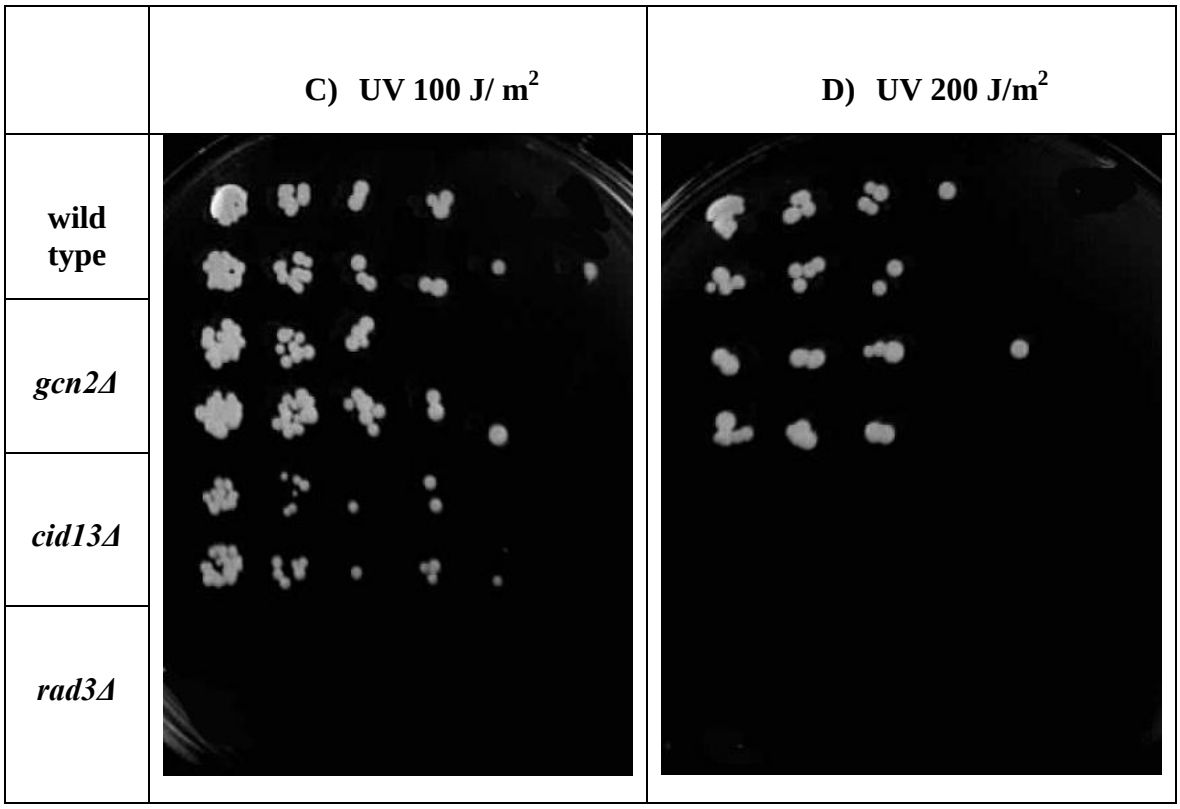

Figure 5.1. Survival of wild type, *gcn2Δ*, *cid13Δ* and *rad3Δ* cells after UV irradiation with 50 J/m^2, 100 J/m^2 and 200 J/m^2 compared to non-irradiated cells (A). All cell cultures were adjusted to OD_{595nm} = 0.25 which corresponds to a cell number of 5x10^6 / mL before arresting them in G1. 3-fold serial dilutions, starting with approximately 4x10^4 cells in the first spot, were spotted on YE (from left to right, two copies of each strain pr plate) and irradiated with UVC.

Wild type cells have a survival rate of approximately 15% when exposed to 200 J/m^2 of UVC on a plate. Very low irradiation doses, as 50 J/m^2, affect viability of wild type cells very little presumably because intact repair mechanisms are able to remove DNA damage efficiently. When the irradiation dose is increased cells begin to struggle in repairing more extensive damage. This tendency can be seen in all four strains.

Compared to the wild type cells *gcn2Δ* cells show equal or slightly lower survival in all irradiation doses after 6 days incubation at 25˚C while most of the *rad3Δ* cells lose viability already at dose of 50 J/m^2. *cid13Δ* cells survive less well than *gcn2Δ* cells when irradiated with medium or high dose of UVC, but they are clearly less sensitive to UVC than *rad3Δ* cells.

We conclude that *cid13Δ* cells are slightly sensitive to UVC irradiation in G1, which is consistent with the proposal that Gcn2 might contribute to regulating RNR levels through Cid13. However, *cid13Δ* cells are more sensitive than *gcn2Δ* cells, indicating an additional role(s) for Cid13.

5.2 The G1/S checkpoint in the absence of *cid13*

The G1/S checkpoint is thought to provide time for DNA repair before replication commences and consequently contribute to survival. Thus, one possible reason for the UV sensitivity of *cid13Δ* cells might be a deficient checkpoint response.

Therefore we investigated whether the deletion of *cid13* affects the time of entry into S phase after UVC irradiation in G1. Wild type, *cid13Δ* and *gcn2Δ* cells (see table 3.1. for genotypes) were analyzed.

Appearance of Cdc2 phosphorylation was used as a molecular marker for S phase entry (1.2.1.) after cells were released from the *cdc10* block. Phosphorylated Cdc2 was detected with an antibody specific for the phosphorylated form. This experiment was done in two biological and four technical replicas, out of which two were successfully completed. Cells were harvested every 30 minutes after the release from *cdc10* block for 120 minutes. Representative results are shown here.

A wild type #489

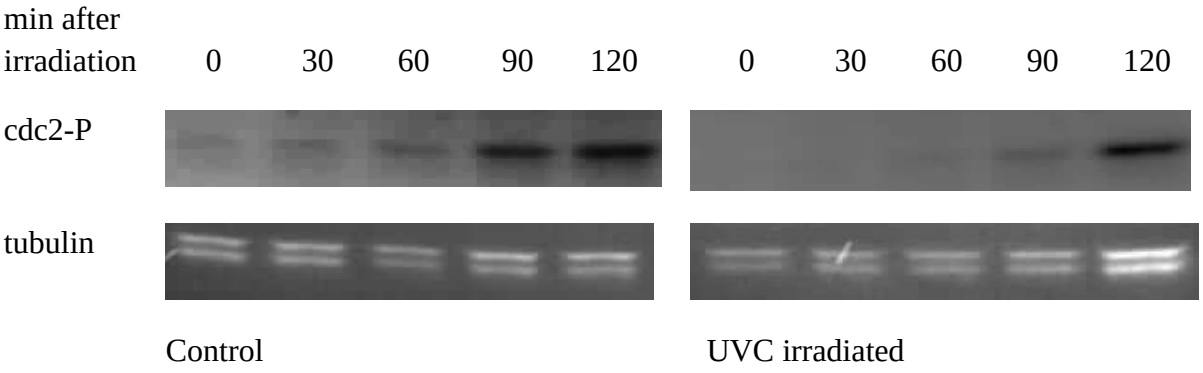

B ***cid13Δ*** **#1639**

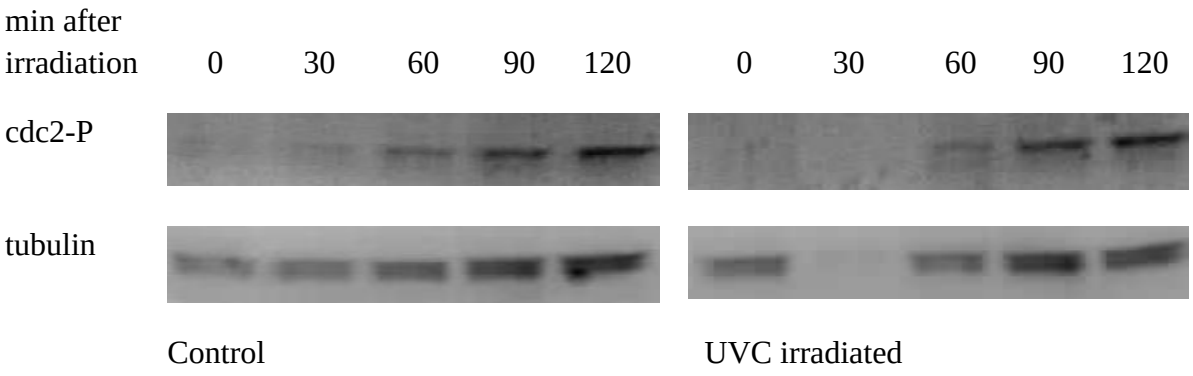

C ***gcn2Δ*** **#1138**

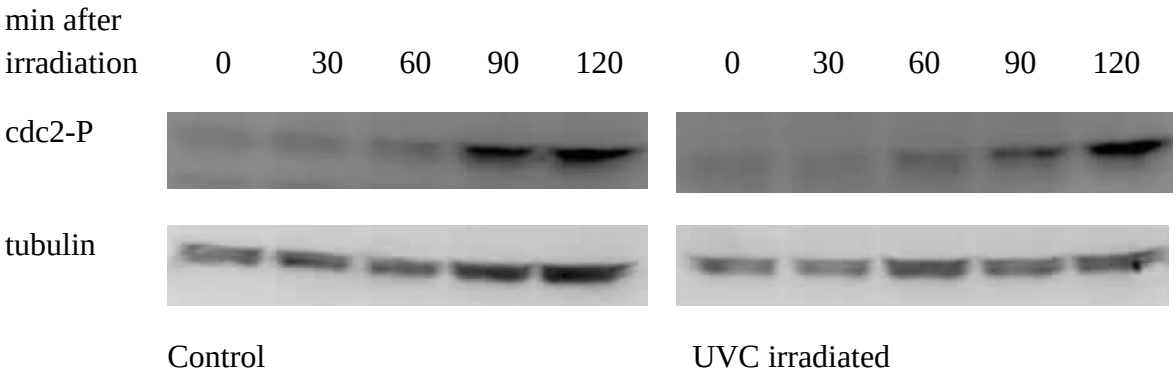

Figure 5.2. Appearance of phosphorylated Cdc2 after release from *cdc10* block. Tubulin is used as a loading control. A) wild type cells (#489). B) *cid13Δ* (#1639) cells. UVC 30min sample was lost in this blot, but the same sample gave no signal for cdc2-P in the other repeats. C) *gcn2Δ* (#1138) cells.

Unirradiated wild type cells enter S phase 60-90 minutes after release from the *cdc10* block and they delay entry into S phase by approximately 30 minutes, consistent with previous results (Tvegard et al. 2007). *gcn2Δ* cells enter S phase at the same time in control and UVC-irradiated cultures.

cid13Δ cells show similar kinetics as *gcn2Δ* cells as there is no delay seen in response to UVC in G1. We conclude that *cid13Δ* cells are deficient in the G1/S checkpoint, similarly to *gcn2Δ* cells. The checkpoint deficiency of *cid13Δ* cells is consistent with the notion that regulating Cid13 levels might be an important function of Gcn2.

5.3 Tagging of *suc22* in *S. pombe*

Since the only known target of Cid13 is the *suc22* mRNA, we decided to explore the hypothesis that after UVC irradiation, regulation of Suc22 levels and thereby the amount of dNTPs in the cells is an important function of Cid13 and, indirectly, of Gcn2.

To be able to study the subcellular localization and quantify the amount of Suc22 in *S. pombe* we tagged the Suc22 with green fluorescent protein, GFP, tag. This was performed by PCR-based gene targeting described by Bahler et al. (1998) which is based on amplifying the wanted sequence by PCR and transforming cells with this DNA (see 4.1.4. and 4.2.2.). The integration of the foreign DNA proceeds via homologous recombination. Therefore the primers used to amplify the GFP tag need to also contain sequences homologous to the target DNA. Furthermore, the primers have to be designed so that the two genes are in the same reading frame to be translated together to give a Suc22-GFP fusion protein. In addition to the GFP tag, an antibiotic resistance gene *nat*^{r} was inserted downstream of the Suc22:GFp construct to be used as a selection marker for transformed cells. *Nat*^{r} confers clonNAT resistance in *S. pombe* cells.

We were concerned that the clonNAT resistance marker may interfere with expression of Suc22-GFP as the marker is in between the fusion protein gene and potential downstream regulatory elements of *suc22*. The total transcript will be very long and it may happen that some transcripts do not become translated correctly. Therefore I decided to remove *nat* ^{r} marker before studying subcellular localization and measuring expression levels of Suc22. This proceeded in two steps described in 5.4.4. and 5.4.5. using PCR-based gene targeting.

The removal of *nat* ^{r} marker did not work despite several trials and thorough trouble shooting. The flow chart on the next page shows the whole tagging procedure including also the removal of *nat* ^{r} marker as it was planned. The description of this part of the work can be found in appendix 6.

Flow chart for tagging of Suc22 in *S. pombe*

Strain	Genotype	Procedure
#1138	*cdc10-M17 ura4-D18 gcn2::ura4+ h-*	
	⇩	Transform with *GFP:natMX6* at *suc22* ➔ Select for *nat*^{r}
#1673	*cdc10-M17 ura4-D18 gcn2::ura4+ suc22:GFP:natMX6 h-*	
	⇩	Cross with *cdc10-M17 suc22:GFP ura4-D18 h+* (1697wt) ➔ Select for *nat*^{s} and *ura4+*
#1693wt	*cdc10-M17 ura4-D18 gcn2::ura4+ suc22:GFP h-*	

#1639	*cdc10-M17 ura4-D18 cid13::LEU2+ h+*	
	⇩	Transform with *GFP:natMX6* at *suc22* ➔ Select for *nat*^{r}
#1674	*cdc10-M17 ura4-D18 cid13::LEU2+ suc22:GFP:natMX6 h+*	
	⇩	Cross with *cdc10M-17 gcn2::ura4+ suc22:GFP ura4-D18 h-* (1673wt) ➔ Select for *nat*^{s} and *ura4-* ➔ Check *cid13::LEU2+*
#1674wt	*cdc10-M17 ura4-D18 cid13::LEU2+ suc22:GFP*	

#1005	*cdc10-M17 ura4-D18 h+*	
	⇩	Cross with *cdc10M-17 gcn2::ura4+ suc22:GFP:natMX6 ura4-D18 h-* (#1673) ➔ Select for *nat*^{r} and *ura4-*
#1697	*cdc10-M17 ura4-D18 suc22:GFP:natMX6 h+*	
	⇩	Replace *natMX6* with *ura4+* ➔ Select for *ura4+* ➔ Screen for *nat*^{s}
	cdc10-M17 ura4-D18 suc22:GFP:ura4+	
	⇩	Loop out *ura4+* at *suc22:GFP* ➔ Select for *ura-*
#1697wt	*cdc10-M17 ura4-D18 suc22:GFP h+*	

5.3.1 Amplification and integration of GFP : clonNAT tag

The DNA sequence for GFP : clonNAT -tag was amplified by PCR as described in chapter 4.2.2. The template and primers are described in figure 1.3. and table 3.2, respectively. Both primers consist of 80 nt long targeting sequences, where homologous recombination with chromosomal DNA takes place, and 20 nt long priming sequences complementary to the amplified region.

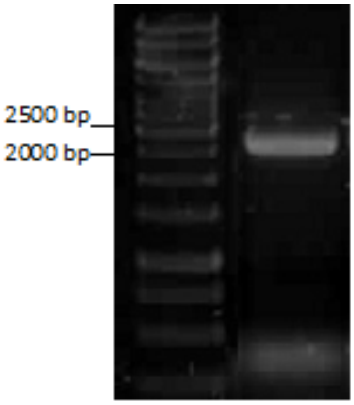

Figure 5.3. Amplified GFP : clonNAT tag was run on agarose gel (right lane) to confirm the right product. Length of the amplified sequence should be 2494 bp. Left lane: 1 kb ladder.

Strains #1005, #1138 and #1639 were transformed with this DNA as described in section 4.1.4. The cells were plated onto selective plates (YE + 100µg/ml clonNAT).

5.3.2 Checking the transformants

After incubating the cells on the selective plate only cells that carry the marker were able to grow. There is a possibility that the transforming DNA is maintained as a stable episome or integration to chromosomal DNA has occurred at other site as expected. This gives growth of false positive colonies on the selective plate, so the integration of the transforming DNA to the correct site must be further confirmed. This can be done by several alternative methods.

We decided to apply immunoblotting as described in section 4.3. Anti-GFP primary antibody was used to detect presence of the Suc22-GFP fusion protein. Suc22 protein has a molecular weight of 45.5 kDa and the GFP protein is 30 kDa. The fusion protein should give a band at 75 kDa. This band was seen in two of the transformed candidates; #1138-8 and #1639-2 (figure 5.4.). None of the #1005 candidates gave a band of the right size so we had to discard them and decided to make a tagged strain of #1005 by crossing it with one of the new strains with the tag.

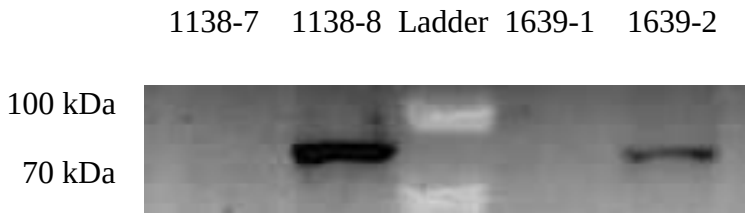

Figure 5.4. Western blot showing the 75 kDa band corresponding to Suc22-GFP fusion protein in samples 1138-8- and 1639-2. The other two samples serve as negative controls.

The strains 1138-8 and 1639-2 were examined further with a fluorescence microscope. Strains 1138-7 and 1639-1 were used as negative controls as they did not give any band in western blot (figure 5.4.).

Cells were stained with DAPI (see 4.5.2.) to visualize DNA. This is an important step as it makes it possible to confirm nuclear localization of Suc22-GFP fusion protein. Suc22 is nuclear during all the others cell-cycle phases than S so most of the cells expressing Suc22 should give a green signal in the nucleus and this can be seen in both candidates examined (figure 5.5.). Control cells do not have a GFP tag and do not give a green fluorescent signal (not shown).

To further confirm the presence of the tag and the wild-type -behavior of the fusion protein, hydroxyurea treatment was applied. Cells were incubated in 10 mM HU for two hours and analyzed after that. Hydroxyurea is an RNR inhibitor and it arrests the cells in S phase (see 1.4.). So, when the cells are incubated in HU, Suc22 is not imported back to nucleus but stays cytoplasmic. This should give a GFP signal scattered throughout the cytoplasm. As my cells showed this behavior it verified that the GFP doesn't significantly alter the Suc22 protein function and these cells could be used in further experiments (figure 5.5.). Previous studies have also shown that the cells with GFP tag at *suc22* locus show normal growth and Suc22 expression pattern (Nestoras et al. 2010).

	1138-8		1639-2	
	- HU	+ HU	- HU	+ HU
GFP	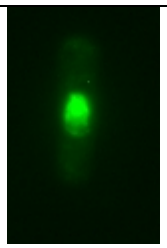	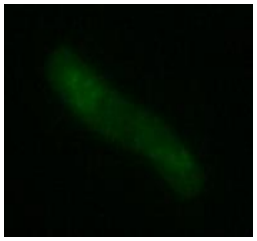	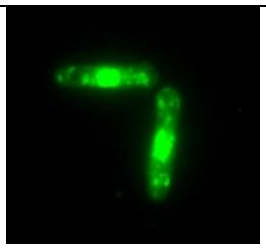	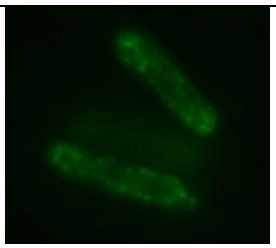
DAPI	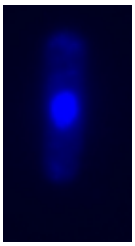	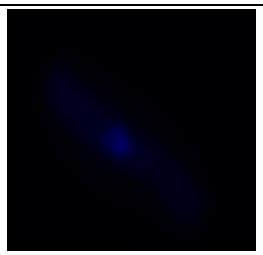	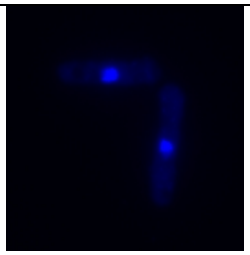	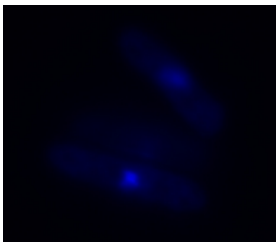

Figure 5.5. Fluorescence microscopy analysis of transformed cells stained with DAPI to confirm the expression of Suc22-GFP fusion protein. 1138-8 and 1639-2 cells show the nuclear localization of Suc22 outside the S phase. After HU treatment the GFP signal is scattered in the cytoplasm.

5.3.3 Genetic cross to make a GFP-tagged strain from *cdc10-M17 ura4-D18 h+* strain

The genetic cross between strains #1005 (*cdc10-M17 ura4-D18 h+*) and #1673 (*cdc10M-17 gcn2::ura4+ suc22:GFP:natMX6 ura4-D18 h-*) strains was performed as described in 4.1.2. and the spores were screened for clonNAT resistance and for uracil auxotrophy by replica-plating (see 4.1.3.). The cells with the desired genotype, *cdc10-M17 suc22:GFP:natMX6 ura4-D18,* should grow in the presence of clonNAT and on EMM with uracil added, but not in EMM alone as it has a defective *ura4+* gene.

All cells should be temperature sensitive (*cdc10-M17*) as both parent strains have this genotype.

The following table shows the possible genotypes after this genetic cross. Columns to the right indicate the selection on different growth media.

Table 5.1. Selection of *S. pombe* spores in different growth media. The genotype wanted written in bold. + indicates growth, - no growth.

Genotype	**YE + clonNAT**	**EMM**	**EMM+URA**
gcn2::ura4+ suc22:GFP:natMX6 ura4-D18 cdc10-M17	+	+	+
gcn2::ura4+ ura4-D18 cdc10-M17	-	+	+
suc22:GFP:natMX6 ura4-D18 cdc10-M17	**+**	**-**	**+**
ura4-D18 cdc10-M17	-	-	+

In addition to analysis by replica-plating, these cells were analyzed with fluorescence microscopy to confirm the genotype, as described above. Mating type was determined as described in 4.1.2.

The result of this cross was a strain with the genotype *cdc10-M17 suc22:GFP:natMX6 ura4-D18* and it was designated #1697.

5.4 Suc22 expression after UVC irradiation in G1

Having successfully tagged Suc22, we have set out to investigate whether there are any changes in Suc22 protein levels and subcellular localization in the cells exposed to UVC irradiation in G1 compared to non-irradiated cells, and whether such changes depend on Cid13 or Gcn2. Again, wild type, *cid13Δ* and *gcn2Δ* cells were used and all three strains express the Suc22-GFP fusion protein. Both immunoblotting (4.3.) and flow cytometry analysis (4.1.9.) were used to analyze the fusion protein levels, and fluorescence microscope (4.5.) was used to study subcellular localization.

The cells were synchronized in G1, irradiated with UVC or left untreated, and the samples were taken at the time points 0, 30, 60 and 90 minutes after the irradiation.

5.4.1 Immunodetection of Suc22 protein levels

All the samples were analyzed as described in 4.3. Primary antibody against GFP was used to detect the fusion protein, and α-tubulin antibody was used to control the loading. This experiment was repeated twice and samples from both experiments were analyzed twice.

Wild type cells show no changes in Suc22 levels in control samples, but in irradiated samples a slight increase can be seen 30 minutes after irradiation (figure 5.6. A). The increase of Suc22 from 0 to 30 minutes in UV samples was quantified by making different dilutions and it was found to be two to three fold.

In *cid13Δ* cells there are no detectable differences in Suc22 levels, either in control samples or in irradiated samples (figure 5.6. B). In *gcn2Δ* cells, the same is seen as in wild type cells; an increase in Suc22 levels 30 minutes after irradiation (figure 5.6. C).

We conclude that there are no major changes in the amount of Suc22:GFP after UVC irradiation. However, our preliminary data suggest a slight Cid13-dependent increase of Suc22:GFP levels in response to UVC irradiation in G1.

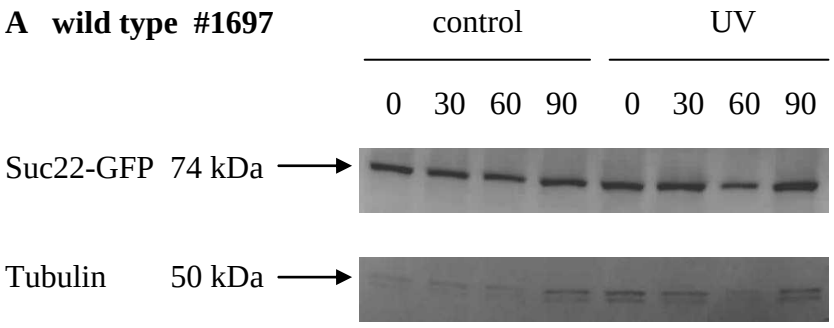

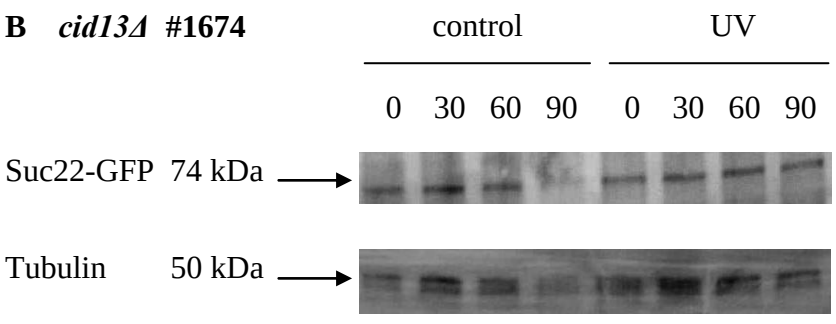

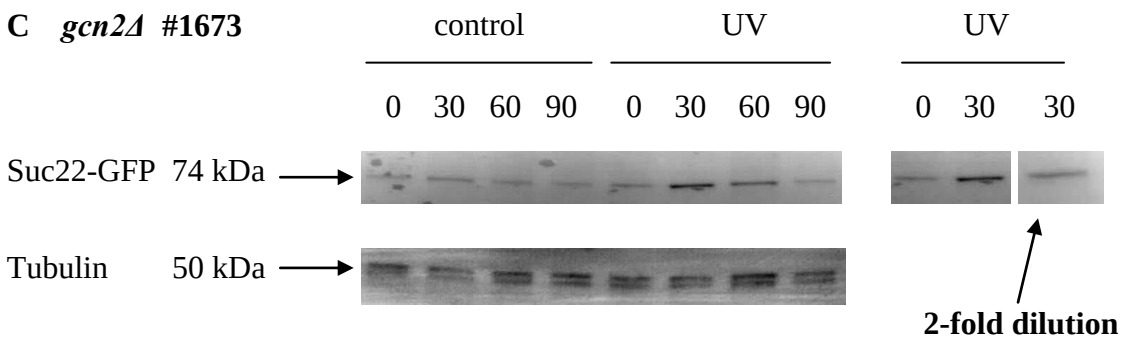

Figure 5.6. A-C) Suc22 levels in control and UVC irradiated samples from wild type, *cid13Δ* and *gcn2Δ* cells were analyzed by western blotting using α-GFP antibody. Tubulin was used as a loading control. The increase in Suc22 levels from 0 to 30 min after irradiation was quantified with a dilution series which revealed that the increase is about 2-fold (shown for *gcn2Δ* cells in panel C).

5.4.2 Flow cytometry analysis of Suc22 protein levels

We explored the possibility that flow-cytometry analysis of the GFP fluorescence might provide a more quantitative method to measure small differences in protein levels. The samples were collected and prepared as described in 4.1.9. The GFP-signal was quantified corresponding to the area under the curve in figure 5.7. (A) and the standard deviation was calculated. The DNA was stained with Hoechst 33258 stain to quantify the DNA content in each nucleus. Flow-cytometry data can be found in appendix 3-5.

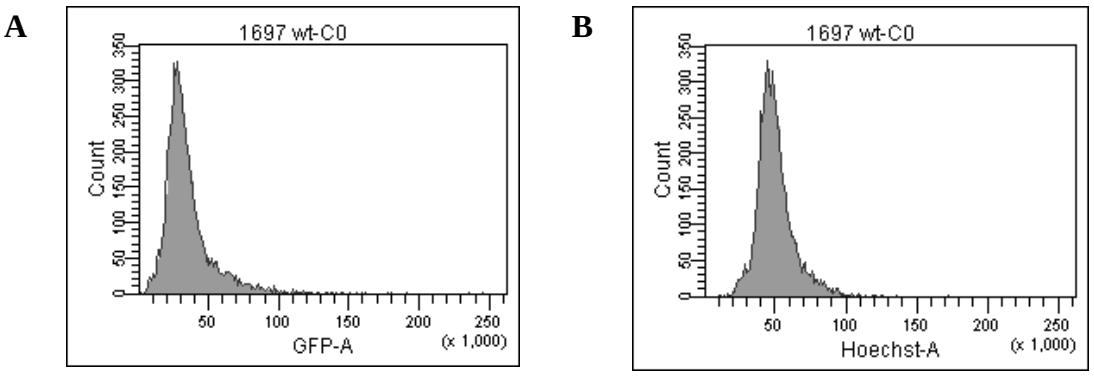

Figure 5.7. Flow cytometry analysis of non-irradiated wild type cells at time point 0. A) A histogram showing the intensity of Suc22-GFP signal as a function of the area under the curve. B) A DNA histogram showing the intensity of the nuclear signal from G1 arrested cells is set to 50 which corresponds to 1C DNA content. Cell number on Y-axis, signal intensity on X-axis.

Only minor fluctuations in Suc22 levels can be observed, but these are not significant. A trend can be observed however, where a slight increase of the GFP signal can be observed at the same time as the cells enter S phase as shown in figure 5.8.

A

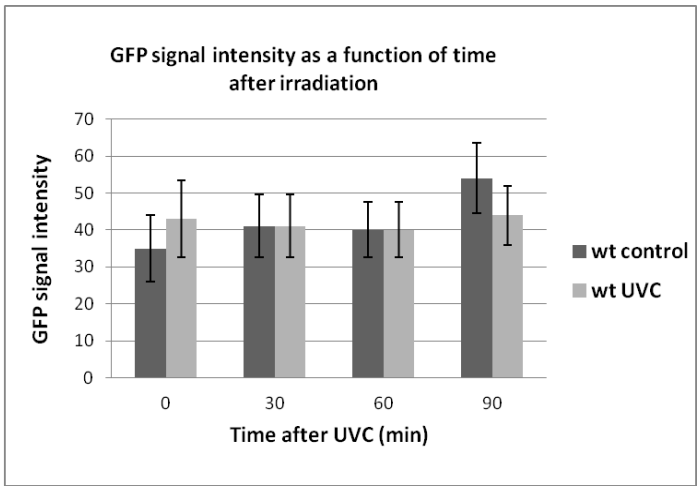

B

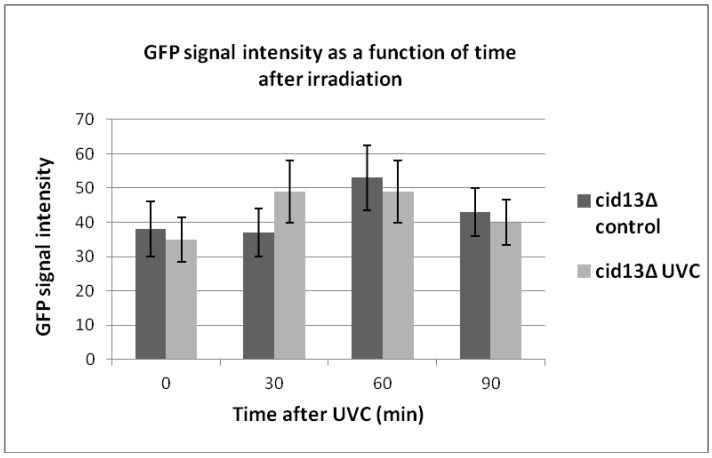

C

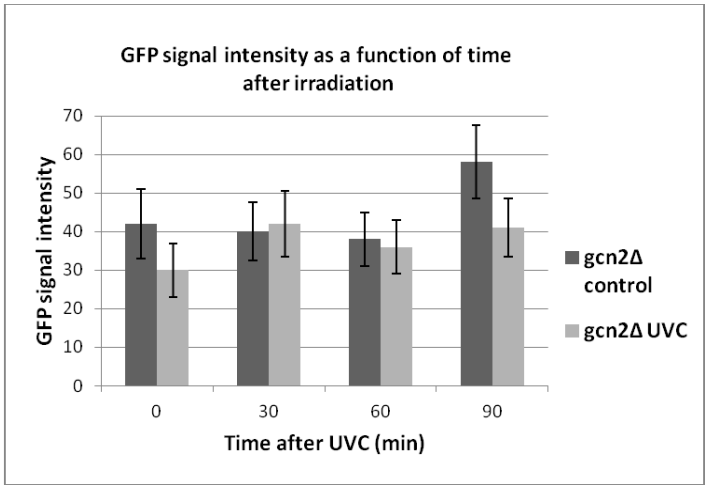

Figure 5.8. GFP signal intensity as a function of time in wild type, *cid13Δ* and *gcn2Δ* cells with and without UVC irradiation in G1. Standard deviation (from cell to cell) is indicated with the vertical bars.

The interpretation of these results is hampered by the slow growth and slow cell-cycle progression after release from *cdc10* block. This resulted in extremely elongated cells (figure 5.9) and indicates that the cells are not able to recover properly from the *cdc10* block. Non-irradiated control cells should enter the S phase approximately 60 minutes after release from the *cdc10* block, which can be detected as an increased DNA content from 1C (50) to 2C (100). DNA histograms in appendix 5 show that the main population in each strain lies far from the 2C DNA content still at time point 90 minutes after irradiation indicating that they have not completed S phase. In addition, both non-irradiated and irradiated *cid13Δ* cells and irradiated *gcn2Δ* cells showed too poor synchrony.

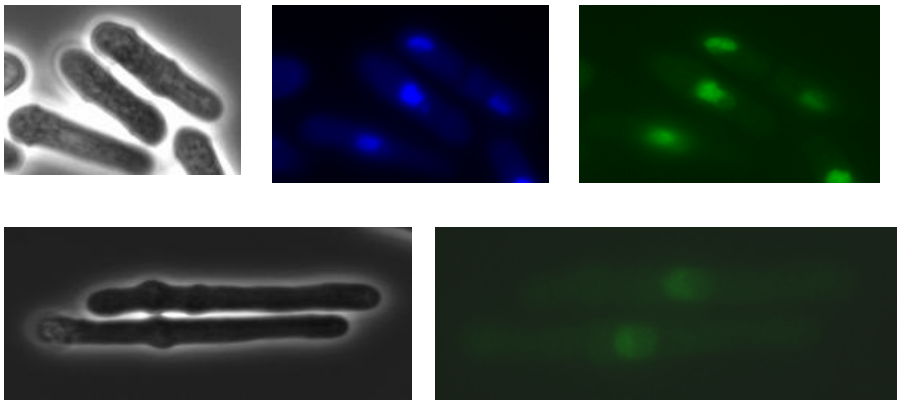

Figure 5.9. GFP-tagged become abnormally highly elongated when synchronized in G1. Upper panel: Logarithmically growing *gcn2Δ* cells expressing Suc22-GFP. From left: phase contrast, DAPI, GFP. Lower panel: The same cells show extremely elongated phenotype 90 minutes after synchronizing with *cdc10* block in G1.

Nuclear staining with Hoechst turned out to be the wrong choice of dye as the peaks on the graphs are very wide making analysis less precise. In other flow cytometry analysis Sytox Green was used, but in this experiment we needed to use another color than green because we were interested in detecting GFP-signal. (Sazer and Sherwood 1990) have studied different DNA staining agents in fission yeast and they showed that *cdc10* arrested cells accumulate mitochondrial DNA while nuclear DNA content is reduced. This is a plausible explanation for unusual wide Hoechst-signal in our experiments as Hoechst show high specificity for A+T rich DNA, which is particularly abundant in *S. pombe* mtDNA. According the same study, the more suitable dye would have been Propidium iodide which emits red fluorescence and its binding to DNA is relatively non-sequence-specific.

5.4.3 Suc22 subcellular localization

We have shown that Suc22-GFP fusion protein is able to localize both in nucleus and cytoplasm indicating that the nuclear transport of this fusion protein is normal (figure 5.5.). Suc22 is known to be exported from the nucleus in S phase and in response to DNA damage to form an active RNR in the cytoplasm. We wanted to explore if Suc22 translocation can be detected after UVC irradiation in G1 and if there is differences between the wild type *cid13Δ* and *gcn2Δ* cells.

The number of cells with nuclear GFP signal was counted in 200 cells in each sample. The results are shown in figure 5.10. The same samples were used in this experiment as in the flow-cytometry analysis of Suc22 levels (5.4.2.).

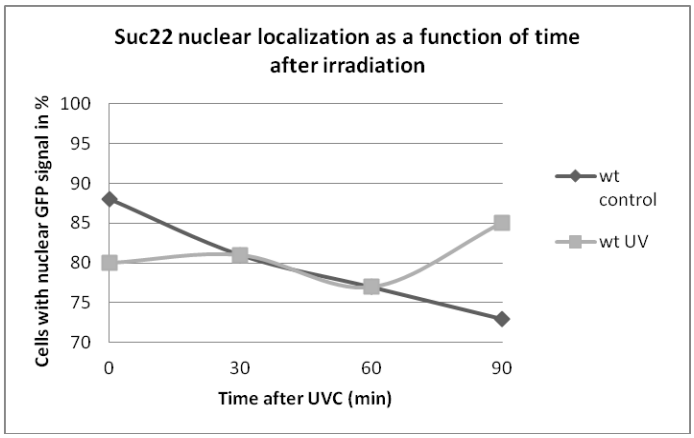

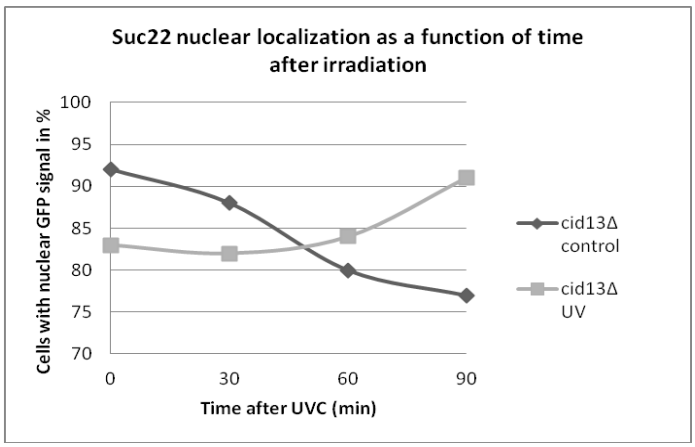

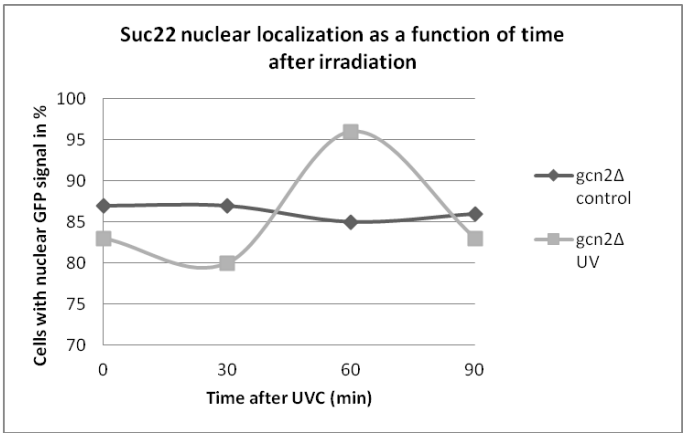

Figure 5.10. Nuclear GFP-signal as a marker for Suc22 localization in the cells expressing Suc22-GFP fusion protein. Wild type (top), *cid13Δ* (middle) and *gcn2Δ* (bottom) cells were analyzed with and without UVC irradiation in G1.

The interpretation of these results is hampered by the same facts as described in flow cytometry analysis (5.4.2.). Abnormally slow cell-cycle progression after release from *cdc10* block detected with flow cytometry can also be seen in the graphs above as the number of cells with nuclear GFP signal is very high (>70%) in each strain even after 90 minutes.

Wild-type cells showed good synchrony in G1 so these results can be analyzed together with flow-cytometry data of cell-cycle progression giving an indication of the localization of Suc22 (appendix 4-5). The slow progression to S phase seems to correspond to slow decrease in nuclear GFP signal in control samples (figure 5.10, top). Irradiated wild-type cells show the opposite tendency as number of cells with nuclear GFP-signal increases slowly. This is consistent with the delayed entry into S phase after UVC irradiation and Suc22 is then kept in the nucleus. Furthermore, it indicates that DNA damage caused by UVC in G1 do not trigger the nuclear export of Suc22.

5.5 dATP levels after UVC irradiation in G1

Our working hypothesis predicts that maintenance of Cid13 translation after UVC irradiation is important in order to provide a sufficient pool of dNTPs via the regulation of Suc22 levels. Following Suc22 levels was hampered by the impaired function of the fusion protein. To directly address the importance of the Gcn2-Cid13 pathway in regulation of dNTP levels after UVC irradiation, we measured dATP levels using polymerase assay (4.4).

Wild type, *cid13Δ* and *gcn2Δ* cells were analyzed. Samples were collected immediately after UVC irradiation in G1 and every 30 minutes for 90 minutes. Efficiency of the *cdc10* block was monitored with flow cytometry and for each strain samples of two experiments with highest % of G1 arrested cells were selected for further analysis.

Because of the limited time for this experiment, concentrations of only one species of dNTPs, dATP, were analyzed.

5.5.1 Normalizing the samples by measuring ATP concentration

Standard ATP solutions were used to create a standard curve.

A

pmol ATP	RLU
0	
20	115
40	218
80	395
200	1156

B

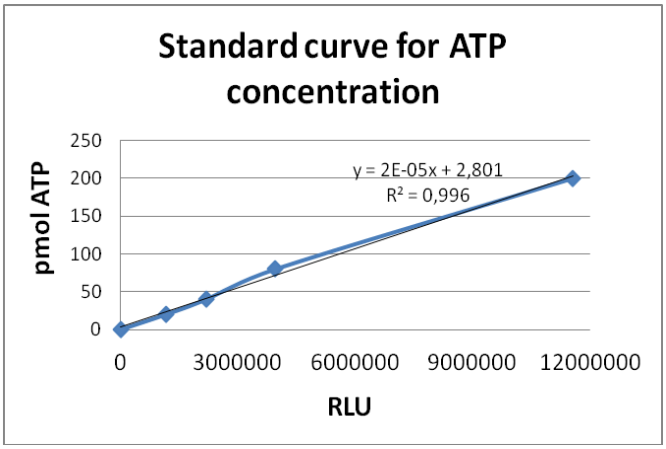

Figure 5.11. A) Luminescence values (RLU) for known ATP concentrations. B) Standard curve with regression line and equation to calculate ATP concentration in unknown samples. The R^2 value very close to 1 indicates good correlation between ATP concentration and relative luminescence.

Samples from two independent experiments were analyzed with the Luciferace assay and ATP concentration was calculated using the standard curve. One set of samples of

each strain with highest ATP concentrations was chosen to continue with; numbers marked in red in table 5.2.

Table 5.2. ATP concentrations of samples from two independent experiments. Samples from experiment 1 in table A, experiment 2 in table B. Red numbers indicate that those samples have higher ATP concentration on average than corresponding samples from the other experiment. These were chosen to further analysis.

A

strain	sample	RLU	pmol ATP/µl
489-1	0	8434421	**85,7**
	30	9493501	**96,3**
	60	10948799	**110,9**
	90	10623477	**107,6**
1138-1	0	8610800	87,5
	30	11509626	116,5
	60	11309955	114,5
	90	3379532	35,2
1639-1	0	3593684	37,3
	30	8344539	84,8
	60	3456430	36,0
	90	3320679	34,6

B

strain	sample	RLU	pmol ATP/µl
489-2	0	4946709	50,9
	30	11151561	112,9
	60	8587792	87,3
	90	10324290	104,6
1138-2	0	7975006	**81,2**
	30	10561372	**107,0**
	60	10159406	**103,0**
	90	7030042	**71,7**
1639-2	0	7116990	**72,6**
	30	5644119	**57,8**
	60	7261246	**74,0**
	90	8029343	**81,7**

5.5.2 Quantifying dATP levels in the samples

The amount of dATP in the cells is measured from the number of dATPs incorporated during primer extension. Possible outcomes include sequences with different lengths from 22 nucleotides (non-elongated primer) to 34 nucleotides (fully elongated primer); see sequences below. Nucleotides to be incorporated are marked in red.

Primer p22: 5' - ^{32}P – GGTAGGGCTTCGCAGCCGTCCA **A T T A T T A T T A T T** -3'

Template: 3'- CCATCCCGAAGCGTCGGCAGGT T A A T A A T A A T A A -5'

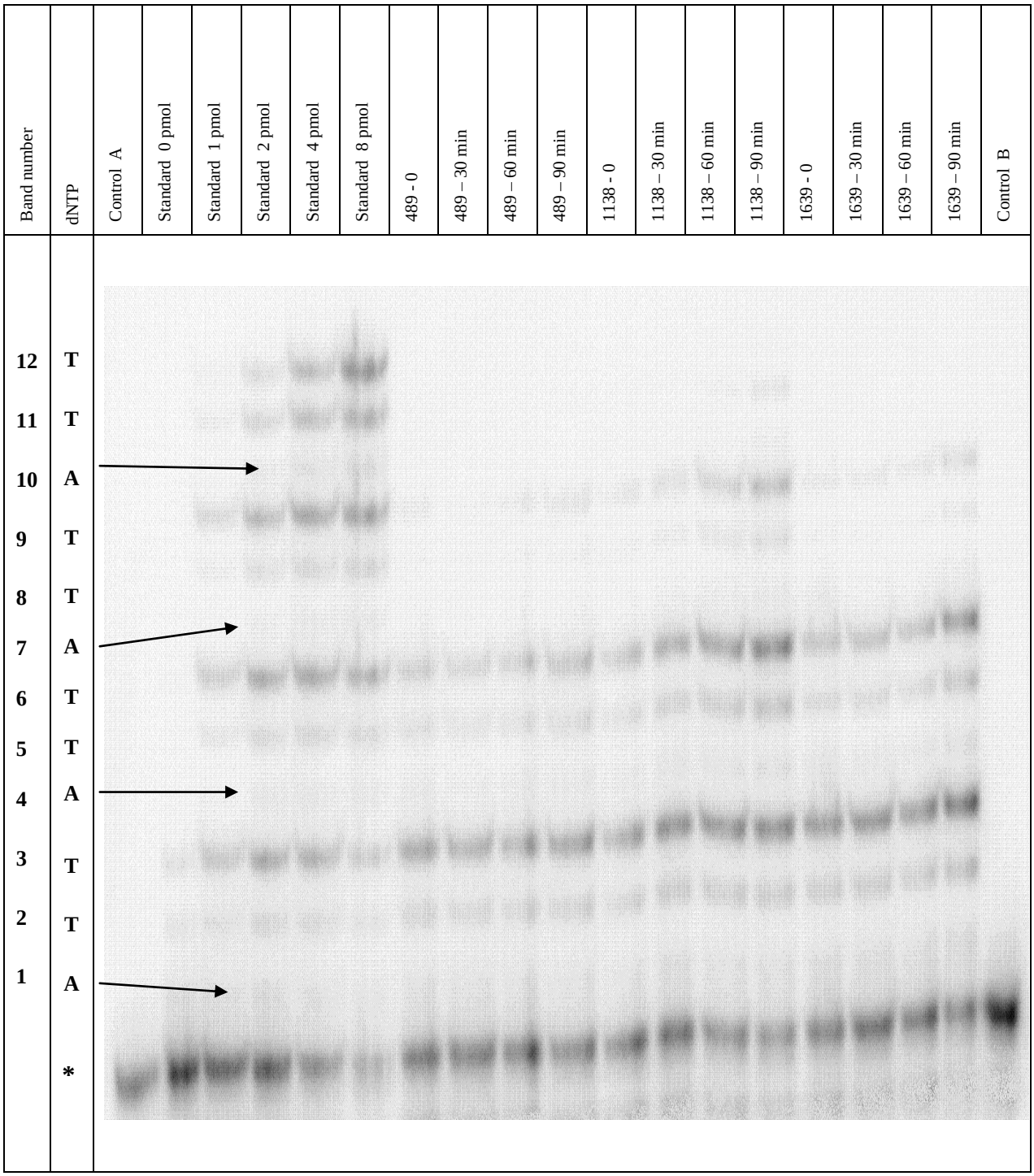

Figure 5.12. A gel picture showing the bands corresponding to elongated primer sequences of different lengths in control samples A and B (no dNTPs added), standard samples and samples to be analyzed. Arrows show the lines where dATP is incorporated. The very bottom bands are the non-elongated primers (the row marked with *).

Intensity of the bands in the standard samples was analyzed first to create a standard curve. The calculations made for the standard samples were as follows:

1) Sum of the intensities of all bands per line = total volume
2) Ratio between volume of each band and the total volume
3) Sum dATP: In tA template used, there are 12 nucleotides to fill $(ATT)_4$, so we calculate:
   (band1+b2+b3) + 2 * (b4+b5+b6) + 3 * (b7+b8+b9) + 4 * (b10+b11+b12).
4) 3 pmol primer was used in all samples so the sum is multiplied with 3.
5) As the dATP concentration of the standard samples is known, the standard curve can now be created (figure 5.13.).

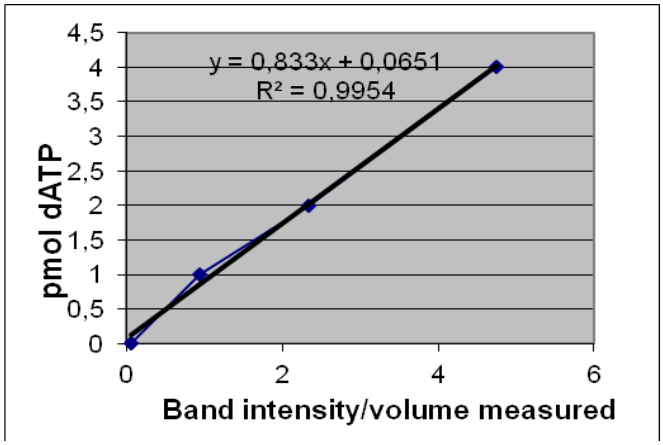

Figure 5.13. Standard curve for dATP concentration as a function of band intensity.

The calculation steps 1.-3. were applied to samples to be analyzed to get a sum of dATP in each sample. As 10 µl of each of my samples was used to the primer extension reaction, the sum is divided by 10 to get a value in pmol dATP/µl. These values are then compared with the values for ATP concentration from the Luciferase assay to achieve dATP/ATP ratio.

5.5.3 UVC irradiation in G1 does not affect the dATP pools

Table 5.3 shows the dATP/ATP values. In addition, I chose to normalize the dATP/ATP value for wild type (#489) sample taken at time point 0 which was set to 1 (figure 5.14.). I emphasize that these measurements have been done only once and therefore the results are preliminary.

Table 5.3. dATP/ATP values in the samples from wild type, *cid13Δ* and *gcn2Δ* cells.

Strain	0 min	30 min	60 min	90 min
489 wt	0,001373	0,001012	0,001004	0,001526
1639 *cid13Δ*	0,002207	0,002315	0,001934	0,002938
1138 *gcn2Δ*	0,001579	0,001628	0,002457	0,004527

Figure 5.14 shows that wild type cells have very stable levels of dATP in the cells until 90 minutes after the UVC irradiation in G1. *gcn2Δ* cells have an equal basal dATP level as wt cells and no immediate increase is seen in response to UVC. The 3-fold increase seen at 90 minutes after irradiation corresponds to the entry into S phase (5.2.) as *gcn2Δ* cells do not arrest the cell cycle in response to UVC irradiation in G1. The basal level of dATP in *cid13Δ* cells is 1.5-fold higher than in the other strains analyzed. *cid13Δ* cells are shown to enter the S phase with the same kinetics as *gcn2Δ* cells (5.2.) and the slow increase in dATP levels is seen from 60 minutes after irradiation.

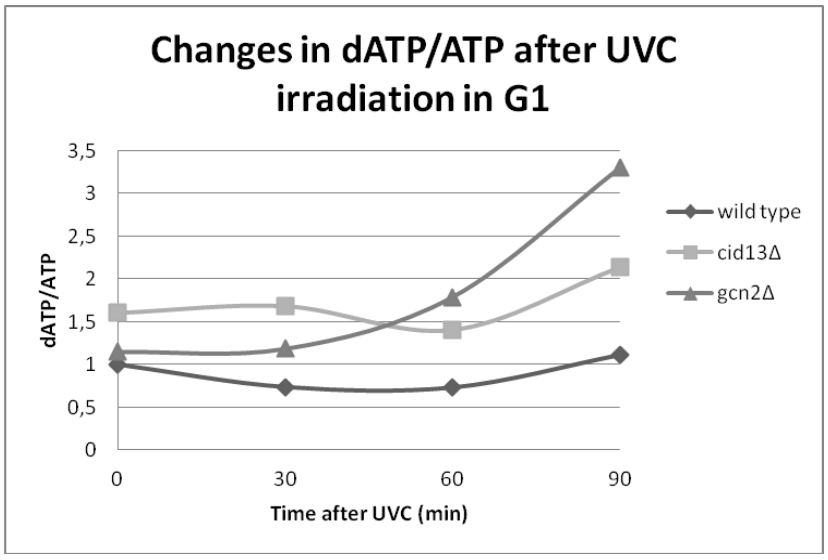

Figure 5.14. Relative changes in dATP/ATP in wild type, *cid13Δ* and *gcn2Δ* cells after UVC irradiation in G1. dATP/ATP value in wild-type sample at time point 0 was set equal 1 and values from the other samples were adjusted after that.

I conclude that the observed changes in dATP pools correspond to S phase entry and the UVC irradiation does not seem to affect dATP pools significantly.

6 DISCUSSION

In this chapter I will discuss my results in light of recent knowledge about G1/S checkpoints, functions of Cid13, and multiple facets of regulation of RNR in fission yeast. I will also go through some troubleshooting concerning the Suc22:GFP yeast strains and the synchronization method used in this study. In the end I will discuss some other possible functions of Cid13 and how it might affect regulation of RNR, to give better understanding of the possible underlying mechanisms.

It should be noted that due to shortage of time the dNTP measurements and the Suc22 localization studies have only been performed once and the results are therefore preliminary. Nevertheless, I shall include them in the discussion and put them in the context of previously published work.

6.1 Deletion of *cid13* leads to loss of the G1/S checkpoint and lower survival after UVC irradiation in G1

Cell survival after UVC irradiation is thought to require an intact checkpoint machinery and efficient DNA repair. Mutations that affect some of these functions can lead to chromosomal aberrancies and lower viability.

The G1/S checkpoint in fission yeast absolutely depends on the Gcn2 kinase (Tvegard et al. 2007) and correlates with a downregulation of general translation. However, some proteins continue to be efficiently translated. One of these proteins is Cid13 (Knutsen, JH. unpublished) and therefore we decided to study the function and significance of this protein in the response to UVC in G1 phase.

We have shown that the *cid13Δ* mutant is more sensitive to UVC irradiation in G1 than the isogenic wild type strain (figure 5.1.). This is consistent with the notion that maintaining the translation of Cid13 is important in response to UVC irradiation in G1. We considered the possibility that *cid13Δ* cells might be checkpoint deficient.

We explored the importance of Cid13 for the G1/S checkpoint function by following the kinetics of entry into S phase with and without UVC irradiation in G1. We found that *cid13Δ* cells do not delay entry into S phase when irradiated with UVC in G1 (figure

5.2.), which suggests that Cid13 is needed for the G1/S checkpoint. The phenotype of *cid13Δ* cells is similar to that of *gcn2Δ* cells which are known to be checkpoint deficient (Tvegard et al. 2007).

We suggest that regulation of the Cid13 level might be an important function of Gcn2 (figure 6.1.). This raises a question why *gcn2Δ* cells are less sensitive to UVC than *cid13Δ* cells. These two mutants might have different mechanisms to respond to DNA damage caused by UVC irradiation. Both *gcn2Δ* and *cid13Δ* cells enter S phase without delay after UVC irradiation in G1 indicating that they do not repair the DNA damage immediately. In S phase, the intra-S checkpoint slows down the DNA replication as long as DNA damage is present. Neither Gcn2 nor Cid13 are reported to be needed for this checkpoint function suggesting that both mutants have an intact intra-S checkpoint. *gcn2Δ* cells show just slightly lower survival after UVC irradiation compared to wild type cells. This indicates that *gcn2Δ* cells are able to repair the DNA damage and continue to mitosis. In contrast, *cid13Δ* cells have clearly lower survival rate after UVC irradiation than *gcn2Δ* cells, indicating that *cid13Δ* cells may encounter some problems in DNA repair.

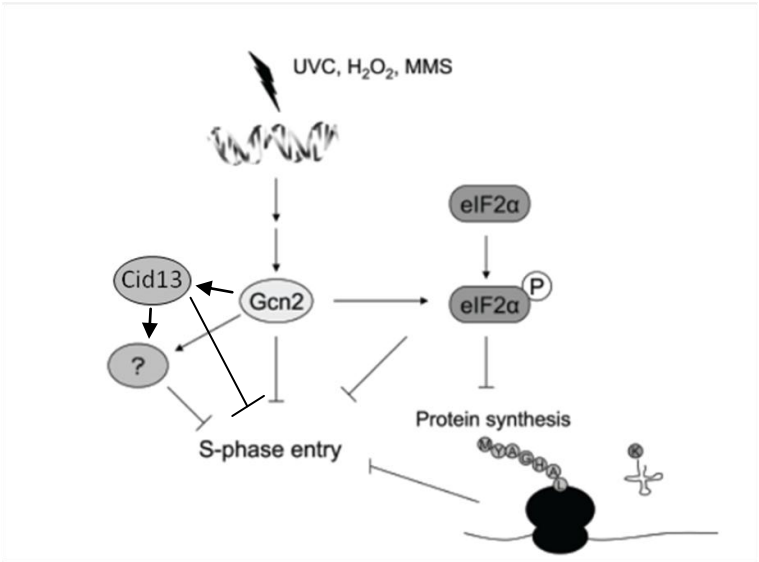

Figure 6.1. A current model for G1/S checkpoint activation (modified from figure 1.3.). Gcn2 may exert its function via several targets leading to a delay in the entry into S phase. We propose that Cid13 is one of the targets of Gcn2 kinase.

6.2 Upregulation of dNTP levels is not essential for the G1/S checkpoint response

The only known target of Cid13 is the RNR subunit Suc22, which prompted us to explore how and whether dNTP levels change in response to UVC irradiation and whether Cid13 is responsible for these changes. We measured dATP pools in wild-type, *cid13Δ* and *gcn2Δ* cells and found that there is no upregulation in response to UVC in G1. On the other hand, the absence of Cid13 correlates with higher basal dNTP levels in G1. (table 5.3 and figure 5.14)

Wild-type cells start increasing dNTP levels when they enter S phase (figure 5.14). Interestingly, they do not increase dNTPs in response to UVC in G1. This is different from what is seen when G2 cells are treated with DNA damaging agents (Hakansson et al. 2006) (Moss et al. 2010). When an asynchronous cell culture is treated with ionizing radiation a two-fold increase in dNTPs is seen. This increase is due to the RNR activation in a checkpoint dependent manner and it is required for efficient DNA repair by homologous recombination (Moss et al. 2010). Hakansson et al. (2006) show a similar increase in dNTPs after treating an asynchronous cell culture (approx. 70% G2 cells) with the UV-mimetic agent 4-NQO. The increase in dNTP levels requires the classic DNA damage checkpoint pathway which trigger the expression of Cdt2, leading to Spd1 proteolysis and RNR activation (Moss et al. 2010). These observations suggest that ionizing radiation and 4-NQO trigger the same response in G2, whilst UVC irradiation in G1 does not activate RNR as no increase in dNTP levels can be seen in wild-type cells (this work). Thus, the response with respect to regulating dNTP levels appears to be dependent on the cell-cycle phase and the prevailing checkpoint mechanisms.

cid13Δ cells have 1.5-fold higher dNTP levels in G1 than wild-type cells (figure 5.14). Interestingly, *cid13Δ* cells do not increase dNTP levels that much when they start to enter S phase. This indicates that *cid13Δ* cells are not able to fully upregulate dNTP levels in S phase and this might interfere with DNA repair during S phase after UVC irradiation in G1. This is consistent with the observations that these cells are more sensitive to UVC than *gcn2Δ* cells.

Our results show further that *gcn2Δ* cells behave as wild-type cells and a clear increase in dNTP levels is seen when the cells enter S phase. As *gcn2Δ* cells do not delay entry into S

phase after UVC treatment the increase in dNTP levels can be seen already 60 minutes after irradiation.

6.3 Effect of the GFP-tag on the cells

In order to address the possible role of Cid13 in the regulation of Suc22 levels, we have tagged Suc22 with a GFP tag in wild-type, *cid13Δ* and *gcn2Δ* cells in *cdc10-M17* background. While doing the experiments with the cells carrying GFP-tagged *suc22* I encountered some problems I would like to discuss here.

First, I noticed that the cells started to lose the GFP-tag and I needed to grow them in selective media taking advantage of the clonNAT marker they carry. Second, when I analyzed the cell-cycle progression by flow cytometry I noticed that these cells grow very slowly. These cells had a generation time up to 5.5 hours, versus 3 hours in wild-type, in YE medium. In addition, microscopic analysis revealed that the tagged cells are more elongated than wild type cells, and they get extremely elongated when arrested in G1 (figure 5.9.) and they use very long time to recover from the arrest. This can be a sign of aberrant growth of these cells. Even though we tested the wild-type behavior of the tagged strains in the presence of HU (figure 5.5.), it does not guarantee that Suc22 is produced in optimal level or that Suc22 function is optimal in those cells.

6.4 Suc22 expression and localization is affected by UVC irradiation in G1

We have shown that there is a slight increase in Suc22 levels in response to UVC irradiation in G1 and this increase is dependent on Cid13 (figure 5.6). As described in 1.4.1, the transcription level of the 1.5 kb *suc22* mRNA is not affected by DNA damage or S phase, but it is the induction of an additional transcript that contributes to an increase in Suc22 protein levels, when required. Our preliminary data supports the hypothesis that UVC irradiation in G1 triggers the transcription of 1.9 kb *suc22* mRNA which is further stabilized in the cytoplasm by Cid13 and this leads to upregulation of total Suc22 level. The maintenance of Cid13 levels seems to be able to counteract downregulated Suc22 translation after UVC irradiation.

Two previous studies report partly conflicting results about Suc22 levels in *cid13Δ* cells. Saitoh et al. (2002) show that the level of the 1.9 kb suc22 mRNA is lower in *cid13Δ* cells than in wild-type cells when exposed to HU and they conclude that Suc22 translation is impaired when Cid13 is deleted. This observation is consistent with our finding that there is a slight Cid13 dependent increase in Suc22 levels in response to DNA damage. On the other hand, Read et al (2002) report opposite observations showing that there are no differences in Suc22 levels in wild-type and *cid13Δ* cells, with or without HU treatment. But it has been shown that the over-expression of either Cid13 (Read et al. 2002) or Suc22 (Liu et al. 2003) could rescue the HU sensitivity of *rad3Δ* mutants, consistent with increased dNTP levels.

For RNR to become active the subunits need to be localized into the same cellular compartment to form a tetramer. Therefore we explored if UVC irradiation in G1 leads to nuclear export of Suc22. Wild-type and *cid13Δ* cells show very similar tendencies with and without UVC irradiation in G1. When the cells are not irradiated there is a continuous decrease in nuclear Suc22 which is consistent with the entry into S phase (figure 5.10). Suc22 has been shown to be exported from the nucleus to the cytoplasm in S phase and in response to DNA damage to contribute to formation of RNR tetramer (see 1.4.3. and 1.5.). When the cells are irradiated in G1 no significant changes can be seen during the first 60 minutes indicating that Suc22 is kept in the nucleus. Surprisingly, both wild-type and *cid13Δ* cells show increased nuclear Suc22 levels 90 minutes after irradiation even though *cid13Δ* cells enter S phase whereas wild-type cells delay S-phase entry (figure 5.10). The observation that also *cid13Δ* cells show increase in nuclear Suc22 levels 90 minutes after UVC irradiation indicates that *cid13Δ* cells are impaired in Suc22 nuclear export. This is consistent with our finding that *cid13Δ* cells are not able to fully upregulate dNTP levels when entering S phase.

6.5 Suc22-Spd1 interplay in RNR regulation

In the previous chapter I already touched upon one important event in RNR regulation: translocation of Suc22 between the cytoplasm and the nucleus, and the possibility that Cid13 is involved in that process. It is not known what triggers Suc22 nuclear import after S phase and after completion of the repair of DNA damage. In contrast, several factors connected to Spd1 degradation and Suc22 nuclear export have been identified. I will

discuss this subject further and put it in context with the G1/S transition, DNA damage and the subsequent need for RNR activation.

6.5.1 Coupling DNA damage and RNR activation

Activation of RNR requires several events to occur at the right place and time. When the cells enter S phase, Cdt2 levels increase to promote degradation of the RNR inhibitor Spd1. Cdt2 is required for this degradation also in response to DNA damage, but the activation of Cdt2 expression occurs in different ways (see 1.3.2 and 1.4.3). Transcription of Cdt2 is shown to correspond to Spd1 degradation profiles (Liu et al. 2005). A very recent study (Salguero et al., in press) suggests that Cdt2 functions as an adaptor protein to Spd1. They show that high Cdt2 level alone is not enough to trigger Spd1 proteolysis in G1/S transition, but the critical step in Spd1 proteolysis is the interaction of Spd1 with the DNA-bound polymerase processivity factor PCNA. They conclude that this provides a direct mechanism to couple DNA synthesis and repair with activation of RNR to increase dNTPs. This is an interesting suggestion and it could be relevant to our finding that instead of exporting Suc22 to the cytosol after UVC irradiation, Suc22 appears to be restrained in the nucleus.

6.5.2 Spd1 plays several roles in RNR activation

Spd1 was found to interact with both RNR subunits (Hakansson et al. 2006) and this has raised several questions concerning the localization of both the subunit dimers, tetramerization and, finally, the active enzyme. The first suggestion for Spd1 acting by anchoring Suc22 inside the nucleus outside of S phase (Liu et al. 2003) has been followed by both supporting and opposing reports, which will be discussed below. Liu et al. (2005) have shown later that Cdt2-dependent Spd1 degradation results in loss of Suc22 from the nucleus and in *cdt2Δ* cells Suc22 remains nuclear. This indicates that Spd1 is not degraded and it could be able to retain Suc22 in the nucleus. When deleting Spd1, Suc22 is dispersed into the cytoplasm, probably due to the loss of ability to retain Suc22 in the nucleus (Takahashi et al. 2007).

In addition, Caf1 is needed to interact with the ubiquitin ligase complex responsible for Spd1 degradation and to release Spd1-Suc22 from the nucleus (Takahashi et al. 2007). Caf1 has been characterized as a multi-functional component that is largely involved in

the transcription of RNR genes. Takahashi et al. (2007) have further shown that the *caf1Δ cid13Δ* double mutant is not synergistically sensitive to HU, indicating that these proteins act in the same pathway. They speculate that Caf1 is also involved in anchoring Suc22 in the nucleus, inhibiting RNR activation outside of S phase and in no-stress conditions.

Nestoras et al. (2010) suggest that Sdp1 contributes to Suc22 nuclear import, but they show that Spd1 and Suc22 are not fully co-localized in the nucleus, indicating that Spd1 does not function as a nuclear anchor for Suc22. So far it remains unclear how Suc22 is kept in the nucleus, since the direct interaction between Suc22 and Spd1 is found to be very weak and transient (Hakansson et al. 2006). Instead, another article from Hakansson (2006) have shown that Spd1 binds to Cdc22 with much higher affinity and this supports the previous hypothesis that Spd1 mostly localizes to the cytoplasm (Borgne and Nurse 2000).

The role of Spd1 in Suc22 subcellular localization and further in RNR activation is getting even more complex after the conflicting finding that the ability of Spd1 to sequester Suc22 to the nucleus does not correlate with reduced RNR activity (Nestoras et al. 2010). In addition, no difference was observed in co-localization of Suc22 and Cdc22 in the FRET analysis before and after Spd1 degradation, suggesting that Spd1 keeps RNR in an inactive form and its degradation would leave the subunits in an optimal conformation for catalytic activity.

Taken together, it seems that Spd1 regulates RNR through several mechanisms. Suc22 subcellular localization is only partly dependent on Spd1 function and Spd1 degradation is required for RNR activation. It is possible that a pool of RNR tetramers with bound Spd1 is formed in the cytoplasm and imported to the nucleus when rapid synthesis of new dNTPs is required. The proteolysis of Spd1 could then take place at the site of DNA damage or synthesis as suggested by Salguero et al (in press). Outside S phase and when there is no DNA damage present there would be only low RNR activity or few active RNR complexes.

6.6 Cid13 may possess other important functions required for resistance to UVC irradiation in G1

6.6.1 Poly(A) polymerases in Cid1 family have multiple functions

Cid13 belongs to the Cid1 family of non-canonical poly(A) polymerases (PAPs). Six members of this family have been identified in *S. pombe* and they all contain a similar catalytic NTP transferase domain and a PAP-associated domain (Stevenson and Norbury 2006). These structural properties are conserved across eukaryotes. The expression of so a many regulatory poly(A) polymerases increases the flexibility for control of gene expression. The modulation of poly(A) tail length both in the nucleus and in the cytoplasm is clearly an evolutionary conserved mechanism for regulating mRNA translation.

In fission yeast, some of the Cid1-family proteins are solely nuclear or cytoplasmic, and some can be detected in both the nucleus and the cytoplasm. Cid13 was previously reported to localize solely in the cytoplasm, but the global analysis of protein localization in fission yeast revealed that Cid13 can also be detected in the nucleus (Matsuyama et al. 2006). However, this finding must be interpreted carefully as the nmt-promoter was used to drive the expression of each protein. This can lead to overexpression and mislocalization of proteins which normally are expressed at low levels.

Cid1-family proteins are also found to associate with ribosomal subunits and assembly factors, and Cid14 is required for silencing heterochromatic genes (Keller et al. 2010). It has also been suggested that both Cid13 and Cid14 are involved in ribosome biogenesis (Stevenson and Norbury 2006). Several ribosomal biogenesis factors have recently found to be involved in other cellular mechanisms both in yeast and higher eukaryotes (Jorgensen et al. 2002; Warner and McIntosh 2009) .

6.6.2 Cid13 interacts with the nuclear transport machinery

The observed nuclear localization of Cid13 is consistent with the finding that Cid13 coimmunoprecipitates with Mog1, a RanGDP-binding protein involved in nuclear transport and mRNA metabolism (Oki et al. 2007). RanGDP binds its cargo in the cytoplasm and this complex is transported to the nucleus where the cargo is released and

Ran-GEF (guanine nucleotide exchange factor) replaces GDP with GTP. Overexpression of Cid13 is also able to rescue the lethality of *mog*^{ts} cells when grown at the restrictive temperature (Oki et al. 2007).

These findings suggest that Cid13 might be involved in the nuclear transport. *S. cerevisiae* Mog1 shares several functional features with its *S. pombe* homolog, such as involvement to RanGDP nuclear transport. Because of that I would like to consider the possibility that *S. pombe* and *S. cerevisiae* share also some other features in the nuclear transport. Dosil (2011) has reported that *S. cerevisiae* utilizes a karyopherin, Kap121 (also called PSE1), dependent route to import one of the small RNR subunits to the nucleus (*S. cerevisiae* has two genes for the RNR small subunit and they form a heterodimer). This transport mechanism is dependent on Rrp12, a protein involved also in ribosome maturation. The same study showed that *rrp12Δ* cells are more sensitive to DNA damage, delay entry into S phase, and have significantly higher dNTP pools both in asynchronous and G1-synchronized cells compared to the wild-type cells. But, upregulation of dNTP synthesis is delayed in *rrpΔ* cells when they enter S phase. *S. pombe* Kap121 ortholog, karyopherin Pse1, is known to cooperate with Kap123, interact with the nuclear pore complex and act as a nuclear import receptor for specific proteins (pombase.org).

It is tempting to suggest that Cid13 might participate in Suc22 translocation. This could be achieved via binding to RanGDP, which carries Suc22 as one of its cargos, and that the nuclear entry of this complex is dependent on karyopherins and Rrp12 interacting with the nuclear pore complex. The defective Suc22 nuclear transport could also explain the increased HU sensitivity of *cid13Δ* cells.

6.6.3 Deletion of Cid13 leads to abnormal RNR function and aberrant dNTP levels

(Saitoh et al. 2002) reported the first observations of Cid13 and cytoplasmic polyadenylation of 1.9 kb mRNA of *suc22* in fission yeast. They showed that *cid13Δ* cells are not able to upregulate the 1.9 kb *suc22* transcript to the same extent as *cid13+* cells when treated with HU. They argued that Cid13 is needed to rapidly enhance dNTP synthesis in response to DNA damage. They also compared dNTP levels in wild type and *cid13Δ* cells in the absence of DNA damage. They reported that dNTP pools of *cid13Δ*

cells are just half of that of wild type cells in asynchronous cell culture. A similar ratio was observed when cells synchronized in G1 enter S phase. However, these results are not consistent with the finding that the 1.9 kb *suc22* mRNA is induced to detectable level only in S phase and in response to DNA damage. How could Cid13 then affect dNTP pools in the cells outside S phase and when DNA damage is not present? The more recent findings considering the additional roles of Cid13 have lead to partly conflicting arguments to those Saitoh et al. (2002) reported and I will discuss these here.

The total amount of RNR complexes formed is dependent on the amount of Suc22 available for tetramerization. If Cid13 contributes to the nuclear import of Suc22 after S phase, deletion of *cid13* would lead to an increase in the total amount of RNR complexes in the cytoplasm. This could lead to an increased RNR activity outside S phase resulting increased basal production of dNTPs in *cid13Δ* cells. This could explain the higher dATP pools measured in our *cid13Δ* cells than in the wild-type cells.

In *S. cerevisiae*, constitutively high dNTP levels are shown to be deleterious as it interferes with the dATP feedback inhibition mechanism of RNR (Chabes and Stillman 2007). It has been suggested that fission yeast has relatively tight feedback inhibition mechanism as only 2-3 -fold increase in dNTP levels is seen both in S phase and in response to DNA damage (Hakansson et al. 2006). This feedback mechanism is very important for the cells to be able to monitor the status of the NTP/dNTP ratio and to be able to shut off the dNTP production when needed. Chabes and Stillman (2007) report also that the DNA damage tolerance is directly correlated to the ability to transiently increase dNTP concentration. Interestingly, they also observed that the DNA-damage checkpoint is inactive in the presence of high concentrations of dNTPs, explaining the sensitivity to DNA-damaging agents of such cells.

We measured 1.5-fold higher dATP levels in G1 in *cid13Δ* cells compared to the wild-type cells. We suggest that because of constitutively higher dNTP pools the dATP feedback inhibition mechanism may be impaired in *cid13Δ* cells in fission yeast, leading to a disability to upregulate dNTP synthesis rapidly when needed. This is consistent with our finding that *cid13Δ* cells do not increase dNTP levels as much as *gcn2Δ* cells even if they enter S phase with the same kinetics after UVC irradiation in G1. We can ask if the loss of G1/S checkpoint in *cid13Δ* cells could be due to abnormal high basal dNTP pools, even though this mechanism is not established yet in *S. pombe*.

Assuming that Cid13 plays a role in the sequestration of Suc22 to the nucleus, that would also explain many of the similarities between *S. pombe cid13Δ* mutants and *S. cerevisiae rrp12Δ* mutants such as DNA damage sensitivity, delay into S phase and higher dNTP levels in G1-synchronized cells (see 6.6.2). So far, *rrp12* ORF is identified in *S. pombe* and the predicted function of that protein is in ribosome biogenesis. This equals to *S. cerevisiae* Rrp12 function, the role of which in nuclear transport was recently revealed (Dosil 2011).

6.7 Working with *cdc10-M17* temperature sensitive strains

The usage of temperature sensitive *cdc10-M17* mutant strains of *S. pombe* is well established. Up to 95% synchrony in G1 can be achieved by using these mutants and this offers a powerful tool to study the G1/S checkpoint (appendix 3). When the cells are released from the temperature block they need to go through some important events, triggered by Cdc10, before entering S phase. Activation of Cdc10 at the permissive temperature leads, for instance, to expression of Cdt2 which is required for several events discussed in this study.

A common problem with *cdc10-M17* strains is that they easily pick up a suppressor that impairs the temperature sensitivity. We encountered this problem with the wild type strain #1005 (*cdc10-M17 ura4-D18*). The difficulties to synchronize these cells appeared when I started to collect cells for dNTP measurements and that is why we decided to run that experiment with another wild type strain, #489, which also has the genotype *cdc10-M17*, but it is *ura4+*. The strain with defective *ura4+* gene was used to generate GFP-tagged cells as it was a helpful feature in the selection process.

The very slow cell-cycle progression of some of the strains used in this study may be due to the slow recovery from the *cdc10* block, or it is an additive effect of slow growth because of the GFP-tag and the transient Cdc10 inactivation. If an increase in the Suc22 level is important for normal completion of S phase, this upregulation might require fully functional Suc22. The presence of a GFP tag may interfere with this and lead to slower S-phase progression.

7 CONCLUSION

One of the important aspects of translational regulation after UVC irradiation appears to be maintaining Cid13 levels. In this work we show that Cid13 is indeed important for an appropriate response to UVC irradiation in G1 phase.

We have shown that deletion of *cid13* leads to lower survival after UVC irradiation. Since *cid13Δ* cells do not delay entry into S phase in response to UVC irradiation in G1 we conclude that *cid13Δ* cells are checkpoint deficient, like *gcn2Δ* cells. This indicates that Cid13 in needed for the G1/S checkpoint and the checkpoint deficiency of *cid13Δ* cells is consistent with the notion that regulating Cid13 levels might be an important function of Gcn2.

Our preliminary data suggest a slight Cid13-dependent increase of Suc22 protein levels in response to UVC irradiation in G1, but this is not reflected in a significant increase of dNTP levels. This indicates that G1/S checkpoint signaling does not lead to RNR activation.

Cid13 seems to have other functions related to dNTP synthesis, in addition to cytoplasmic polyadenylation of *suc22* mRNA, which affect the G1/S checkpoint. There is some evidence that Cid13 participates in RanGDP-mediated nuclear transport and could therefore play a role in Suc22 translocation.

REFERENCES

al-Khodairy, F. and A. M. Carr (1992). "DNA repair mutants defining G2 checkpoint pathways in Schizosaccharomyces pombe." Embo J **11**(4): 1343-1350.

Alberts, B. J., A; Lewis, J; Raff, M; Roberts, K; Walter, P (2008). "Molecular Biology of the Cell."

Arias, E. E. and J. C. Walter (2006). "PCNA functions as a molecular platform to trigger Cdt1 destruction and prevent re-replication." Nat Cell Biol **8**(1): 84-90.

Baber-Furnari, B. A., N. Rhind, M. N. Boddy, P. Shanahan, A. Lopez-Girona and P. Russell (2000). "Regulation of mitotic inhibitor Mik1 helps to enforce the DNA damage checkpoint." Mol Biol Cell **11**(1): 1-11.

Bahler, J., J. Q. Wu, M. S. Longtine, N. G. Shah, A. McKenzie, 3rd, A. B. Steever, . . . J. R. Pringle (1998). "Heterologous modules for efficient and versatile PCR-based gene targeting in Schizosaccharomyces pombe." Yeast **14**(10): 943-951.

Benito, J., C. Martin-Castellanos and S. Moreno (1998). "Regulation of the G1 phase of the cell cycle by periodic stabilization and degradation of the p25rum1 CDK inhibitor." Embo J **17**(2): 482-497.

Bentley, N. J., D. A. Holtzman, G. Flaggs, K. S. Keegan, A. DeMaggio, J. C. Ford, . . . A. M. Carr (1996). "The Schizosaccharomyces pombe rad3 checkpoint gene." Embo J **15**(23): 6641-6651.

Borgne, A. and P. Nurse (2000). "The Spd1p S phase inhibitor can activate the DNA replication checkpoint pathway in fission yeast." J Cell Sci **113 Pt 23**: 4341-4350.

Breeden, L. L. (2003). "Periodic transcription: a cycle within a cycle." Curr Biol **13**(1): R31-38.

Caspari, T. and A. M. Carr (1999). "DNA structure checkpoint pathways in Schizosaccharomyces pombe." Biochimie **81**(1-2): 173-181.

Chabes, A. and B. Stillman (2007). "Constitutively high dNTP concentration inhibits cell cycle progression and the DNA damage checkpoint in yeast Saccharomyces cerevisiae." Proc Natl Acad Sci U S A **104**(4): 1183-1188.

Dosil, M. (2011). "Ribosome synthesis-unrelated functions of the preribosomal factor Rrp12 in cell cycle progression and the DNA damage response." Mol Cell Biol **31**(12): 2422-2438.

Elledge, S. J., Z. Zhou, J. B. Allen and T. A. Navas (1993). "DNA damage and cell cycle regulation of ribonucleotide reductase." Bioessays **15**(5): 333-339.

Fernandez Sarabia, M. J., C. McInerny, P. Harris, C. Gordon and P. Fantes (1993). "The cell cycle genes cdc22+ and suc22+ of the fission yeast Schizosaccharomyces pombe encode the large and small subunits of ribonucleotide reductase." Mol Gen Genet **238**(1-2): 241-251.

Forsburg, S. (2003). "Current Protocols in Molecular Biology."

Gordon, C. B. and P. A. Fantes (1986). "The cdc22 gene of Schizosaccharomyces pombe encodes a cell cycle-regulated transcript." Embo J **5**(11): 2981-2985.

Hakansson, P., L. Dahl, O. Chilkova, V. Domkin and L. Thelander (2006). "The Schizosaccharomyces pombe replication inhibitor Spd1 regulates ribonucleotide reductase activity and dNTPs by binding to the large Cdc22 subunit." J Biol Chem **281**(3): 1778-1783.

Harder, J. and H. Follmann (1990). "Identification of a free radical and oxygen dependence of ribonucleotide reductase in yeast." Free Radic Res Commun **10**(4-5): 281-286.

Harris, P., P. Kersey, C. McInerny and P. Fantes (1996). "Cell cycle, DNA damage and heat shock regulate<i>suc22</i>⁺ expression in fission yeast." (3): 284-291.
Hartwell, L. H. and T. A. Weinert (1989). "Checkpoints: controls that ensure the order of cell cycle events." Science **246**(4930): 629-634.
Holmberg, C., O. Fleck, H. A. Hansen, C. Liu, R. Slaaby, A. M. Carr and O. Nielsen (2005). "Ddb1 controls genome stability and meiosis in fission yeast." Genes Dev **19**(7): 853-862.
Jorgensen, P., J. L. Nishikawa, B. J. Breitkreutz and M. Tyers (2002). "Systematic identification of pathways that couple cell growth and division in yeast." Science **297**(5580): 395-400.
Kastan, M. B. and J. Bartek (2004). "Cell-cycle checkpoints and cancer." Nature **432**(7015): 316-323.
Keller, C., K. Woolcock, D. Hess and M. Buhler (2010). "Proteomic and functional analysis of the noncanonical poly(A) polymerase Cid14." RNA **16**(6): 1124-1129.
Knutsen, J. H., I. D. Rein, C. Rothe, T. Stokke, B. Grallert and E. Boye (2011). "Cell-cycle analysis of fission yeast cells by flow cytometry." PLoS One **6**(2): e17175.
Krohn, M., H. C. Skjolberg, H. Soltani, B. Grallert and E. Boye (2008). "The G1-S checkpoint in fission yeast is not a general DNA damage checkpoint." J Cell Sci **121**(Pt 24): 4047-4054.
Kronja, I. and T. L. Orr-Weaver (2011). "Translational regulation of the cell cycle: when, where, how and why?" Philos Trans R Soc Lond B Biol Sci **366**(1584): 3638-3652.
Kumar, D., J. Viberg, A. K. Nilsson and A. Chabes (2010). "Highly mutagenic and severely imbalanced dNTP pools can escape detection by the S-phase checkpoint." Nucleic Acids Res **38**(12): 3975-3983.
Liu, C., M. Poitelea, A. Watson, S. H. Yoshida, C. Shimoda, C. Holmberg, . . . A. M. Carr (2005). "Transactivation of Schizosaccharomyces pombe cdt2+ stimulates a Pcu4-Ddb1-CSN ubiquitin ligase." Embo J **24**(22): 3940-3951.
Liu, C., K. A. Powell, K. Mundt, L. Wu, A. M. Carr and T. Caspari (2003). "Cop9/signalosome subunits and Pcu4 regulate ribonucleotide reductase by both checkpoint-dependent and -independent mechanisms." Genes Dev **17**(9): 1130-1140.
Lowndes, N. F., C. J. McInerny, A. L. Johnson, P. A. Fantes and L. H. Johnston (1992). "Control of DNA synthesis genes in fission yeast by the cell-cycle gene cdc10+." Nature **355**(6359): 449-453.
Maqbool, Z., P. J. Kersey, P. A. Fantes and C. J. McInerny (2003). "MCB-mediated regulation of cell cycle-specific cdc22+ transcription in fission yeast." Mol Genet Genomics **269**(6): 765-775.
Martin-Castellanos, C., K. Labib and S. Moreno (1996). "B-type cyclins regulate G1 progression in fission yeast in opposition to the p25rum1 cdk inhibitor." Embo J **15**(4): 839-849.
Matsuyama, A., R. Arai, Y. Yashiroda, A. Shirai, A. Kamata, S. Sekido, . . . M. Yoshida (2006). "ORFeome cloning and global analysis of protein localization in the fission yeast Schizosaccharomyces pombe." Nat Biotechnol **24**(7): 841-847.
Moss, J., H. Tinline-Purvis, C. A. Walker, L. K. Folkes, M. R. Stratford, J. Hayles, . . . T. C. Humphrey (2010). "Break-induced ATR and Ddb1-Cul4(Cdt)(2) ubiquitin ligase-dependent nucleotide synthesis promotes homologous recombination repair in fission yeast." Genes Dev **24**(23): 2705-2716.

Nestoras, K., A. H. Mohammed, A. S. Schreurs, O. Fleck, A. T. Watson, M. Poitelea, . . . C. Liu (2010). "Regulation of ribonucleotide reductase by Spd1 involves multiple mechanisms." Genes Dev **24**(11): 1145-1159.

Nilssen, E. A., M. Synnes, N. Kleckner, B. Grallert and E. Boye (2003). "Intra-G1 arrest in response to UV irradiation in fission yeast." Proc Natl Acad Sci U S A **100**(19): 10758-10763.

Nurse, P. (1990). "Universal control mechanism regulating onset of M-phase." Nature **344**(6266): 503-508.

Oki, M., L. Ma, Y. Wang, A. Hatanaka, C. Miyazato, K. Tatebayashi, . . . T. Nishimoto (2007). "Identification of novel suppressors for Mog1 implies its involvement in RNA metabolism, lipid metabolism and signal transduction." Gene **400**(1-2): 114-121.

Read, R. L., R. G. Martinho, S.-W. Wang, A. M. Carr and C. J. Norbury (2002). "Cytoplasmic poly(A) polymerases mediate cellular responses to S phase arrest." Proceedings of the National Academy of Sciences **99**(19): 12079-12084.

Rhind, N. and P. Russell (1998). "Mitotic DNA damage and replication checkpoints in yeast." Curr Opin Cell Biol **10**(6): 749-758.

Rhind, N. and P. Russell (2001). "Roles of the mitotic inhibitors Wee1 and Mik1 in the G(2) DNA damage and replication checkpoints." Mol Cell Biol **21**(5): 1499-1508.

Rustici, G., J. Mata, K. Kivinen, P. Lio, C. J. Penkett, G. Burns, . . . J. Bahler (2004). "Periodic gene expression program of the fission yeast cell cycle."

Saitoh, S., A. Chabes, W. H. McDonald, L. Thelander, J. R. Yates Iii and P. Russell (2002). "Cid13 Is a Cytoplasmic Poly(A) Polymerase that Regulates Ribonucleotide Reductase mRNA " Cell **109**: 563-573.

Sazer, S. and S. W. Sherwood (1990). "Mitochondrial growth and DNA synthesis occur in the absence of nuclear DNA replication in fission yeast." J Cell Sci **97 (Pt 3)**: 509-516.

Stevenson, A. L. and C. J. Norbury (2006). "The Cid1 family of non-canonical poly(A) polymerases." Yeast **23**(13): 991-1000.

Stubbe, J. and P. Riggs-Gelasco (1998). "Harnessing free radicals: formation and function of the tyrosyl radical in ribonucleotide reductase." Trends Biochem Sci **23**(11): 438-443.

Takahashi, S., K. Kontani, Y. Araki and T. Katada (2007). "Caf1 regulates translocation of ribonucleotide reductase by releasing nucleoplasmic Spd1-Suc22 assembly." Nucleic Acids Res **35**(4): 1187-1197.

Torrents, E., P. Aloy, I. Gibert and F. Rodriguez-Trelles (2002). "Ribonucleotide reductases: divergent evolution of an ancient enzyme." J Mol Evol **55**(2): 138-152.

Tvegard, T., H. Soltani, H. C. Skjolberg, M. Krohn, E. A. Nilssen, S. E. Kearsey, . . . E. Boye (2007). "A novel checkpoint mechanism regulating the G1/S transition." Genes Dev **21**(6): 649-654.

Wang, S. W., T. Toda, R. MacCallum, A. L. Harris and C. Norbury (2000). "Cid1, a fission yeast protein required for S-M checkpoint control when DNA polymerase delta or epsilon is inactivated." Mol Cell Biol **20**(9): 3234-3244.

Warner, J. R. and K. B. McIntosh (2009). "How common are extraribosomal functions of ribosomal proteins?" Mol Cell **34**(1): 3-11.

Wood, V., R. Gwilliam, M. A. Rajandream, M. Lyne, R. Lyne, A. Stewart, . . . P. Nurse (2002). "The genome sequence of Schizosaccharomyces pombe." Nature **415**(6874): 871-880.

APPENDIX

Appendix 1: Internet references

Appendix 2: Molecular weight standards

Appendix 3: Analysis of G1 arrested cells

Appendix 4: Measuring Suc22 levels by flow cytometry

Appendix 5: Cell-cycle progression of Suc22:GFP cells

Appendix 6: Results chapters

5.3.4. Replacing the clonNAT marker with the *ura4+* cassette,

5.3.5. Removing *ura4+* from the *suc22:GFP* sequence,

5.3.6. Removing clonNAT marker from #1673 and #1674 strains

Appendix 1: Internet references

http://www.biochem.arizona.edu

http://old.genedb.org/genedb/pombe

http://www-bcf.usc.edu/~forsburg

http://www.pombase.org

http://biology.berkeley.edu

Appendix 2: Molecular weight standards

O'GeneRuler 1kb DNA Ladder, Fermentas

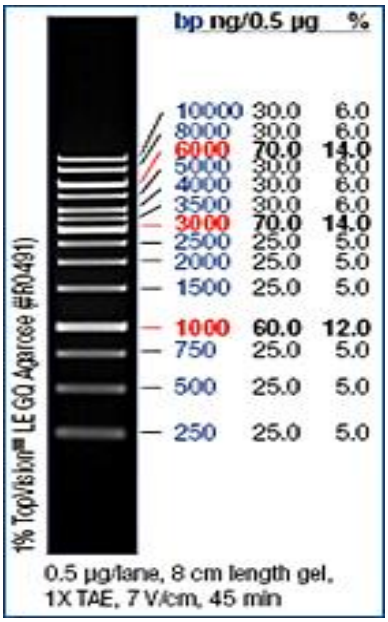

PageRuler Prestained Protein Ladder, Fermentas

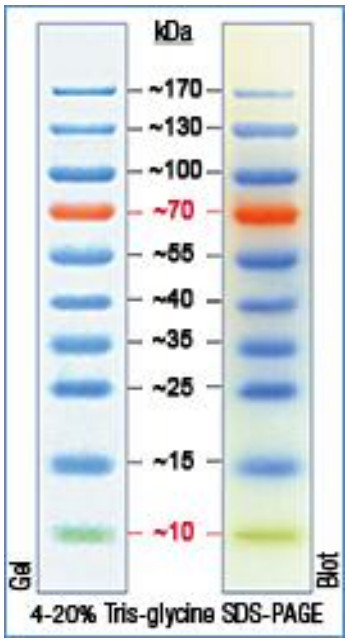

Novex Sharp Protein Standard, Invitrogen

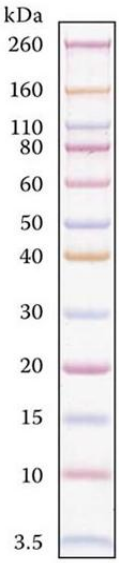

Appendix 3: Analysis of G1 arrested cells

Flow cytometry data showing analysis of cells arrested in G1 with *cdc10* block:

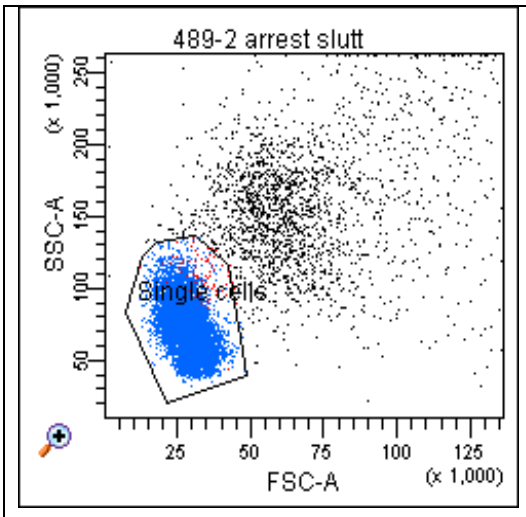	A light scatter cytogram (forward scatter (FSC) vs. side scatter (SSC) dot plot) showing the cell population after G1 arrest. The gated subpopulation represents single cells with one nucleus, a 1C DNA content and low FSC/SSC values. When analyzing the samples, 10 000 cells from this particular subpopulation are counted. The dots outside this subpopoulation, and with higher FSC/SSC values, represent cell dublets. (Figure: this study)
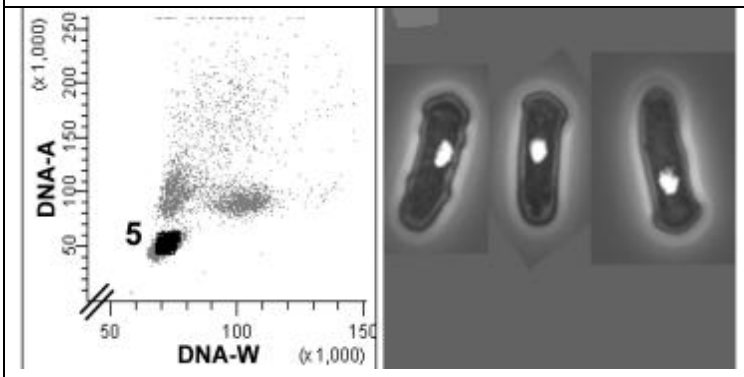	Left: A DNA cytogram based on DNA-width and DNA-areal signals showing the same population as above. The gated cells are here marked with 5. Right: Cells representing subpopulation 5 with one nucleus and 1C DNA content. (Figure: Knutsen et al. 2011)
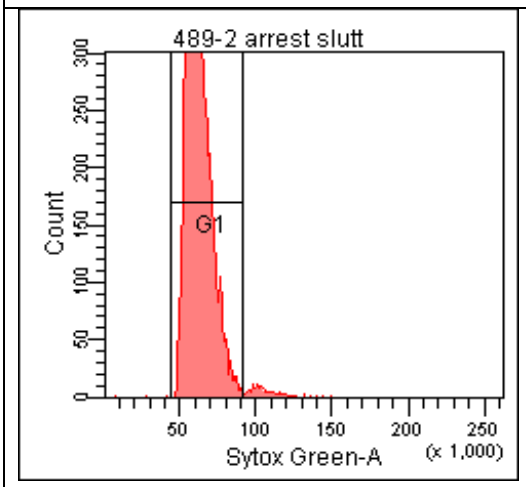	A DNA histogram showing the DNA content of 10 000 cells belonging to the subpopulation of single cells gated in the figure on top. The G1 gate in this figure defines the final cell population in G1 phase. Amount of cells in this gated population is given in persentage out of the population of single cells in the figure on top. With *cdc10* block up to 95% synchrony in G1 can be achieved. (Figure: this study)

Appendix 4: Measuring Suc22 levels by flow cytometry

Flow cytometry analysis of Suc22 protein levels.

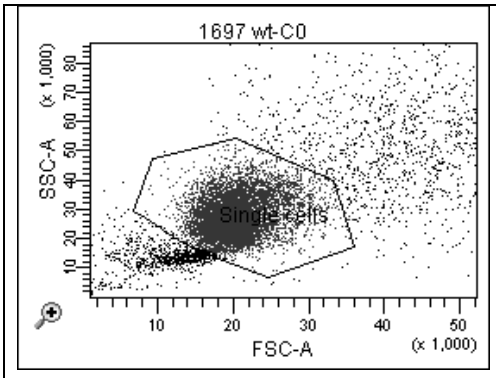

A light scatter cytogram showing the population of single cells gated from the total cell population. These cells are used to analyze the samples. The dots in the upper right corner represent cell duplets and the dots in the lower left corner are most likely signals from mitochondrial DNA due to Hoechst staining. (results chapter 5.4.2)

Histograms showing the intensity of GFP-signal in the cell population expressing Suc22-GFP fusion protein. The samples taken in time points 0 and 90 minutes after the release from *cdc10* block. Wild type, *cid13Δ* and *gcn2Δ* cells, with and without UVC irradiation in G1. Number of cells counted on Y-axis, GFP-signal intensity on X-axis. The total GFP-signal intensity corresponds to the area under the curve. (results chapter 5.4.2)

Wild type Control	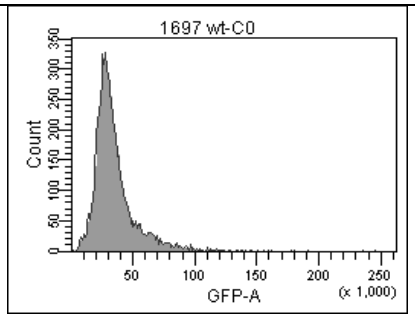	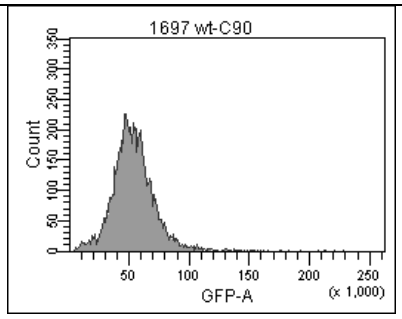
Wild type UVC irradiated	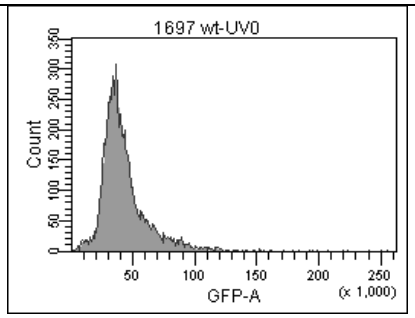	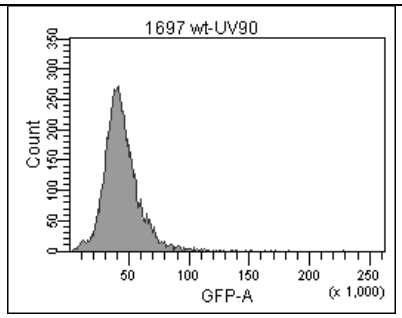

cid13Δ Control	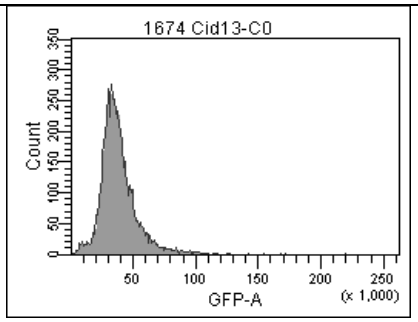	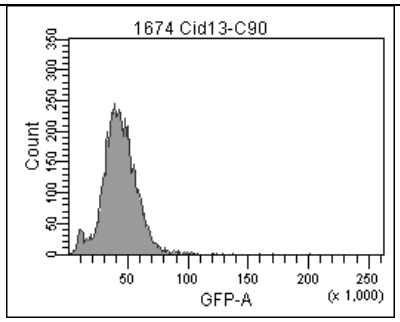
cid13Δ UVC irradiated	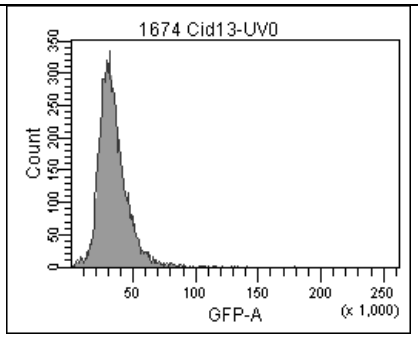	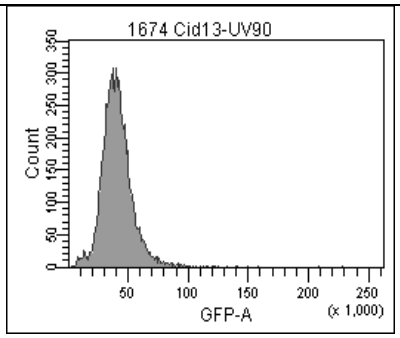
gcn2Δ Control	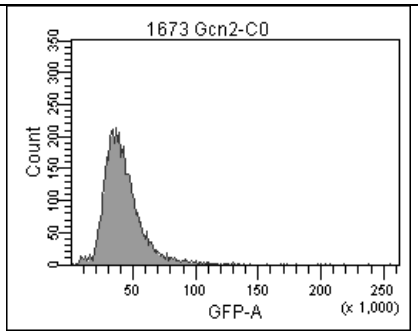	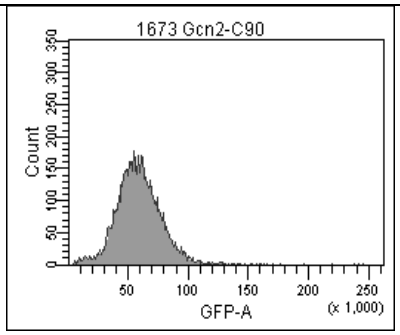
gcn2Δ UVC irradiated	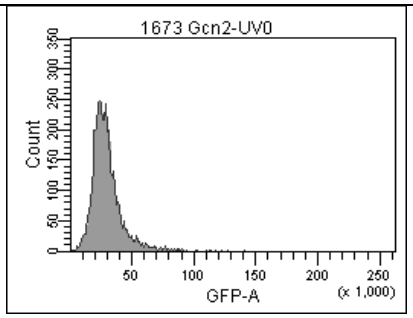	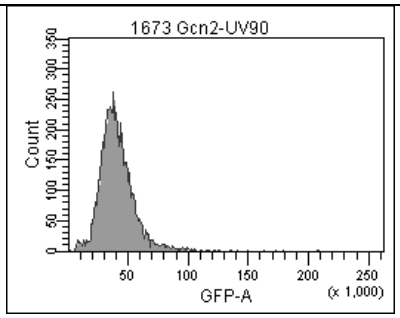

Appendix 5: Cell-cycle progression of Suc22:GFP cells

Flow cytometry analysis of cell-cycle progression of Suc22:GFP cells.

DNA histograms showing the total DNA content as an indicator of the cell-cycle progression after the release from the *cdc10* block. The samples from time points 0 and 90 in wild type, *cid13Δ* and *gcn2Δ* cells, with and without UVC irradiation in G1, are shown. Cell number on Y-axis, signal intensity from Hoechst-stained DNA on X-axis. Abnormally wide peaks appear due to an increase in amount of mitochondrial DNA during the *cdc10* block. Hoechst stain show high specificity to the A+T rich DNA which is particularly abundant in fission yeast mtDNA. (results chapters 5.4.2 and 5.4.3)

Wild type Control	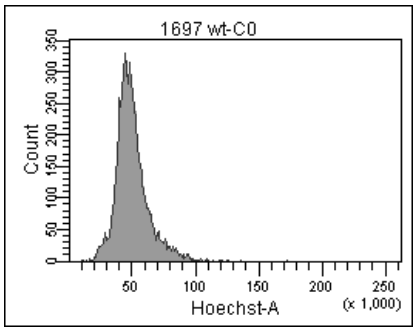	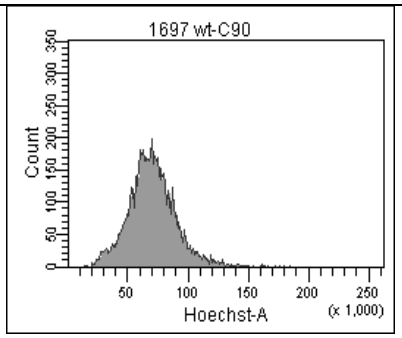
Wild type UVC irradiated	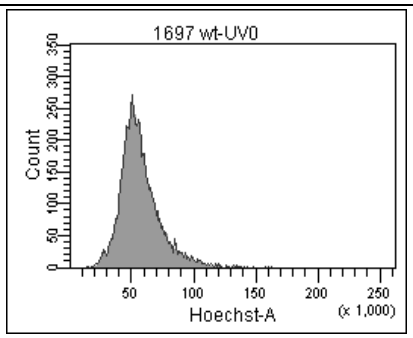	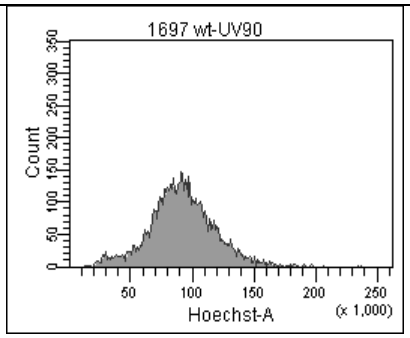
cid13Δ Control	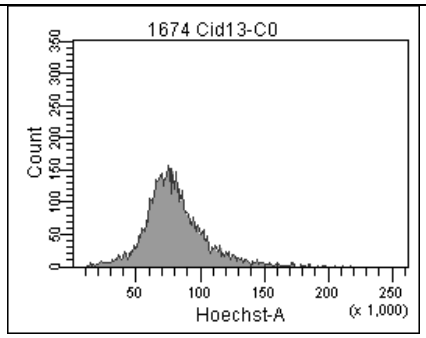	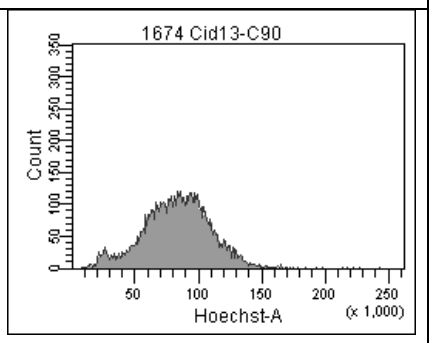

cid13Δ UVC irradiated	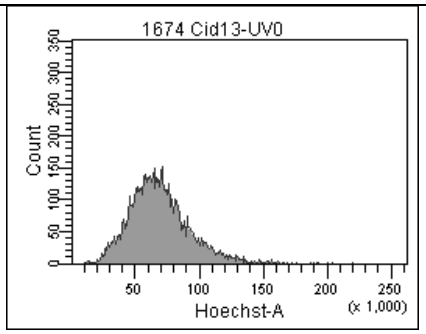	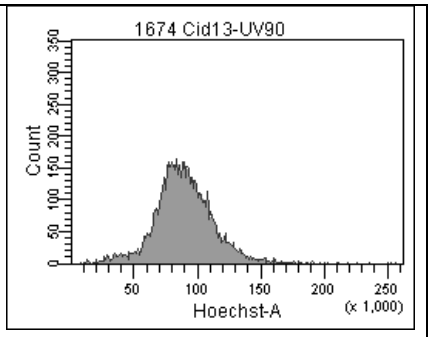
gcn2Δ Control	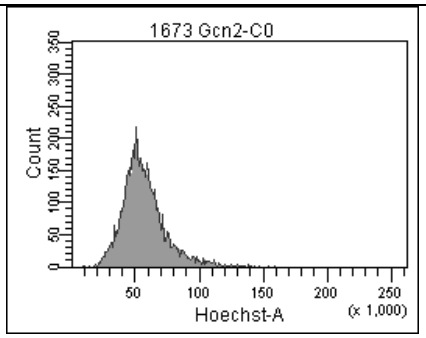	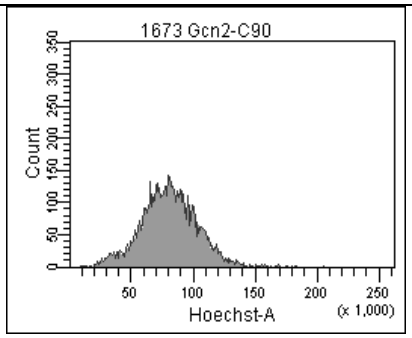
gcn2Δ UVC irradiated	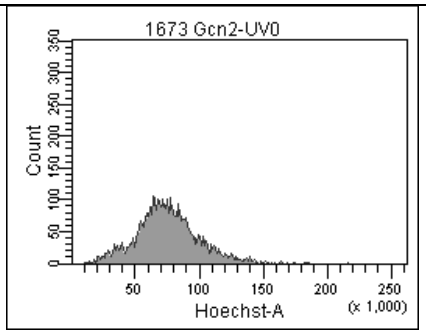	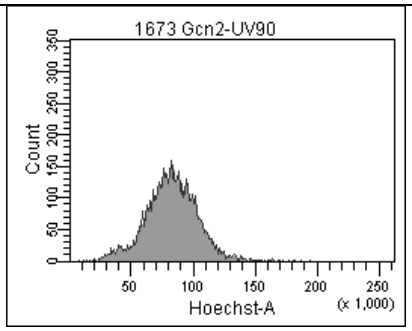

Appendix 6: Results chapters 5.3.4, 5.3.5 and 5.3.6

5.3.4. Replacing the clonNAT marker with the *ura4+* cassette

We decided to remove the clonNAT resistance marker from suc22:GFP:natMX6 construct. The first step was to replace it with the *ura4+* cassette which was removed in the second step. PCR of the *ura4+* cassette was run as described in 4.2.2.

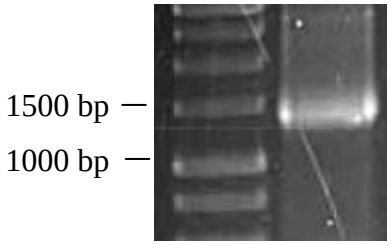

Figure A6.1. The amplified *ura4+* cassette was run on agarose gel (right lane) to confirm that we indeed generated the right product. The length of the amplified sequence should be 1332 bp. Left lane: 1 kb ladder.

Transformation of the wild type (#1697), *cid13Δ* (#1674) and *gcn2Δ* (#1673) strains with *ura4+* sequence was performed as described in 4.1.4.

The transformed cells were plated out onto selective plates (EMM) in different concentrations to screen for the cells which have taken up the *ura4+* gene. Two colonies appeared on one plate with #1697 cells after incubation and these were further streaked out to get several single colonies on YE plate. This was replica plated to YE + clonNAT plates to confirm that the cells have lost the clonNAT resistance marker, ie that the *ura4+* gene is integrated at the *suc22* locus. This new strain has the genotype *cdc10-M17 suc22:GFP:ura4+ ura4-D18 h+* and I called it #1697ura4+.

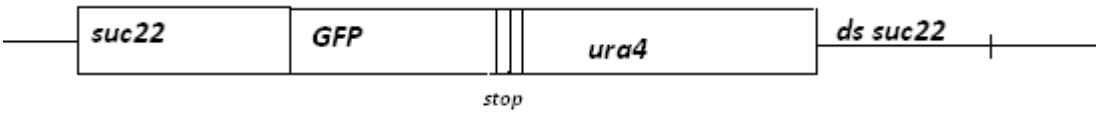

Figure A6.2. *ura4+* replacing the *nat*^{r} marker giving a suc22:GFP:ura4+ construct.

I decided to finish the procedure with #1697ura4+ to produce the genotype *cdc10-M17 suc22:GFP ura4-D18 h+*. This could then be used to cross the *suc22:GFP* into the *cid13Δ* (#1674) and *gcn2Δ* (#1673) strains.

5.3.5. Removing *ura4+* from the *suc22:GFP* sequence

The second step in removing the clonNAT resistance marker from the original *suc22:GFP:natMX6* construct was to loop out the *ura4+* cassette from the *suc22:GFP:ura4+* sequence in #1697ura4+ strain as described in 4.2.2 (figure 4.6). One-step gene replacement using this fragment was expected to remove the *ura4* marker and restore the wild-type sequences downstream of *suc22:GFP*.

Transformation of strain #1697ura4+ with the wild type sequence was performed as described in 4.1.4. The transformed cells were plated out onto selective YE plates containing 5-FOA. This compound has the ability to inhibit growth of *ura4+ S. pombe* cells and therefore selects for uracil auxotrophs. When colonies appeared, several of them were further streaked out to EMM with uracil and EMM alone to be able to pick clean *ura4-* colonies. This new strain was designated #1697wt.

5.3.6. Removing clonNAT marker from #1673 and #1674 strains

Performing a genetic cross to remove nat^r from #1673 strain

I continued with crossing the new 1697wt strain *(cdc10-M17 suc22:GFP ura4-D18 h+)* with #1673 *(cdc10M-17 gcn2::ura4+ suc22:GFP:natMX6 ura4-D18 h-),* to produce GFP-tagged *gcn2Δ* mutant strain without the *nat^r* marker. Genetic cross was performed as described in 4.1.2. and the spores were screened for uracil auxotrophy and clonNAT sensitivity by replica-plating (4.1.3.). The genotype wanted, *cdc10-M17 gcn2::ura4+ suc22:GFP ura4-D18*, should grow both in EMM and in EMM with uracil added, but not in the presence of clonNAT. The following table A6.1 shows the possible genotypes after this genetic cross. Columns to the right indicate the selection on different growth media. All spores will have *cdc10-M17* and *ura4-D18* genotype. This new strain was designated #1673wt.

Table A6.1. Selection of *S. pombe* spores in different growth media. The genotype wanted written in bold. + indicates growth, - no growth.

Genotype	**YE + clonNAT**	**EMM**	**EMM+URA**
gcn2::ura4+ suc22:GFP:natMX6 ura4-D18 cdc10-M17	+	+	+
gcn2::ura4+ suc22:GFP ura4-D18 cdc10-M17	**-**	**+**	**+**

gcn2+ suc22:GFP:natMX6 ura4-D18 cdc10-M17	+	-	+
gcn2+ suc22:GFP ura4-D18 cdc10-M17	-	-	+

Mating type was determined as described in 4.1.2. I needed to have an h- strain as I continued with crossing this strain further with GFP-tagged *cid13Δ* strain, #1674, to remove the *nat*^{r} marker from that.

Performing a genetic cross to remove nat^r from #1674 strain

I followed the same procedure as described above to construct the last strain. This time I crossed #1673wt *(cdc10-M17 gcn2::ura4+ suc22:GFP ura4-D18 h-)* with #1674 *(cdc10-M17 cid13::LEU2+ suc22:GFP:natMX6 ura4-D18 leu1-32 h-)* and screened first for clonNAT sensitivity and uracil auxotrophy (table A6.2). All spores will have *cdc10-M17* and *ura4-D18* genotype. This new strain was designated #1674wt.

Table A6.2. Selection of *S. pombe* spores in different growth media. The genotype wanted written in bold. + indicates growth, - no growth.

Genotype	**YE + clonNAT**	**EMM**	**EMM+URA**
gcn2::ura4+ cid13::LEU2+ suc22:GFP:natMX6 ura4-D18 cdc10-M17	+	+	+
gcn2+ cid13::LEU2+ suc22:GFP:natMX6 ura4-D18 cdc10-M17	+	-	+
gcn2::ura4+ cid13::LEU2+ suc22:GFP ura4-D18 cdc10-M17	-	+	+
gcn2+ cid13::LEU2+ suc22:GFP ura4-D18 cdc10-M17	**-**	**-**	**+**
gcn2::ura4+ cid13+ suc22:GFP:natMX6 ura4-D18 cdc10-M17	+	-	+
gcn2+ cid13+ suc22:GFP ura4-D18 cdc10-M17	-	-	+

There are two possible genotypes left after these selections: *gcn2+ cid13::LEU2+ suc22:GFP ura4-D18* and *gcn2+ cid13::LEU2+ suc22:GFP ura4-D18*. The last step

was to identify the colonies carrying the *cid13* deletion exploiting the HU sensitivity of the *cid13Δ* cells. This was done with a plate assay described in 4.1.8.

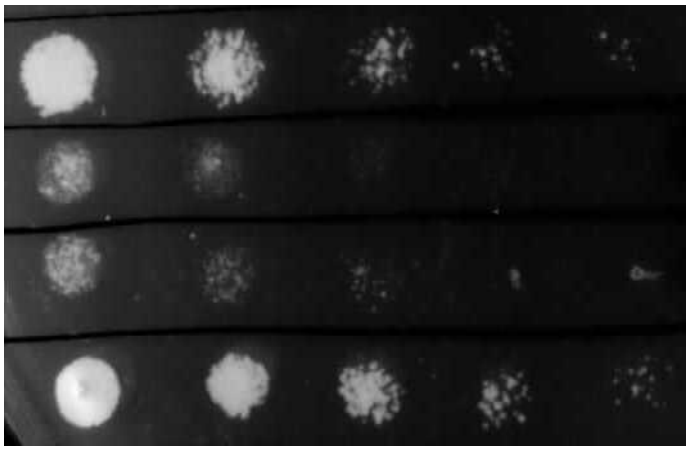

Figure A6.3. Four different strains were spotted to YE plate containing 7 mM HU and incubated for 5 days. Top and bottom rows, #1005 and #1673, respectively, are negative controls and grow normally in the presence of 7 mM HU. The two rows in the middle show the strains that are more sensitive to HU: one positive control (#1674) and one strain to be tested for HU sensitivity.

Confirming the presence of the GFP-tag

The #1674wt candidate strain (shown in figure A6.3), and #1673wt and #1697wt strains were further examined under the fluorescence microscope to confirm the presence of the GFP-tag. Surprisingly, the GFP signal was not present in any of the three strains. All primers, templates and genomic sequences used in this procedure were checked once more and the whole procedure was started from the beginning. This time I noticed that the GFP signal was not present after removing *nat*^{r} with the *ura4+* deletion cassette. The same occurred in all three strains at the same time as they lost the *nat*^{r} and gained the ability to grow without added uracil. Western blot analysis with α-GFP primary antibody couldn't detect the presence of GFP either. After several trials with the same strange result we decided to continue working with the strains still carrying the clonNAT resistance marker.

ACKNOWLEDGMENTS

I owe my sincere thanks to my supervisors Erik Boye and Beáta Grallert for the opportunity to be a part of your group for the last two years. I also appreciate the opportunity to join you for congresses and seminars.

Erik, thank you for being positive, encouraging and available during this work. You have an extraordinary gist for scientific communication and daily conversation.

Beáta, thank you for sharing your phenomenal knowledge in pombe-biology with me, to not to forget the understanding for stiff shoulders caused by infrequent training.

I have had such a good time with all of you at the lab and you have helped me a lot. I would especially thank Lilian and Christiane, I would have not been able to complete this work without you.

I would also like to thank my friends and family for being patient with me for the last months and for reminding me that there is more to life than these green cells. In particular, I would like to thank my friend Marja for believing in me in all these years more than I believe in myself.

Anette, Nina and Kristiane, I'm very glad that I have gotten to know you. The years at the university wouldn't have been as enjoyable without you.

Arne, thank you for bringing so much joy to my life.

Oslo, February 2012

Riikka Taipale